A LABORATORY AND MATHEMATICAL STUDY OF THE 'THERMAL BAR'

by

G.H. ELLIOTT

B.Sc., University of Toronto, 1965
M.Sc., University of British Columbia, 1967

A THESIS SUBMITTED IN PARTIAL FULFILMENT OF
THE REQUIREMENTS FOR THE DEGREE OF
DOCTOR OF PHILOSOPHY

in the Department
of
Physics
and
Institute of Oceanography

We accept this thesis as conforming to the
required standard

THE UNIVERSITY OF BRITISH COLUMBIA
October, 1970

In presenting this thesis in partial fulfilment of the requirements for an advanced degree at the University of British Columbia, I agree that the Library shall make it freely available for reference and study. I further agree that permission for extensive copying of this thesis for scholarly purposes may be granted by the Head of my Department or by his representatives. It is understood that copying or publication of this thesis for financial gain shall not be allowed without my written permission.

Department of Physics
Institute of Oceanography,
The University of British Columbia
Vancouver 8, Canada

Date October 16/70

ABSTRACT

The 'migrating thermal bar' phenomenon, known to occur in certain large, dimictic, freshwater lakes, has been studied in laboratory and mathematical models. The temperature fields observed in the laboratory agreed with those observed in Lake Ontario and a linear physical model for the speed of the 'thermal bar', based on negligible horizontal advection and diffusion of heat, gave reasonable values for both the laboratory model and Lake Ontario. Observations were also made of the associated velocity field. On the basis of this laboratory model, which suggests that horizontal advection and diffusion of heat were not of primary importance, mathematical models were developed. First the temperature field was calculated from the one-dimensional heat diffusion equation. Then the velocity field was calculated assuming that the flow was driven by buoyancy forces and balanced by viscous forces. On the basis of the similitude between the temperature fields found in my models and those observed in the lakes, it seems possible that the velocity field of the models also provides a good approximation to the circulation associated with the bar in lakes. There are no direct measurements of the velocities associated with the bar in lakes and they will be difficult to obtain as such velocities are expected, in Lake Ontario, to be only of the order of 1 cm sec^{-1}.

TABLE OF CONTENTS

page

LIST OF FIGURES

Figure page

ACKNOWLEDGEMENTS

The author would like to express her gratitude to Dr. P.H. LeBlond who suggested the problem and provided advice, encouragement and funds for the experimental work; to Dr. G.K. Rodgers of the Great Lakes Institute, University of Toronto who generously provided observational material from his work on the Great Lakes; to Dr. E.L. Lewis of the Frozen Sea Research Group, Department of Energy, Mines and Resources who kindly permitted the use of the cold chambers; to all who took their time to discuss and advise including Dr. R.W. Stewart, Dr. A. Gill, Dr. R.W. Burling, Dr. Z. Rotem, Dr. L.A. Mysak and Dr. G.W. Bluman; and to Dr. J.A. Elliott for his invaluable assistance in the experimental work. The author was most fortunate to be financially supported during this work by a National Research Council of Canada Studentship and a MacMillan Family Fellowship.

Finally the author wishes to thank her husband, Dr. J.A. Elliott, for his patience and help in the preparation of this thesis.

1. INTRODUCTION

The term 'thermal bar' (or rather 'barre thermique') was first coined 90 years ago when a Swiss scientist (Forel, 1880) tried to explain a curious winter temperature pattern in Lake Geneva. The deeper part of the lake remained above 4°C, the temperature of maximum density of fresh water, while during severe winters there was ice at the shore. The 4°C isotherm at the surface was situated just on the shallow side of a drop off to deep water and was quite stationary. The water was not observed to mix across this isotherm, which thus seemed to mark some sort of limnological barrier.

However most of the literature on the thermal bar is from the last decade. In 1963 Tikhomirov published a paper describing a migrating thermal bar observed on Lake Ladoga during both the spring heating-up period and the fall cooling-off period. The bar was observed to move from near shore to the centre of the lake where it disappeared. The most detailed observational studies have been done by G.K. Rodgers of the Great Lakes Institute, University of Toronto, who for many years has been studying the migrating thermal bar in Lake Ontario (Rodgers, 1963, 1965a, 1966a, 1966b, 1967, 1968).

A migrating thermal bar thus occurs in some large freshwater lakes in the spring and late fall (e.g., Lake Michigan: Church, 1942; Great Lakes: Richards *et al*, 1969; Lake Ontario: Rodgers, 1966a; Lake Ladoga: Tikhomirov, 1963). It is a thermal structure in which a surface 4°C isotherm appears first near the shores and then progresses towards the centre of the lake, where it eventually disappears. Strong surface temperature gradients, a marked change in turbidity, and indications of a convergence are usually associated with the 'bar', defined by the 4° surface isotherm, which

separates stable, stratified, shoreward water from almost homogeneous deeper water (Rodgers, 1966a). The thermal bar exists because fresh water attains its maximum density above its freezing point (Figure 1). During heating or cooling through the temperature of maximum density in certain large lakes, in which the 'bar' exists, the vertical mixing does not occur uniformly over the whole lake. Instead the mixing is first completed near the shores which then become stable. The migrating thermal bar exists at the transition between the stable and unstable regions.

The situtation is well illustrated by what happens in Lake Ontario. In early spring Lake Ontario is everywhere colder than 4°C, typically below 2°C. As the lake heats up, the mean water temperature at the shore increases more rapidly than in the deeper parts of the lake. The surface 4°C isotherm appears first near the shore around the lake and gradually moves in towards the centre of the lake, remaining roughly parallel to the depth contours. It takes one and a half to two months from its appearance at the shore until it disappears below the surface at the centre of the lake. By the beginning of June a temperature section across Lake Ontario is similar to those shown in Figure 2 (Rodgers, 1966a and Rodgers, unpublished, 1965). Flotsam along the surface 4°C isotherm suggests some associated convergence. The higher turbidity on the shoreward side of the 4°C isotherm indicates that this water does not mix quickly with the remainder of the lake. This is the reason for the name 'thermal bar' meaning 'barrier'. In the warmer water on the shoreward side of the 4°C isotherm a thermocline and a strong surface temperature gradient exist (Figure 2) (see Rodgers, 1966a, 1966b).

This phenomenon can also occur in the fall as the temperature

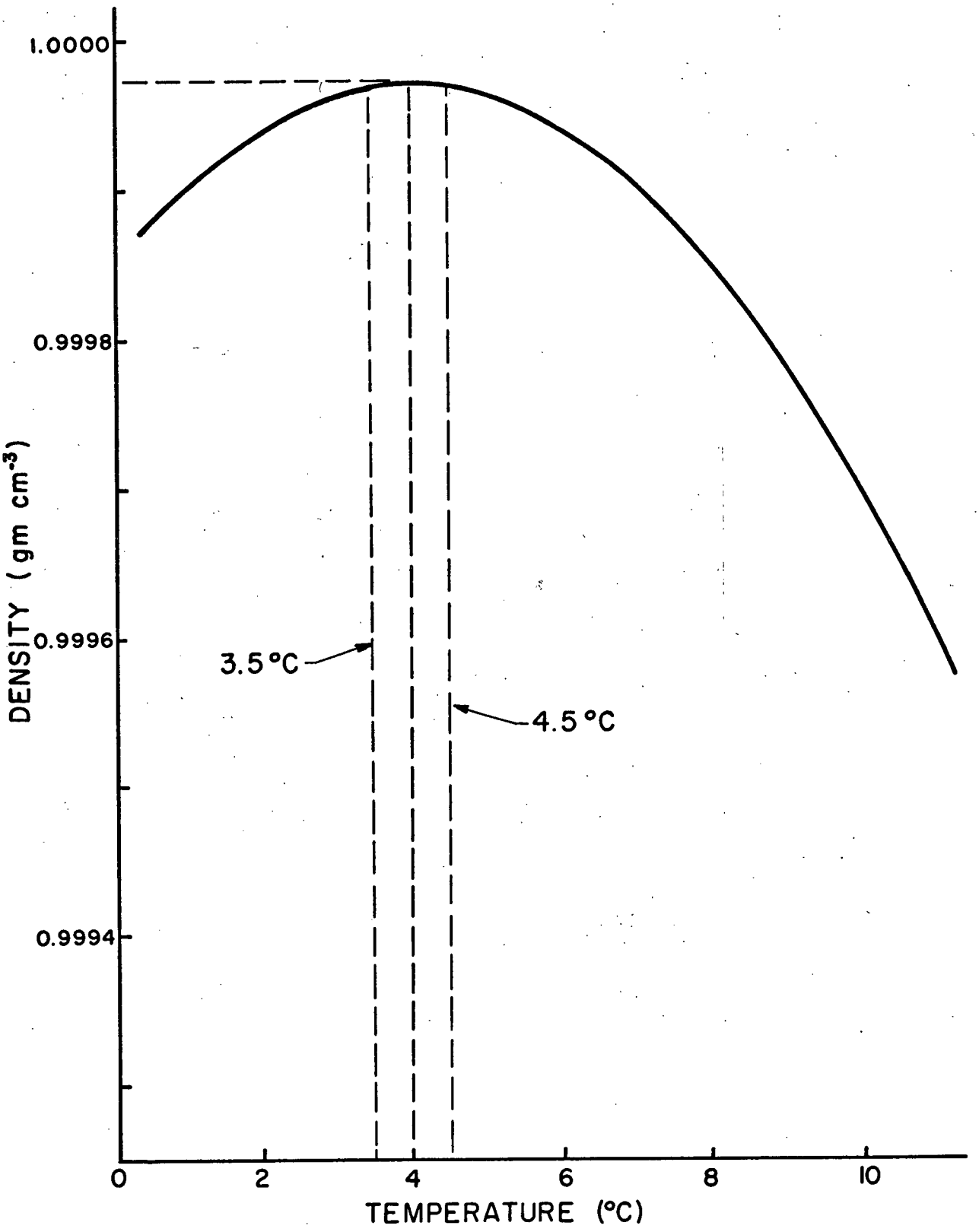

Figure 1. The density of fresh water as a function of temperature (Handbook)

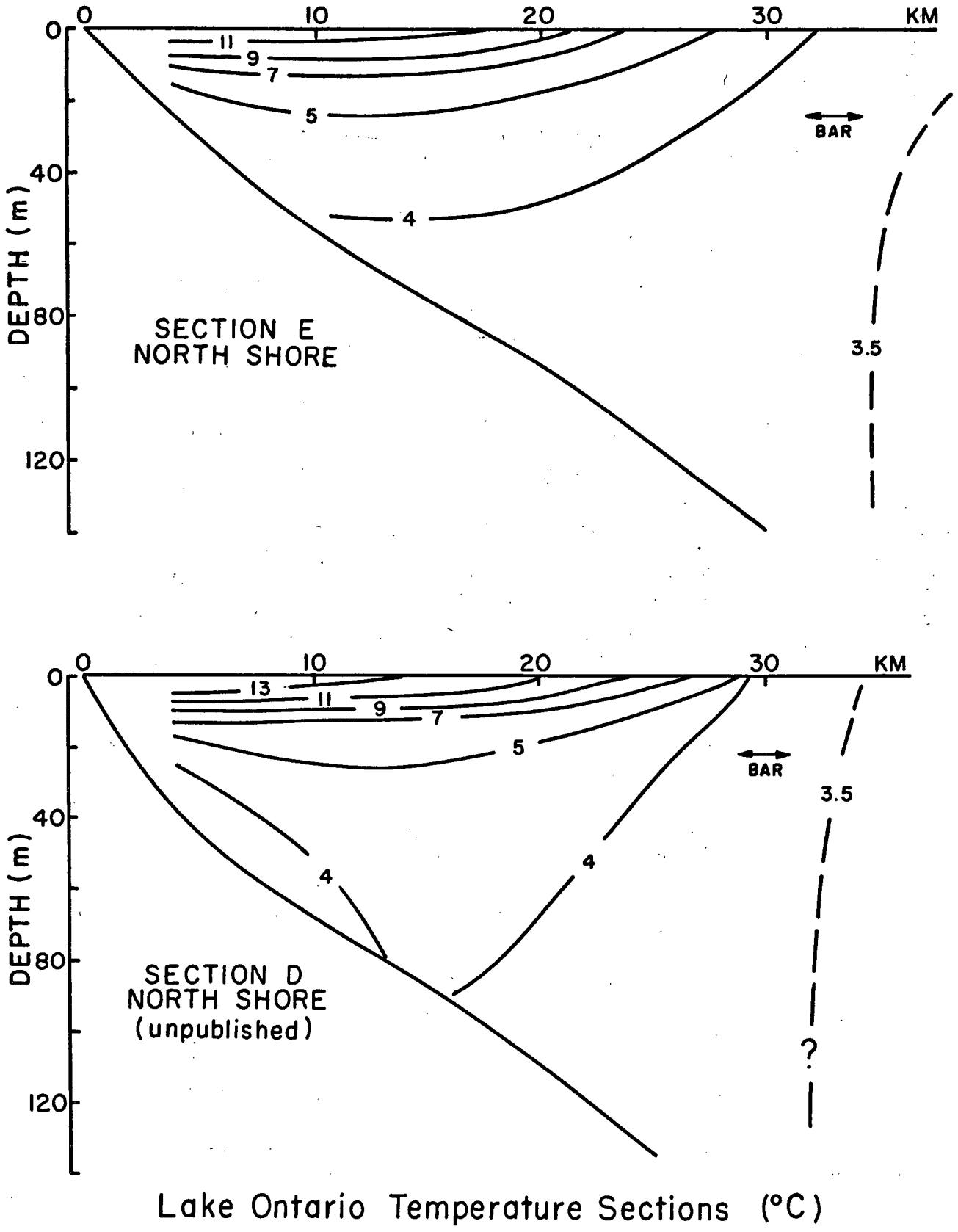

Figure 2. Temperature sections for Lake Ontario for two N-S mid-lake sections (Section E, Rodgers 1966a; Section D, Rodgers, unpublished, 1965)

near the shore decreases more rapidly than near the middle of the lake resulting in a 4°C isotherm that then progresses towards the centre of the lake in a manner similar to the situation in the spring (Church, 1942; Richards *et al*, 1969; Rodgers, 1966a). This is not as prominent a condition since the stable shoreward side cannot become as strongly stratified, the maximum temperature difference being 4C°.

The only previous mathematical consideration of the thermal bar phenomenon was the recent work pertaining to Lake Michigan by Huang (1969). His approach assumed that the pressure gradients induced by thermal effects were balanced by Coriolis forces (that is, he used the thermal wind equation) except in thin viscous boundary layers. The equations were linearized by ordering in terms of the Rossby number; the zeroth and first order solutions were considered. These solutions are not at all time dependent, as the migrating thermal bar obviously is. The confining of viscous effects to thin boundary layers confines the horizontal flow prependicular to the bar to these boundary layers, which does not seem reasonable in the light of our model studies. Also his calculated flow is in the form of cells, one on either side of the bar, with mixing and sinking at the bar. This was not what I found in my experimental observations.

A simple prediction scheme for the time of disappearance of the thermal bar in Lake Ontario was developed by Sato (1969) using observational data. He found the time to depend primarily on the heat content in the central portions of the lake in the early spring (arbitrarily using April 1); that is, the time interval was that necessary to heat the central waters to the point where the surface temperature was 4°C.

In my opinion a theoretical approach to the problem of the thermal bar was hampered by the lack of knowledge of the velocity field involved in the phenomenon; for example, no measured currents have been directly related to this phenomenon. For this reason I have studied the thermal bar in a laboratory model (Elliott and Elliott, 1969, 1970) (see section 2). This study compared favourably with lake observations.

From these laboratory studies and the observations taken by others of the thermal bar in lakes, a linear physical model for the speed of the migrating bar was developed. A temperature field was developed mathematically which compared reasonably well with the laboratory model studies. Using an analytical approximation of the observed temperature field, a velocity field was then found, using an approximated vorticity equation, which again agreed reasonably well with the observations from the work in the laboratory (see section 3). These results were then scaled, on the basis of the laboratory studies and compared to the conditions in Lake Ontario during the presence of the thermal bar.

The laboratory and theoretical studies produce reasonable approximations to the temperature fields observed in Lake Ontario and the associated velocity field is not unreasonable, but has not been directly measured in the lakes.

2. LABORATORY MODEL

2.1 Apparatus

The experiments were conducted in a rectangular tank 1.5 meters long and 30 centimeters wide that was insulated on the sides and bottom (Figure 3). The end walls and bottom were plywood with 4 centimeter styrofoam insulation. The long walls were a double thickness of 0.6 centimeter plexiglas separated by a 1.2 centimeter air space. A desiccating agent was inserted in the air space to prevent condensation. To provide a sloping bottom, wedges of styrofoam covered with sheets of plastic were sealed into the tank with masking tape and a silicone sealant. This tank was used to simulate both the spring and fall conditions.

The spring condition or heating period was simulated by first cooling water in the tank down to about 0°C and then heating the surface from above with heat lamps (Westinghouse, 250 watt, reflector, infrared heat). The fall or cooling period was simulated by cooling cold (6° to 8°C) tap water in a cold chamber (facilities of the Frozen Sea Research Group, DEMR, Victoria). Since the spring conditions have been more frequently reported for the Great Lakes and the heated system is easier to simulate in the laboratory this system was studied in more detail.

2.2 Experimental Techniques

For the heating experiments the tank was first filled with fresh tap water. About 1 c.c. of liquid detergent was added; this was necessary to decrease surface tension effects during the addition of dye. If the detergent was not present when the flecks of dye came in contact with the water, surface velocities resulted which distorted any 'thermal bar effects'

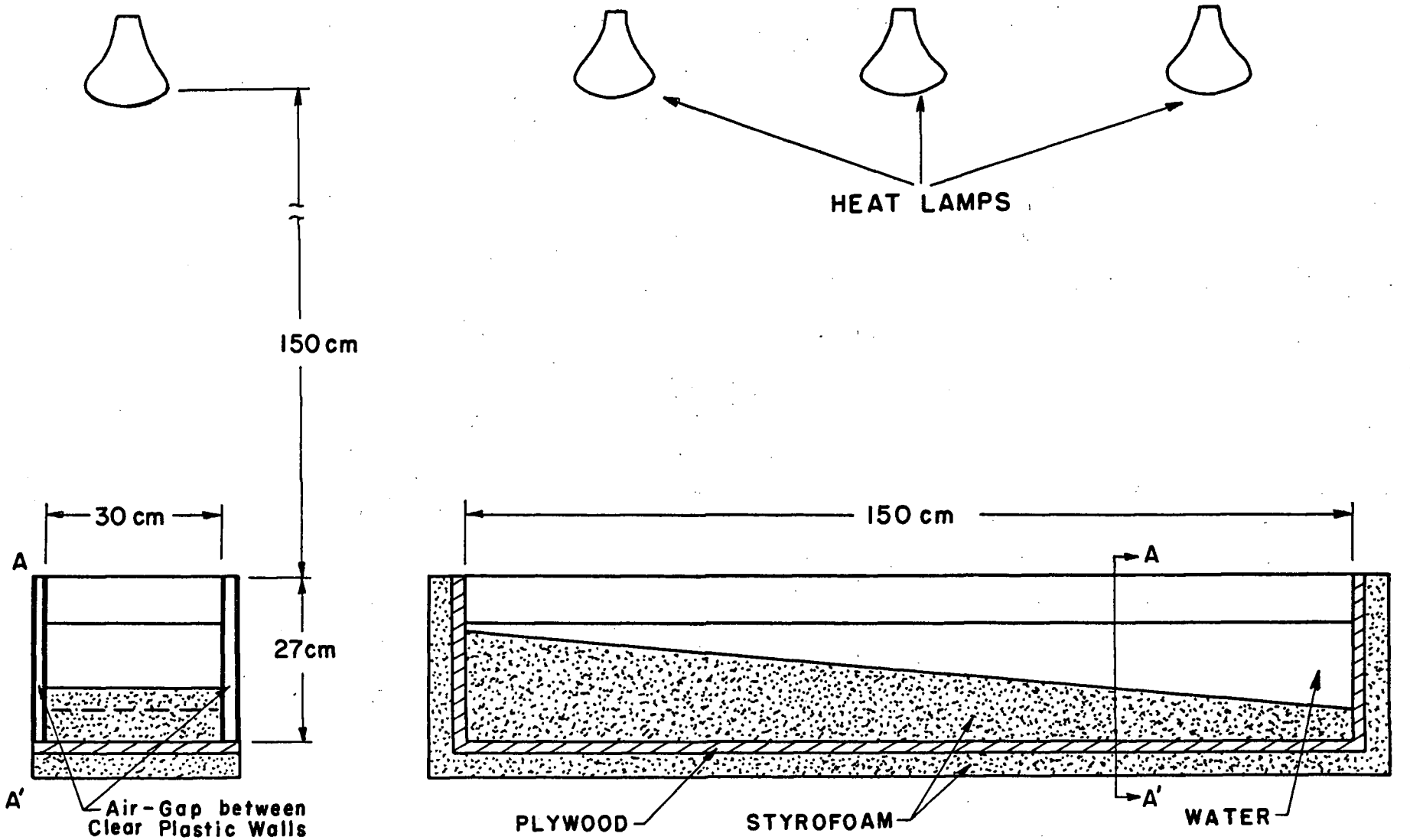

Figure 3. Experimental tank

present. Crushed ice was stirred into the water to lower the temperature of the water to near 0°C; then excess ice was removed, the mean temperature measured, and the heat lamps turned on. In approximately one half hour the shallow end had reached a temperature slightly above 4°C. A temperature and current pattern developed (see subsection 2.3) which maintained itself throughout the experiment, progressing from the shallow end to the deep end in a further half hour.

The current structure was followed by dropping flecks of Rhodamine B dye on the surface; these sank to the bottom leaving vertical red traces which were subsequently distorted by the currents. The dye trace was positioned with respect to a centimeter grid on the back wall of the tank. The motion was timed with a stop-watch. Relative motions were obtained from time series photographs and from 16 mm movies of the dye streaks.

To obtain temperature profiles a thermistor bead (VECO 32A5), attached to the end of a 40 cm, thin glass rod with centimeter markings, was lowered vertically through the water. The resistance of the thermistor was measured directly with a Fairchild Multimeter (Model 7050). This instrument uses sufficiently small current (1 μa) that self heating of the thermistor is negligible. To prevent thermal contamination from water dragged by the glass rod, measurements were made only while lowering the thermistor. Resistances were usually read at depths of 0.5 cm, 1 cm, 2 cm, 3 cm, etc., to the bottom. The thermistor was calibrated against a mercury and glass thermometer before, during, and after the experiments. Its calibration did not change. A calibrated, battery-operated thermistor thermometer was situated at the deep end of the tank at all times in order to measured the temperature here periodically during the experiments.

The heat flux was obtained from the difference in heat content of the

water in the tank just before the heat lamps were turned on and just after the heat lamps were turned off. Normally the tank was heated with three heat lamps equally spaced with respect to the tank and at a height of 1.5 meters above the water surface (Figure 3). The water was also heated by long wave radiation and heat conduction through the walls. The effects of this radiation and conduction were evaluated as follows. With the heat lamps off, a tank of 0°C water was allowed to sit for about an hour. This gave a heat flux which included both long wave radiation balance and heat gained by conduction through the walls. Then a tank of water at 0°C, with an insulated top, was allowed to sit for approximately an hour. This gave an estimate of the heat flux through the walls. Using three lamps the heating rate was about 9×10^{-3} cal cm^{-2} sec^{-1} (Figure 4). Of this 2×10^{-3} cal cm^{-2} sec^{-1} was from the long wave radiation and 2×10^{-3} cal cm^{-2} sec^{-1} from heat conduction through the walls. A higher heating rate of 12×10^{-3} cal cm^{-2} sec^{-1} could be obtained using five heat lamps. Thus a maximum of about one fifth of the heating of the water in the tank is through the walls and not through the surface of the water.

In the first series of experiments a bottom slope of 5° and a heating rate of 9×10^{-3} cal cm^{-2} sec^{-1} were used. This slope is five to twenty times those found in Lake Ontario, the prototype for this model, however it gave a reasonable change in water depth over the length of the tank (about 1 cm of water at shallow end, 14 cm at deep end). The heating rate is only slightly higher than the 7×10^{-3} cal cm^{-2} sec^{-1} typically experienced in the spring on Lake Ontario. Figure 5 shows the penetration of the surface heating from the heat lamps, calculated from the spectral energy distribution of the lamps and known absorption coefficients (Sverdrup *et al*, 1942; Dorsey, 1940). Also shown is the penetration of

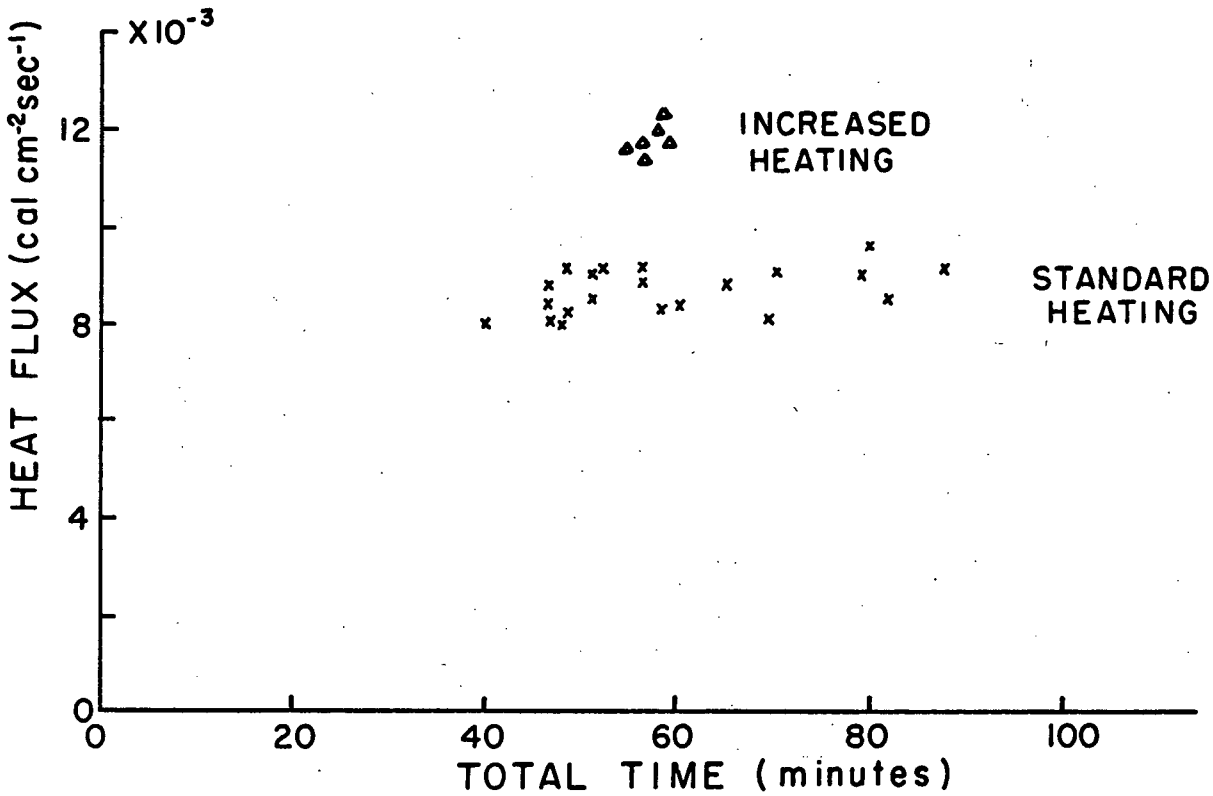

Figure 4. Heat fluxes used in the experiments plotted against total time of heating

solar radiation into pure water (Sverdrup *et al*, 1942). In the tank most of the heat was absorbed in the upper centimeter of the water; this simulates solar heat absorption in the upper few meters in the lake. Thus Figure 5 suggests a vertical scaling of approximately 1/1000. The 5° bottom slope, compared to the north shore of Lake Ontario, in turn suggests a horizontal scaling of approximately 1/20,000. In making a comparison with the lakes, the tank could then be viewed as representing a section from the shore to the centre of the lake, however these tank experiments are not meant to be an example of strict dynamic modelling.

The experimental work was done in two stages. The first series of experiments were done primarily to investigate the possibility of studying the thermal bar in a laboratory model and to investigate its behaviour during heating and cooling. The velocity field was also studied at this time. Later, a further series of experiments were done to study my 'thermal bar' in a more quantitative manner.

2.3 Description of the 'Bar' in the Tank

Initially the surface heating produces vertical convection everywhere in the tank. The temperature in the shallow end rises faster than that in the deep end making the water in the shallow end denser. However downslope flow due to this horizontal density gradient is inhibited by the convection. Eventually the temperature in the shallow end reaches 4°C while in the deep end it is still less than 2°C. By this time some flow of dense water along the bottom slope can be observed in spite of the vertical convection. This weak mean circulation is superimposed on the convection; towards the deep end at the bottom and towards the shallow end at the top. Further heating produces, at the shallow end, a stable thermocline of water warmer than 4°C.

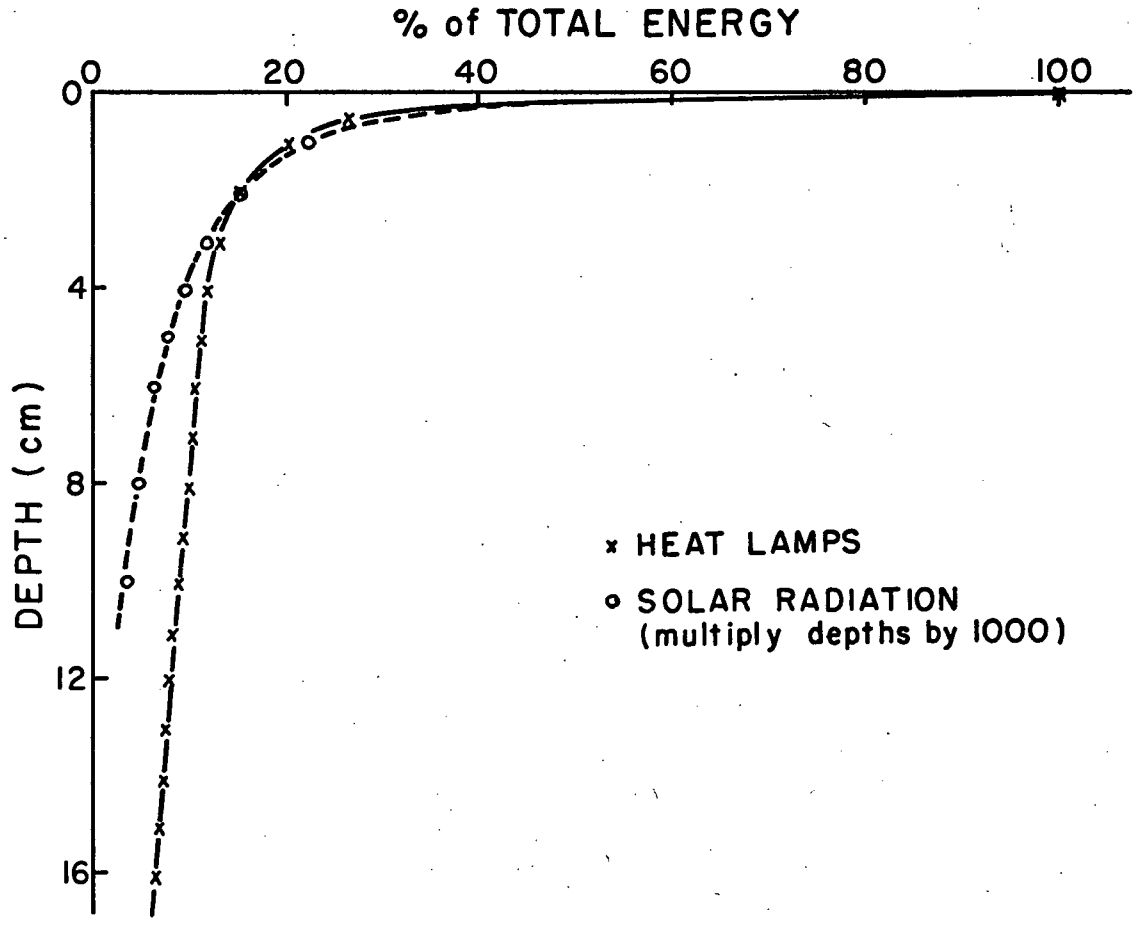

Figure 5. Percentage of total surface heat reaching different depths

This thermocline progresses towards the deep end and its forward edge marks a boundary between the now stable shallow region of the tank and the deeper convecting region (Figure 6). A mean flow towards the deep end is observed in the thermocline with a counter-flow underneath. In the deep end of the tank a flow near the surface travels towards the stable thermocline. This current sinks at the front edge of the thermocline and divides, a part providing the upslope current in the shallow end and the other part a downslope current in the deep end. The sinking zone (Figure 6) in front of the stable thermocline is made up of water between 3.5 and 4.5°C (maximum density region). This dense water is the result of heating colder, lighter water from the deep end of the tank and does not include water from the stable thermocline on the shallow side. In these experiments, this sinking zone will be referred to as the 'thermal bar' or simply the 'bar'. The 4°C isotherm does not always extend to the surface since eventually a shallow thermocline also develops on the deep side due to the intense heating at the surface. This thermocline is slightly unstable and more active convective mixing would dissipate it. The surface velocities go to zero because of surface tension effects, often referred to as 'surface pressure' (see Davies and Rideal, 1961, p.218); this is due to the presence of nearly unavoidable surface contamination. The temperature and current pattern maintains itself until the bar has reached the deep end of the tank. The results for the cooling system are similar (see Appendix A).

2.4 Similitude to Lake

Comparing these results from the tank to field observations, there are several obvious similarities. A 'bar' moves from the shallow end or shore to the deep end or centre of the lake. A thermocline develops on the

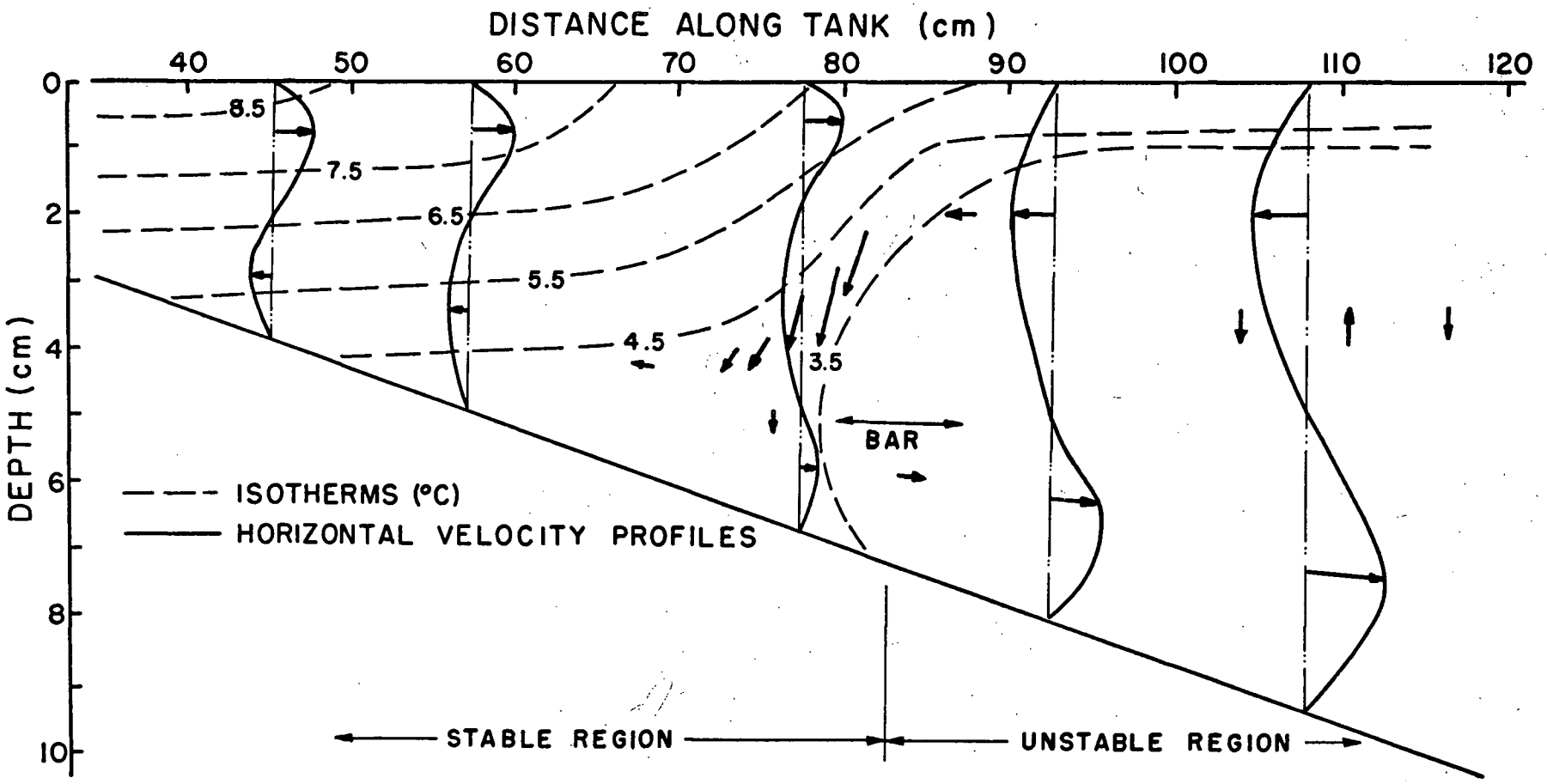

Figure 6. Generalized current and temperature results for the heated system. Averaged velocities are shown by arrows, their length indicating the motion observed in a minute (i.e., cm min^{-1}) in the same scales as used for the axes.

shallow side and the front edge is marked by water near 4°C. On the deep side a more uniform temperature region exists in both, indicating convection. The motion observed in the thermocline in the experiment has also been deduced from heat budget calculations for Lake Ontario (Rodgers, 1968). The sinking plume observed in the experiment in front of the thermocline would produce the convergence that has been suggested from the field observations. In the experiment there was no horizontal motion across the bar from the thermocline region to the deeper region. This agrees with the fact that the bar is observed to be a limnological barrier to offshore motion. The shallow thermocline which developed on the deep side in the experiment would not generally exist in lakes, due to wind mixing. Nevertheless under very stable, light wind conditions such a shallow thermocline has been observed on Lake Ontario (Elder and Lane, 1970). Also the surface velocities would not, of course, be expected to go to zero. Thus the tank experiment appears to represent a heat driven circulation similar to the thermal bar phenomenon observed in the Great Lakes.

2.5 Linear Model for the Speed of the Bar

A simple linear model based on the above results was used to evaluate the speed of the bar. The model assumes that horizontal advection and diffusion of heat are not of primary importance. This means that most of the heat entering the surface of a unit column remains within that column. The position of the bar is then at the transition from an unstable to a stable water column. The time taken for the bar to travel from a point A to a point B is the time taken to heat the column of unit area at point B up to 4°C. The model gives the speed of the bar, S, since

$$\text{time} = \frac{L}{S} = \frac{\text{change in heat content}}{Q},$$

as

$$S = \frac{Q\ L}{\Delta T\ \rho c_p\ D} \qquad (2.5.1)$$

where Q is heat flux through the surface in cal cm^{-2} sec^{-1};

L is the horizontal distance (in cm) between the bar and some deeper position where the mean temperature is known;

ΔT is the temperature difference (in C°) between 4°C and the mean temperature at the deeper position;

D is the depth of the water (in cm) at the deeper position where the mean temperature is known;

and ρc_p is the density of the water times its specific heat. To the accuracy of the experimental data this has a value of 1 cal $C°^{-1}cm^{-3}$.

Thus if the mean temperature at some position in the convective region is known, together with the heat input, the arrival time of the bar can be calculated.

The above formula was compared to actual speeds observed in the experiments and its dependence on the three variables D/L, Q, and ΔT was examined. Each of these was varied in turn. The data used in the formula were the depth at the deep end of the tank, the temperature at the deep end, usually when the bar was about 30 cm from the shallow end, and the distance from this position of the bar to the deep end. Figure 7 shows a comparison of the actual and predicted speeds for a heat flux of approximately 9×10^{-3} cal cm^{-2} sec^{-1} and three different slopes: $2\frac{1}{2}°$, 5°, $7\frac{1}{2}°$. The poorer observational data from the $2\frac{1}{2}°$ slope resulted from the longer time required before the bar properly developed; there tended to be a lack of two-

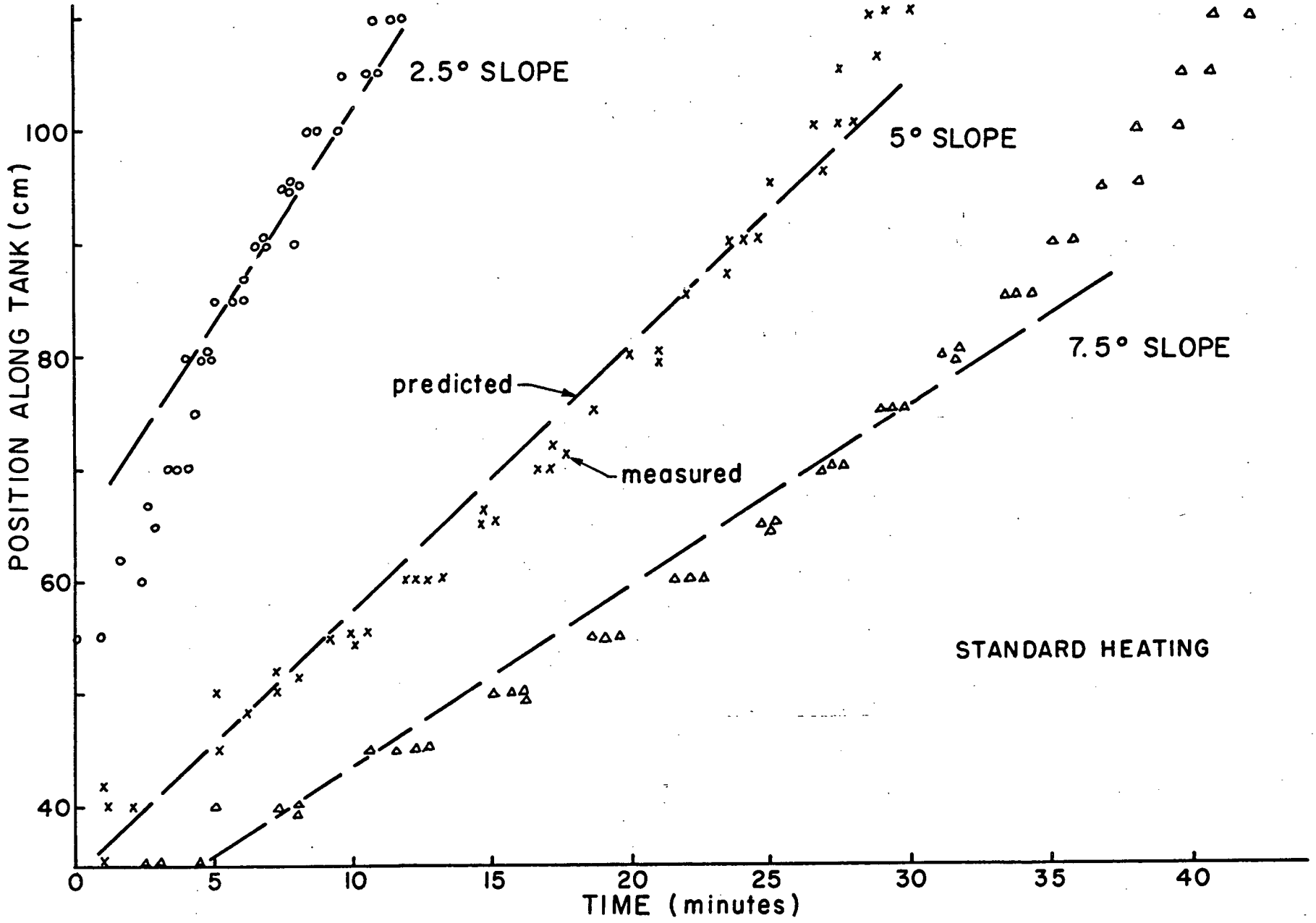

Figure 7. Position of the bar, measured and predicted, for standard heating and bottom slopes of 2.5°,5°, 7.5°. The SLOPE of these curves is BAR SPEED.

dimensionality and current structures often were not uniform across the tank. This prevented using slopes smaller than $2\frac{1}{2}°$. Figures 8 and 9 show a similar comparison for two different surface heat fluxes at slopes of 5° and $7\frac{1}{2}°$. Figure 10 is a comparison of speeds for different ΔT's. The predicted speeds compare well with the measured speeds in all cases. The increase in the speeds as the bar approaches the end of the tank seems to be due to an interaction with the shallow thermocline which has developed on the deep side by this time. The main thermocline is then able to develop faster by incorporating the partially warmed surface layer from the deep side and the region referred to as the bar becomes more diffuse.

The dashed curve, Figure 8, shows the speed of the bar that resulted when an insulated lid was put on the tank at the time indicated by the arrow; this shows the strong dependence of the speed on the surface heat input rather than on the horizontal density gradient or on other heat tranfers.

Temperature sections were used to calculate mean temperatures along the tank in order to compare with the temperatures predicted by the approximations leading to equation 2.5.1. Figure 11 is a temperature section through the bar for a 5° bottom slope and heat input of approximately 9×10^{-3} cal cm^{-2} sec^{-1}. The positions at which observations were made are designated by the vertical marks along the top line in the diagram. From this figure the mean temperature and change in heat content from the time the heat lamps were turned on are calculated and in the lower diagrams of Figure 11 are compared with values predicted by the model. As can be seen the model gives a good first approximation to the temperature or heat content along the tank. Differences from the predicted heat content may be accounted for by the presence of advective effects (see subsection 2.7).

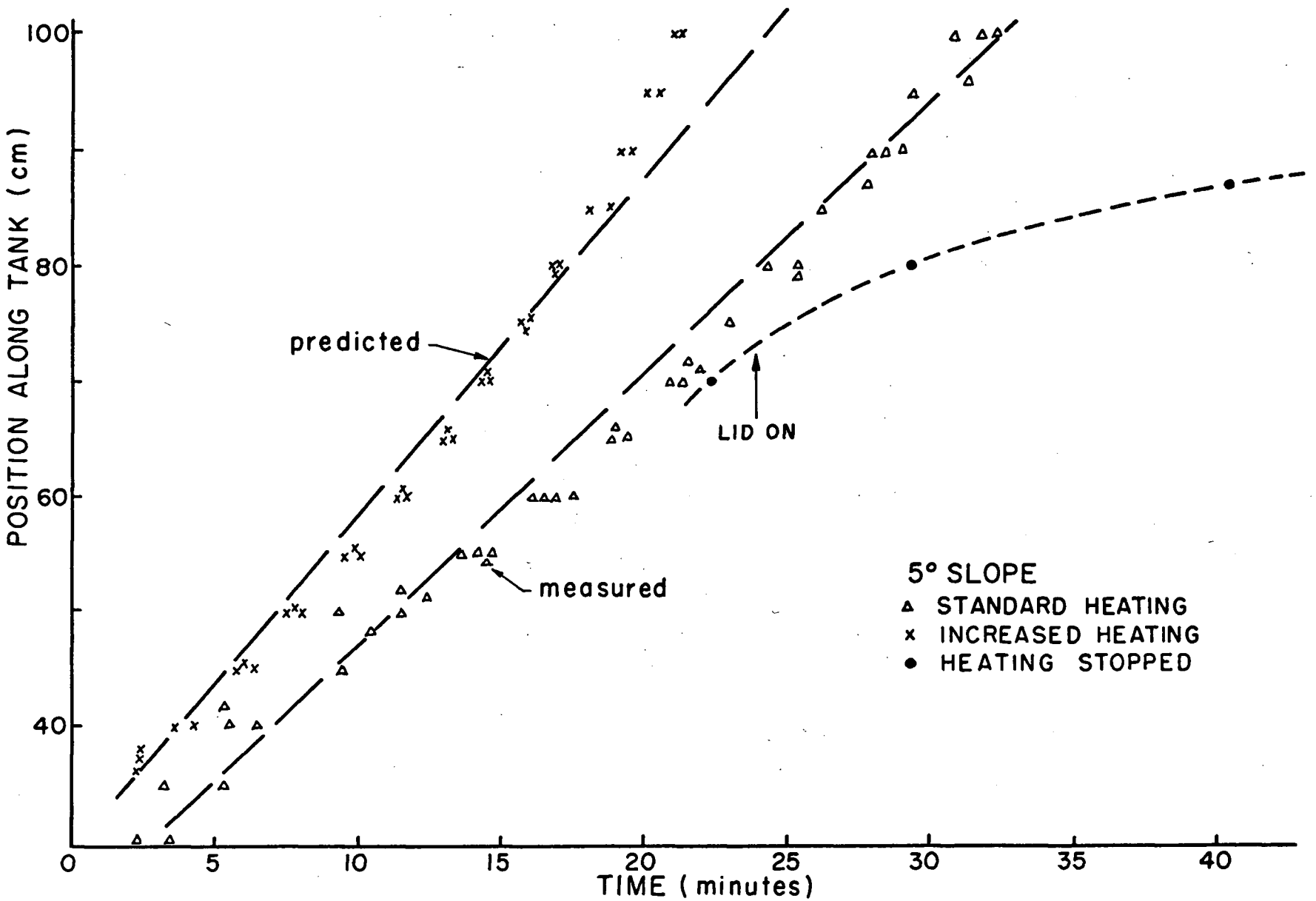

Figure 8. Position of the bar, measured and predicted, for 5° bottom slope and the two heating rates ($\sim 9 \times 10^{-3}$ and $\sim 12 \times 10^{-3}$ cal cm^{-2} sec^{-1}).
The SLOPE of these curves is BAR SPEED.

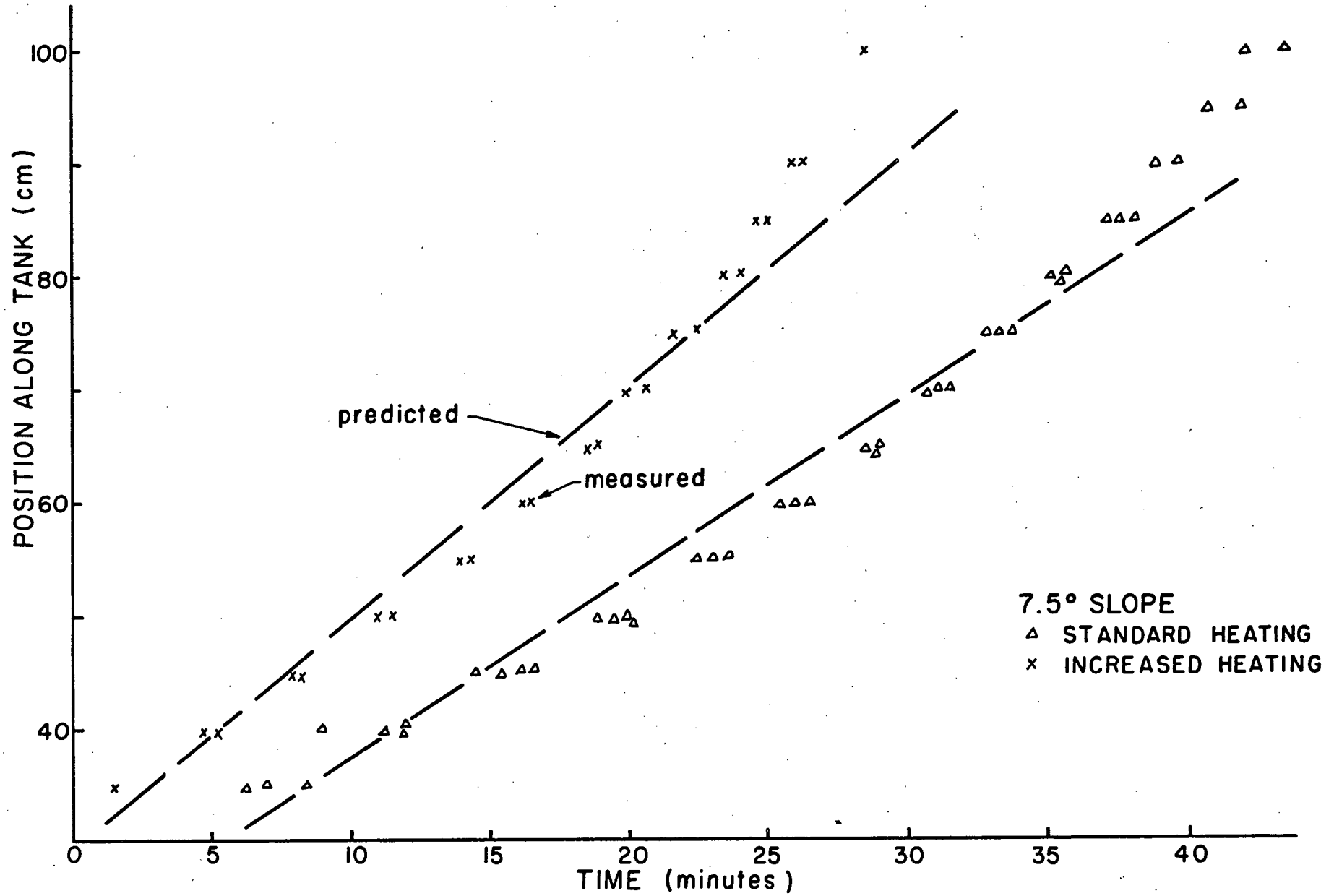

Figure 9. Position of the bar, measured and predicted, for 7.5° bottom slope and the two heating rates ($\sim 9 \times 10^{-3}$ and $\sim 12 \times 10^{-3}$ cal cm^{-2} sec^{-1}).
The SLOPE of these curves is BAR SPEED.

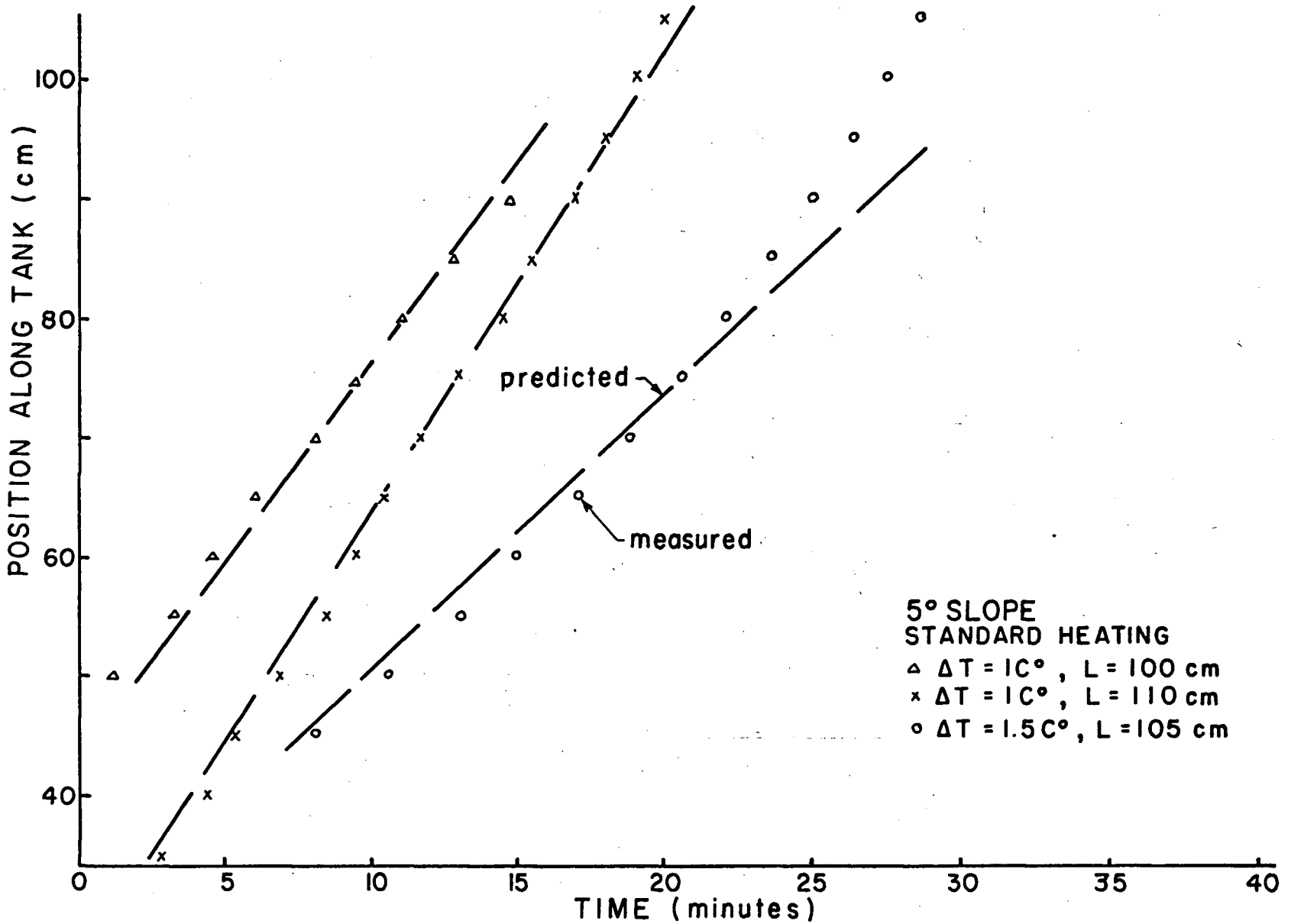

Figure 10. Position of the bar, measured and predicted, for 5° bottom slope, standard heating and different ΔT, L combinations.
The SLOPE of these curves is BAR SPEED.

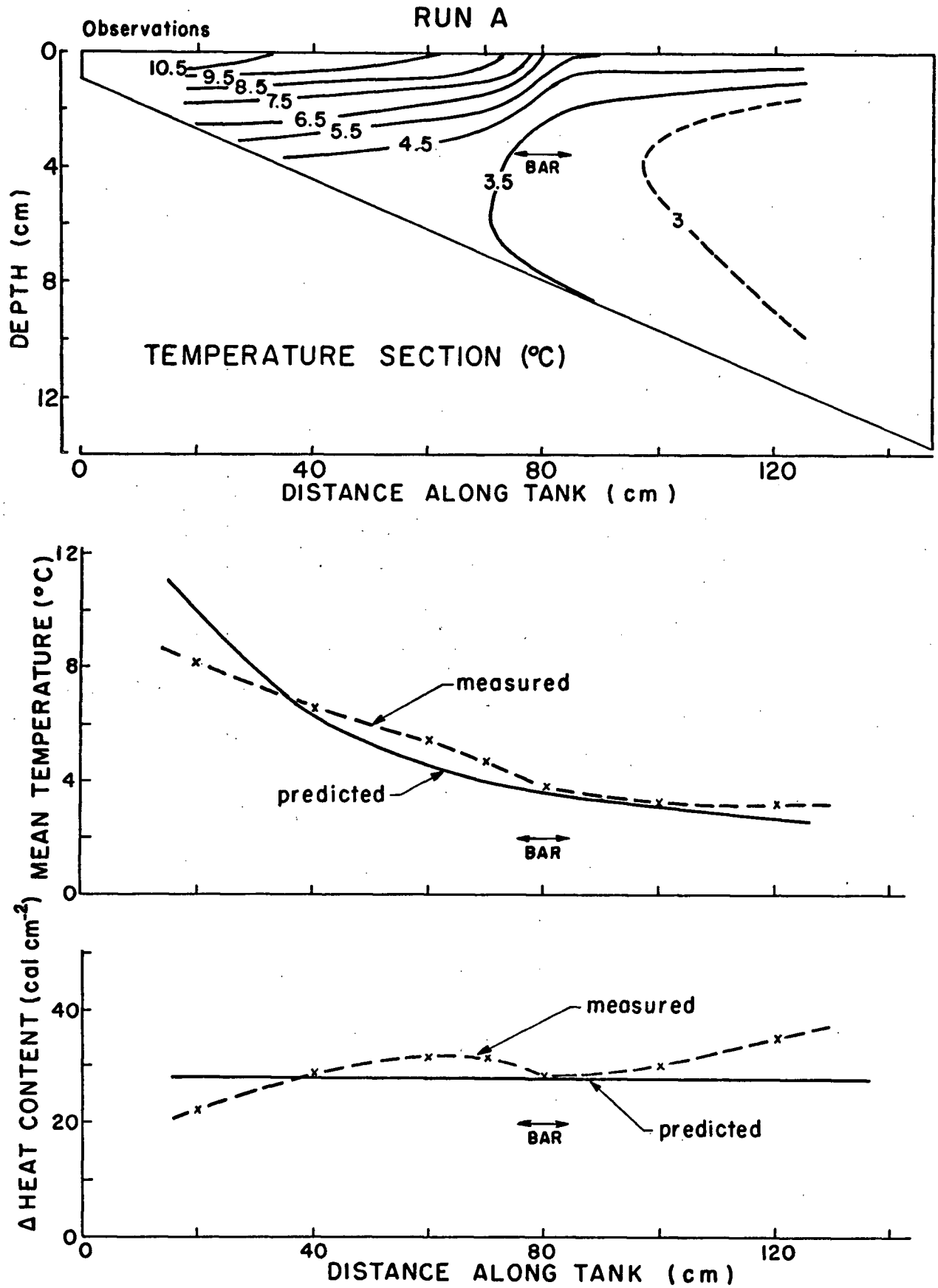

Figure 11. Temperature section, mean temperatures (vertically averaged), and changes in heat content for Run A: 5° bottom slope and standard heating. The initial temperature (Ti) when the heat lamps were turned on was 0.2°C.

Similar data from the other experiments are contained in Appendix B. The results at the different slopes and heating rates are similar to the above.

2.6 Comparison of the Linear Model to Lake Ontario

The model for the speed of the bar was also compared with data taken in Lake Ontario. The data used to make the comparison were taken from Rodgers (1965b, 1966a, 1968) and Rodgers and Anderson (1961). The net surface heat transfer is approximately uniform over the surface of the Lake, as assumed in the calculations. Using the temperature data from Rodgers (1966), the speed of the bar was calculated and compared to the value predicted by the model. Calculated values were 0.95 cm sec^{-1} (north shore) and 0.3 cm sec^{-1} (south shore). The predicted values were 0.7 and 0.4 respectively. The model also gave a reasonable approximation to the speed of the bar in Lake Michigan from the work of Church (1942). To make a closer check on the accuracy of the model, better data from the lakes are needed.

Values of the change in heat content in a unit column for a cross section through the thermal bar from Rodgers (1968) are plotted in Figure 12. Also shown, for comparison, is a plot of similar values for a tank experiment (from Figure 11). As seen from the figure the approximation of negligible advection of heat (uniform change in heat content) is not as good for the Lake as it is for the tank. However the distribution of heat is strikingly similar in both cases. The effect of advection is illustrated in more detail in Figure 13 which shows the cross section temperature anomalies for the tank and the Lake. The 'temperature anomaly' is the difference between the observed temperature and the mean temperature predicted from the heat flow through the surface, assuming no

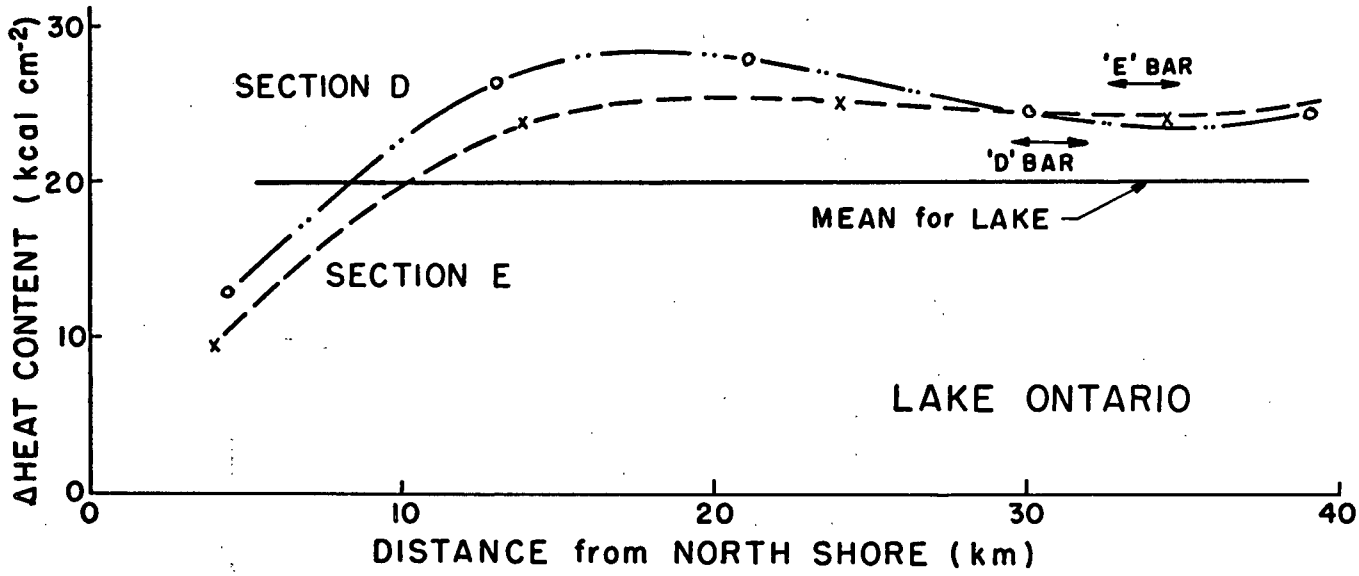

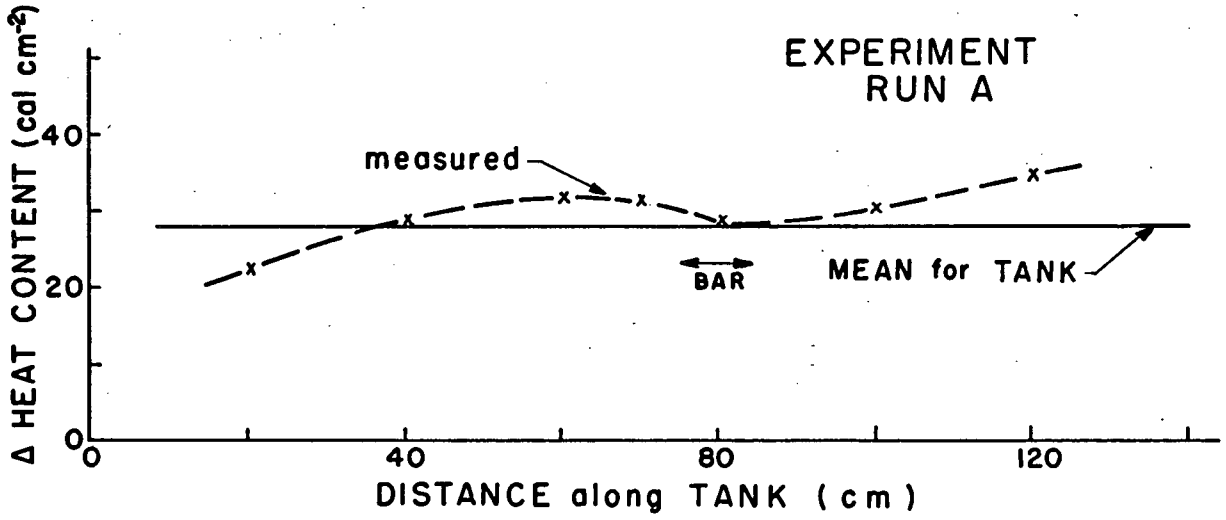

Figure 12. Changes in heat content for Lake Ontario (for sections shown in Figure 2, p.4). Also a similar plot for the tank for Run A.

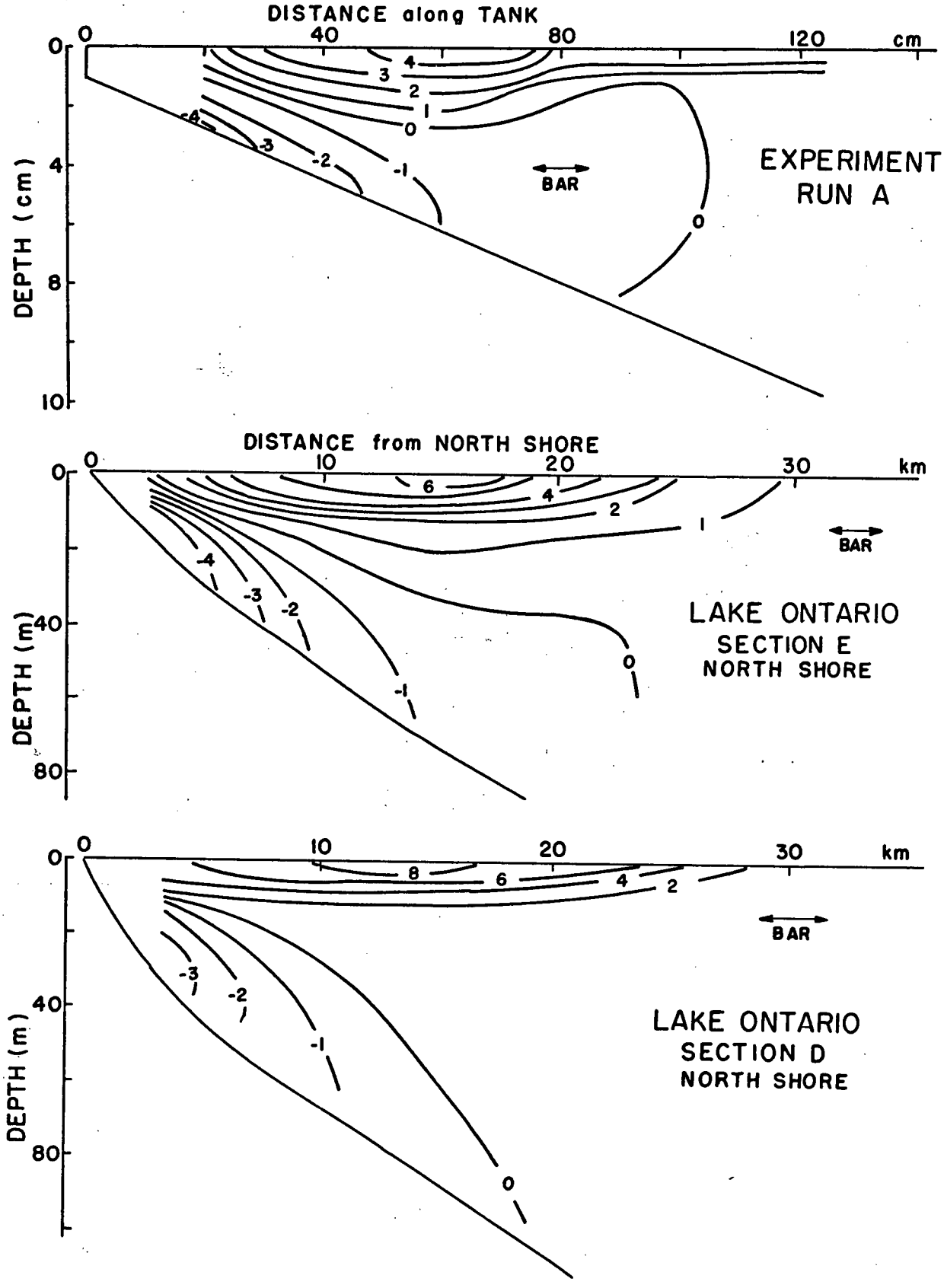

Figure 13. Temperature anomaly sections for the tank experiment (for Run A) and for Lake Ontario (for sections in Figure 2, p.4).

advection. As can be seen from the figure, the sections are similar. Therefore advective effects similar to those observed in the tank could occur in the Lake. Anomaly sections for the other experiments are shown in Appendix B.

2.6 Discussion

As has been shown a reasonable first approximation to the heat content of a water column and the speed of the bar for both the tank and Lake Ontario can be obtained from the assumption of negligible horizontal advection and diffusion. In both cases, in the deeper regions, most of the heat is carried by convective processes. These strong vertical convections inhibit horizontal advection and produce the basic features of the thermal bar.

A further refinement to the first approximation would require including the effects of horizontal advection. The importance of these effects is illustrated by the differences between the actual and predicted values seen in the Lake and in the tank. Three important advective regions exist (Figure 6, p.15). One is the advection of warm water towards the bar in the shallow end. This is a flow of the light, upper thermocline water replacing part of the sinking water at the bar. This results in advection of heat towards the bar for both the tank and the Lake. This flow is aided by the horizontal density gradient toward the bar, but for the tank this density gradient is not sufficient for the flow to cross the bar. There is a counter-flow beneath the above advection. This brings cold water to the shallow end from the vicinity of the bar; that is, heat flux of the

same sign. The other advective region is the downslope flow of 4° water from the vicinity of the bar toward the deep end. This advects heat to the deep regions. For the tank this flow was found to be weaker for smaller bottom slopes. Its effect was also reduced by turbulent mixing. Figure 12 (p.25) suggests that there was some heat advected towards the centre of Lake Ontario. However the importance of this flow in lakes is difficult to judge because of the smaller slope, the unknown nature of the convective mixing, and irregularities in the bottom. In spring, the net effect of advection is that the heat content is higher than would otherwise be expected in the central portions of the Lake and in the regions next to the bar, while regions near the shore have been depleted of heat. The advective velocities observed in the tank are all of the same order of magnitude as the speed of the bar.

The influence of bottom irregularities was tested in two experiments. In both a slope of 5° was used for half the tank, followed by a flat section in one and by a vertical drop of 12 cm to a flat section in the other. The main influence of bottom irregularity was on the speed of the bar; advection produced an averaging effect over the irregularities. The speed observed was roughly that which, from equation 2.5.1, would have been associated with a bottom slope that was the weighted average of the actual slopes. Otherwise the temperature and current structure were similar to the others. The results are given in Appendix C. Thus bottom irregularities do not seem to be of primary importance in the development of the thermal bar in lakes.

An important effect not studied in this experiment is wind mixing. In smaller lakes the resulting wind driven horizontal advections would

likely keep the temperature uniform and not permit a bar to develop. A trip was made to the Merritt region of British Columbia to see if the bar could be found in smaller lakes, however they were found to be too thoroughly wind mixed. In the larger lakes where the thermal bar develops, this wind induced advection might result in mixing across the bar. If this brings water below 4°C adjacent to water above 4°C, more active convection would be expected which would include water from the warmer side. An experiment that brought together 8°C water and 2°C water, by removing a barrier separating the two, produced convection at a stationary mixing zone (see Appendix D). This indicated that mixing across the bar would immediately produce convection but would not dissipate the bar.

Further experimental studies on the thermal bar should await more detailed observations of this phenomenon in lakes. Information on the current structure is particularly necessary.

2.8 Summary

In this laboratory study, a temperature structure has been produced which is similar to that associated with the thermal bar in lakes. The existence of my 'bar' in the tank depends entirely on the temperature dependence of the density and on the presence of heat flux and a sloping bottom. A simple model for the speed of the bar, which also applies to the bar in the lakes, is based on horizontal heat advection and diffusion not being of primary importance. The success of this model indicates that effects of wind mixing, Coriolis force, etc., which exist for lakes but not in the model, are not important factors in the formation of the 'thermal bar'.

3. MATHEMATICAL MODELS

These theoretical studies are an attempt to explain more quantitatively the details of the temperature and velocity fields observed in the laboratory studies and to understand the dynamic balance of the flow. The results may then be tentatively extended to describe the situation in lakes.

3.1 The Temperature Field

From the two-dimensional laboratory model reasonable first approximations to the heat content and to the speed of the bar were obtained by assuming that horizontal advection and diffusion of heat were not of primary importance. This suggests that the temperature distribution may be derived from the one-dimensional heat diffusion equation:

$$\frac{\partial T}{\partial t} = \kappa \frac{\partial^2 T}{\partial z^2} \tag{3.1.1}$$

where z is taken vertically upwards,

t is the time,

T is the temperature in °C,

and κ is the thermal diffusivity

with boundary conditions

$$\kappa \frac{\partial T}{\partial z} = q \qquad \text{at } z = 0 \quad \text{(top)} \tag{3.1.2}$$

$$= 0 \qquad \text{at } z = -D \quad \text{(bottom)} \tag{3.1.3}$$

where q is the heat flux through the surface in C° cm sec^{-1} (= $Q/\rho c_p$, equation 2.5.1, p.17). D = αx where α is the slope of the bottom and x is the distance along the tank from the shallow end. (This assumes that D = 0 at the shallow end, equivalent to a shore). Finally, T = 4°C at z = 0 at the 'bar'.

Since when one is discussing the thermal bar all temperatures are relative to the temperature of maximum density of fresh water, the equation and boundary conditions can be rewritten:

$$\frac{\partial \theta}{\partial t} = \kappa \frac{\partial^2 \theta}{\partial z^2} \qquad (3.1.4)$$

at z = 0 $\qquad \kappa \frac{\partial \theta}{\partial z} = q \qquad (3.1.5)$

at z = -D $\qquad \frac{\partial \theta}{\partial z} = 0 \qquad (3.1.6)$

at z = 0, at the 'bar', $\qquad \theta = 0 \qquad (3.1.7)$

where $\theta = T - 4°C$.

From the laboratory work the temperature field may be considered in two regions, on either side of the bar: a deeper, highly convective region and a shallower, stable region. For the purposes of the theoretical work, the bar will be defined by the 4° surface isotherm as is done in lake studies.

i) The deep, convective side

The aim here is to provide a rough, but reasonable, approximation to the temperature field on the unstable side of the bar. No attempt

will be made to consider convective effects in detail, nor to model the shallow thermocline that develops over this end in the latter stages of the bar in the tank and occasionally forms on Lake Ontario. Instead my reasoning will be based on the observation that the temperature in the deeper region of both tank and lake tends to be nearly uniform vertically, implying a thorough mixing process and hence a high vertical eddy (or convective) diffusivity. Integrating equation 3.1.4 vertically from $z = -D$ to $z = 0$ one obtains

$$D \frac{\partial \theta}{\partial t} \simeq \kappa \frac{\partial \theta}{\partial z} \Big|_{-D}^{0} \qquad (3.1.8)$$

and using the z boundary conditions:

$$\frac{\partial \theta}{\partial t} = \frac{q}{D}$$

or $$\theta = -\theta_o + \frac{qt}{D}$$

where $-\theta_o$ is the temperature in C° at $t = 0$. Using the simple model for the speed of the bar (equation 2.5.1, p.17)

$$S = \frac{q\,x}{\theta_o D} \qquad (2.5.1)$$

where $\theta_o = \Delta T$, the temperature difference, in this case between the shallow end and a position x along the tank, at time $t = 0$ and choosing the origin of time to be when the 'bar' is 'at' $x = 0$, the temperature

for the deeper region can be written:

$$\theta = \theta_o \left(\frac{St}{x} - 1 \right) \qquad (3.1.9)$$

This could have been written empirically from the observational data.

If $t = 0$ is defined, as above, as the time when the 'bar' is 'at' $x = 0$, then θ_o is clearly a function of x, the distance down the tank. The assumption is made that at some time $-t_i$, before heating begins, the entire fluid is at a uniform temperature; this is obviously true for the tank experiments, and roughly valid for the lakes. If heating is uniform over the surface of the water, if the bottom has a constant slope, and if the assumption is made that horizontal advection and diffusion of heat are not of primary importance, then the temperature at any time until the bar appears will be a linear function of x. Thus at $t = 0$ one can write

$$-\theta_o = -\frac{\Theta x}{X}$$

where Θ is the temperature at position X and X is the length of the tank or the distance from the shore to the deeper portions of a lake.

Thus equation 3.1.9 may be rewritten as

$$\theta = \frac{\Theta}{X} (St - x) \qquad \text{for } x > St \qquad (3.1.10)$$

ii) The shallow, stable side

The temperature field on this side of the bar is clearly more complicated than on the deeper side. Since it is desirable to match the two regions, the boundary condition at the 'bar' (equation 3.1.7) will be rewritten as

$$\theta = 0 \qquad \text{at } t = \frac{x}{S} , \tag{3.1.11}$$

where the origin of x is at the shallow end and the origin of time is defined as when the 'bar' is 'at' x = 0.

The solution to

$$\frac{\partial \theta}{\partial t} = \kappa \frac{\partial^2 \theta}{\partial z^2} \tag{3.1.4}$$

for a semi-infinite body with boundary conditions

$$\text{at } z = 0 \qquad \kappa \frac{\partial \theta}{\partial z} = q \tag{3.1.5}$$

and 3.1.11 is

$$\theta = \frac{2q}{\sqrt{\kappa}} \sqrt{t - \frac{x}{S}} \; \text{ierfc} \left(\frac{-z}{2\sqrt{\kappa(t - \frac{x}{S})}} \right) \qquad x < St \tag{3.1.12}$$

If an error in the bottom boundary condition (3.1.6) is 'tolerated'

up to a heat flux that is 20% of the surface heat flux, then the above represents the temperature to within 20 cm of the shallow end of the tank for a 5° bottom slope. This 'error' in bottom heat flux is likely not more than the error involved in neglecting horizontal advection of heat in the shallow end.

An attempt to consider the diffusion equation for a wedge (see Arlinger, 1965) would not improve the temperature solution as the bottom effects tend to make the shallower portions more uniform in temperature vertically. This is not the case in the observations.

Neglecting the bottom heat flux in this manner is equivalent to removing some of the heat input in the shallower portions and thus approximates the advective effects observed in this region.

In order to calculate actual values from this mathematical model it is necessary to choose a value for κ. Since the motion appears to be laminar in the tank, κ ought to have the value of molecular thermal diffusivity, 1.4×10^{-3} cm^2 sec^{-1}. However, in assuming that all the heating occurred at the surface, the penetrative effects of the surface heating (see Figure 5, p.13) have been neglected. These are included roughly in the above model by increasing κ.

iii) Comparison with the tank

The temperature model developed above is

$$\theta = \frac{2q}{\sqrt{\kappa}} \sqrt{t - \frac{x}{S}} \; \text{ierfc}\left(\frac{-z}{2\sqrt{\kappa(t - \frac{x}{S})}}\right) \qquad x < St$$

$$\theta = \frac{\Theta}{X}(St - x) \qquad x > St \qquad (3.1.13)$$

To compare this to the measured temperature field the position of the bar had to be set. In the generalized temperature field shown in Figure 6 (p.15), extending the 4° isotherm to the surface shows the 'bar' at 90 cm. This defines the value of t as 90 times S, the speed of the bar. The value for the speed of the bar is taken to be the average value observed in the tank; that is, 3.9×10^{-2} cm sec^{-1}. q is taken to be the standard heating rate of 9×10^{-3} C° cm sec^{-1} (assuming $\rho c_p \simeq 1$ cal $C^{\circ -1} cm^{-3}$). The value of Θ is obtained using the formula for the speed of the bar (2.5.1), the average observed value of S, the standard value for q, the length of the tank, and the depth at the end of the tank; this gives a value of 2.6 C°. It remains to determine a value of κ; a reasonable fit for the temperature cross-section was found using a value for κ of 5.8×10^{-3} cm^{-2} sec^{-1}, see Figures 14 and 6(p.15). This reasonable fit with the tank results together with general similarity with the lake suggests the temperature model is good for the lake too. This will be discussed in more detail at the end of the theoretical section (see subsection 3.4).

In order to further check on the degree to which the model matched the general picture in the tank, θ was plottted against distance down the tank at fixed values of depth for both the tank and the mathematical model (see Figure 15). In order to make the plot for the tank the 4.5 and 3.5°C isotherms were extended to intersect with the surface rather than form a shallow thermocline over the deeper region. The reason for the interest in the θ versus x plot will become apparent when the vorticity equation is considered in the next subsection. As

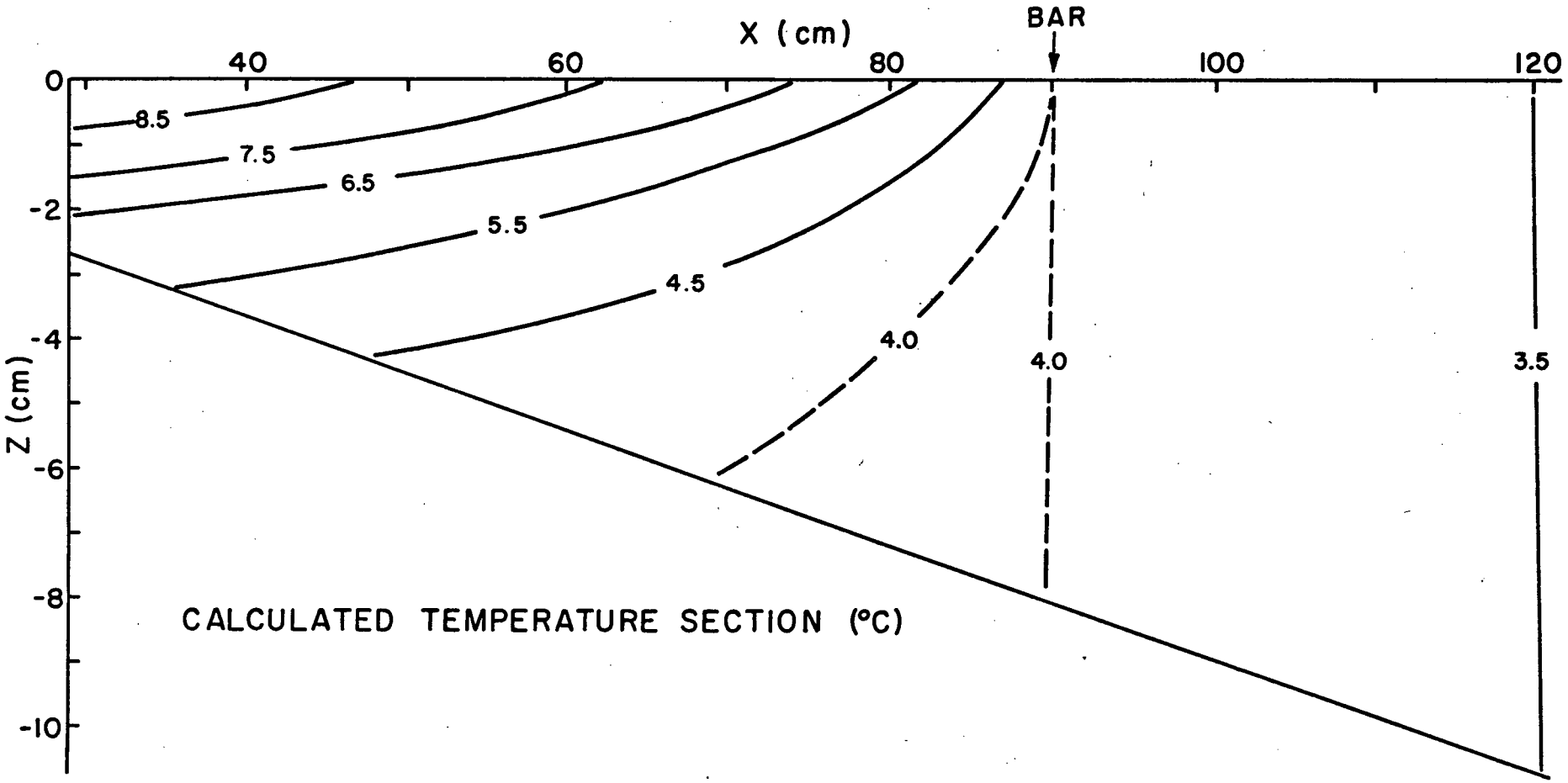

Figure 14. Temperature section (°C) calculated from equations 3.1.13.

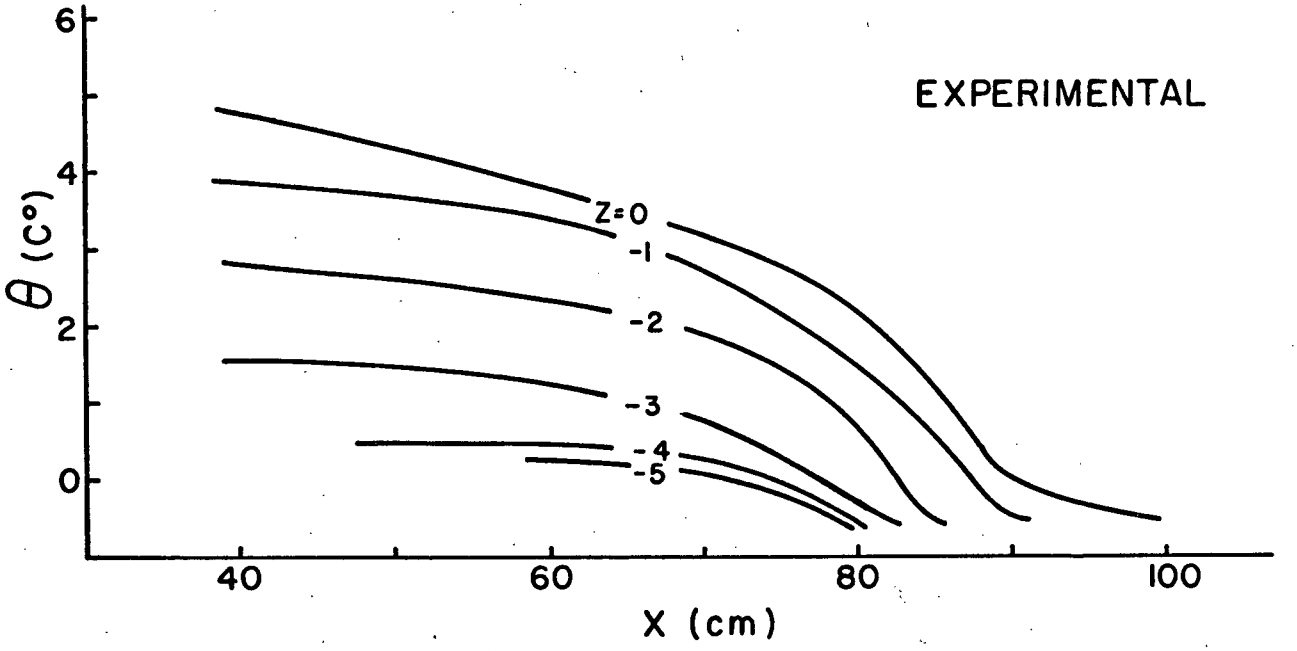

(a)

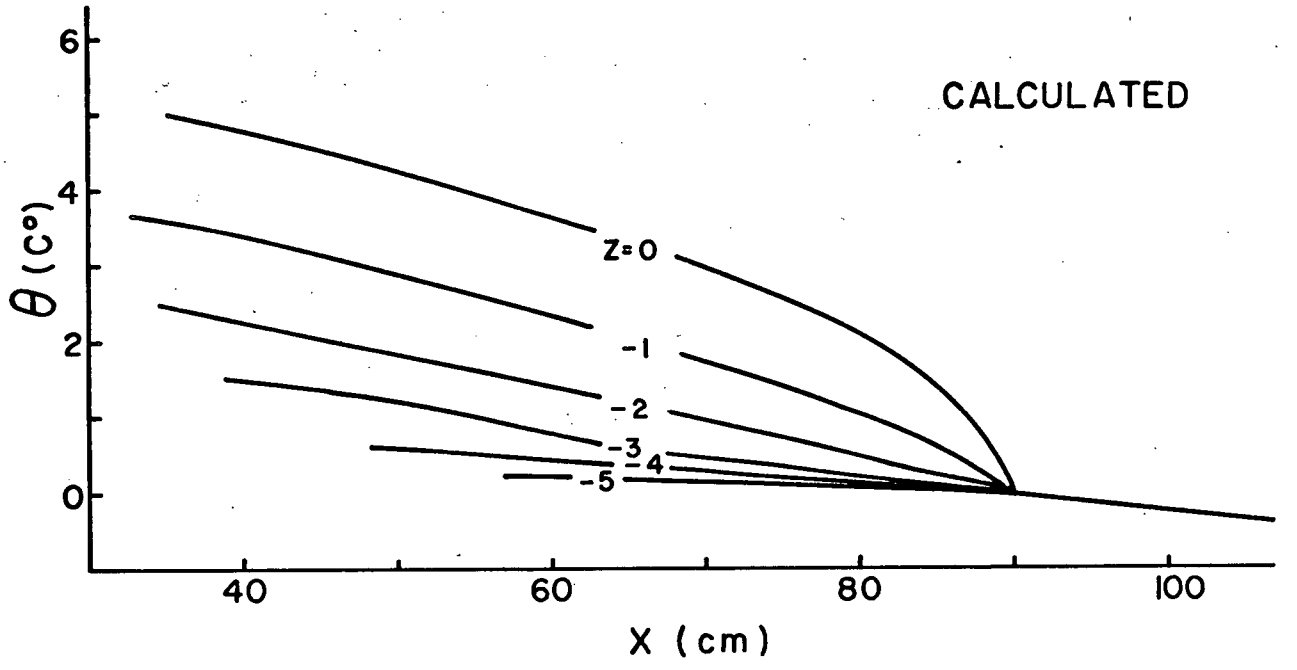

(b)

Figure 15. θ in C° against distance along the tank for fixed values of z (in cm).
(a) generalized measured values
(b) calculated from equations 3.1.13

can be seen the curves are similar.

3.2 The Velocity Field

The velocity field is most readily investigated through the vorticity equation:

$$\frac{\partial \underset{\sim}{\omega}}{\partial t} - \nabla \times (\underset{\sim}{v} \times \underset{\sim}{\omega}) = \frac{1}{\rho^2} (\nabla\rho \times \nabla p) - \nu \nabla \times (\nabla \times \underset{\sim}{\omega}) \qquad (3.2.1)$$

where $\underset{\sim}{\omega}$ is the vorticity vector, $\underset{\sim}{v}$ is the velocity vector, ρ is the density, p is the pressure, and ν is the viscosity.

Assuming two-dimensional flow, neglecting non-linear advective effects and making the hydrostatic approximation for pressure, equation 3.2.1 reduces to

$$\frac{\partial \omega_2}{\partial t} = \frac{g}{\rho} \frac{\partial \rho}{\partial x} + \nu \nabla^2 \omega_2 \qquad (3.2.2)$$

where g is the value of the acceleration due to gravity,

$$\nabla^2 = \frac{\partial^2}{\partial x^2} + \frac{\partial^2}{\partial z^2}$$

and $\omega_2 = \frac{\partial u}{\partial z} - \frac{\partial w}{\partial x}$ where u and w are the x and z velocity components respectively.

Introducing a stream function, ϕ, where

$$u = \frac{\partial \phi}{\partial z}, \qquad w = -\frac{\partial \phi}{\partial x},$$

equation 3.2.2 may be rewritten

$$\frac{\partial}{\partial t} \nabla^2 \phi = \frac{g}{\rho} \frac{\partial \rho}{\partial x} + \nu \nabla^4 \phi \qquad (3.2.3)$$

where $\nabla^4 = \nabla^2 . \nabla^2$. The first term in equation 3.2.3 is the time rate of change of the vorticity and the last term represents effects of viscous diffusion. However the first term on the right hand side, the buoyancy term is not so familiar and perhaps needs further discussion.

Recalling that the buoyancy term in vector notation is $\frac{1}{\rho^2} \nabla\rho \times \nabla p$, it is evident that pressure forces are being considered. In the presence of gravity, a horizontal change in density results in a horizontal pressure gradient which tends to produce a flow down the density gradient.

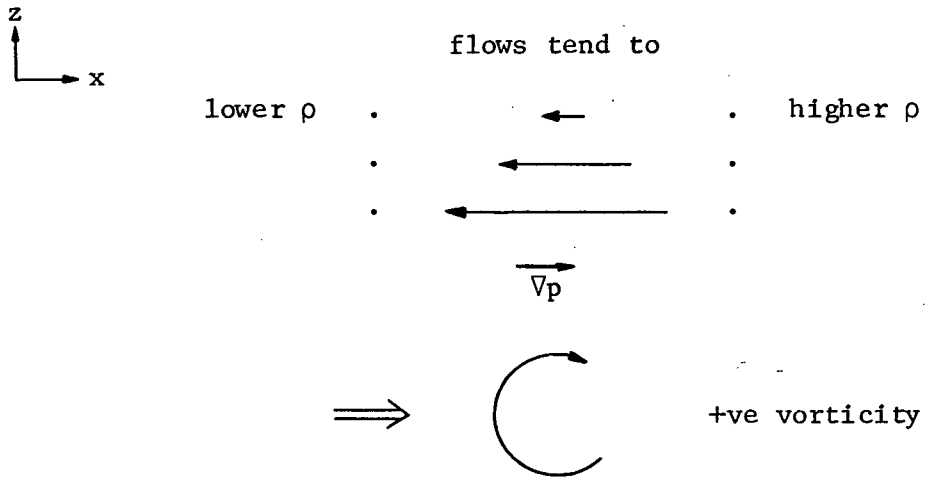

The effect of the buoyancy term

If an horizontal density gradient of the same sign occurs at all depths in a fluid, the pressure gradients at the bottom will be larger than those nearer the surface due to the strong vertical density gradient

($-\rho g$ under the hydrostatic approximation, valid for the tank and lake).

In the tank gradients in the directions shown above are set up on the shallow side due to the effects of surface heating. Flow towards the shallow end results in a slight surface slope downwards towards the bar which is sufficient to produce the flow in the positive x-direction in the upper regions of the tank.

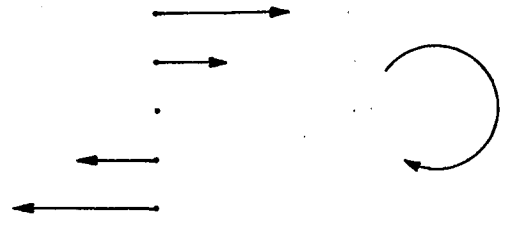

In the deeper end the density gradients are reversed, resulting in flows in the opposite directions (and vorticity of the opposite sign).

Because of viscosity a shear develops which opposes the flow, producing vorticity of the opposite sign to that produced by the buoyancy term. This occurs mainly on the boundaries of the tank although the interior contribution, for the low Reynolds number flow considered, is also important.

Consider the operator $\nabla^4 = \partial_z^4 + 2\partial_x^2\partial_z^2 + \partial_x^4$ in equation 3.2.3. Since the vertical shears greatly exceed horizontal shears almost everywhere in the tank (with the main exception of side walls and the region of the bar itself), I neglect the last two terms of ∇^4 and approximate equation 3.2.3 by

$$\frac{\partial}{\partial t}\frac{\partial^2\phi}{\partial z^2} = \frac{g}{\rho}\frac{\partial \rho}{\partial x} + \nu\frac{\partial^4\phi}{\partial z^4} \qquad (3.2.4)$$

Because the flow changes only slowly, it appears that the buoyancy term and the viscous term roughly balance each other. Thus equation 3.2.4 may be approximated, at least heuristically, by

$$\frac{\partial^4\phi}{\partial z^4} = -\frac{g}{\nu\,\rho}\frac{\partial \rho}{\partial x} \qquad (3.2.5)$$

Given a density field, $\rho(t,x,z)$ and appropriate boundary conditions, equation 3.2.5 may be solved for the stream function and hence for the flow pattern of this model.

The density of fresh water in the region of its maximum density may be expressed as

$$\rho = \rho_o (1 - A\,\theta^2) \qquad (3.2.6)$$

where ρ_o is the density in gm cm^{-3} at 4°C and $A \simeq 8 \times 10^{-6}$ $C^{\circ -2}$. Substituting 3.2.6 into equation 3.2.5 gives

$$\frac{\partial^4\phi}{\partial z^4} = \frac{2gA}{\nu}\,\theta\frac{\partial \theta}{\partial x} \qquad (3.2.7)$$

where I have used $\rho \simeq \rho_o$ when not differentiated.

The boundary conditions are simply that u and w vanish at the top and the bottom (recalling the effect of surface contamination):

$$\text{at } z = 0, \quad u = 0 \quad \text{and} \quad w = 0$$
$$\text{and} \quad \text{at } z = -D, \quad u = 0 \quad \text{and} \quad w = 0 \qquad (3.2.8)$$
(bottom)

where $D = \alpha x$ where α is the slope of the bottom.

Specifying a suitable temperature field is not such a simple matter. Obviously equation 3.2.7 cannot be used with a temperature field given separately for the two sides of the bar as it would not be possible to match the displacements and stresses across the bar. The temperature field 3.1.13 suggested previously (p.35) is thus not only awkward, due to the presence of the error function, but unmanageable for integration of equation 3.2.7 throughout the model.

The solution will be quite sensitive to the chosen temperature field, as may be seen from the presence of the product of θ and θ_x in what is essentially the forcing term (see equation 3.2.7). Thus much care and trial was necessary to find for the temperature field a reasonable compromise which would be both readily integrable and a reasonable representation of the experimental results. Looking at the plots (Figure 15, p.38) of θ versus x for the tank and for the temperature field as given by equations 3.1.13 suggests the use of hyperbolic tangent functions. The compromise which finally produced a reasonable fit to the velocity field for the bar at the position shown in the generalized observations (Figure 6, p.15) (that is,

at 90 cm and a 5° bottom slope) is

$$\theta \simeq \{[\, 1 + \tanh(0.392[\, \frac{St-x}{10} - 2\,])](2.9)(1 + 0.2z + 0.01z^2) - 1\} \quad (3.2.9)$$

in C°. This is plotted in cross-section in °C and as θ versus x at constant z's in Figure 16. As can be seen this produces a reasonable approximation to both the observed (Figure 6, p.15 and Figure 15, p.38) and the calculated (Figure 14, p.37, and Figure 15, p.38) temperature fields.

The analytical temperature field, equation 3.2.9, was then used in equation 3.2.7 and the stream function and the velocity field were calculated(see Appendix E). The resulting velocity field is shown in Figures 17 a and b. As in Figure 6 (p.15) the lengths of the arrows indicate motion expected in a minute (i.e. cm min^{-1}) in the same scales as used for the axes. Comparison of Figures 17a and 6 shows close agreement between the two. Again in Figures 17 the temperature field has been included (dashed lines). The velocities are all in the correct directions and the change in direction of the flows along the tank occurs slightly behind the surface 4°C isotherm as was suggested by the laboratory model studies. The largest downward velocities occur in the region of maximum density as was observed in the tank. In general the velocities are of the same magnitude as those observed.

The differences between the calculated and observed velocity fields can be explained first in terms of the inadequacies of the hyperbolic tangent temperature approximation. The magnitude of the calculated

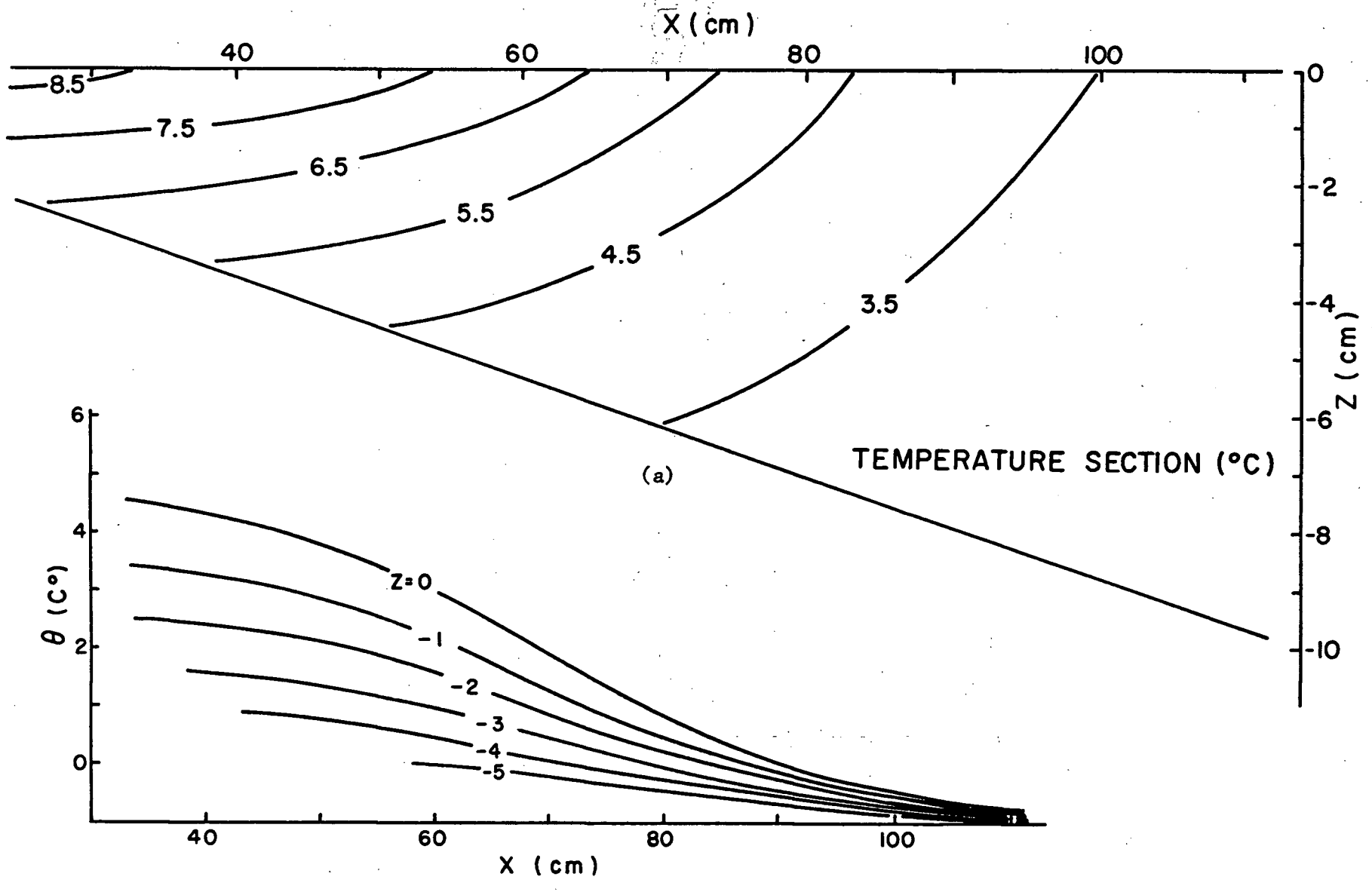

Figure 16. Analytical temperature approximation, equation 3.2.9, used for the velocity calculations:
(a) cross-section (T in °C)
(b) θ in C° against x in cm for fixed values of z (in cm)

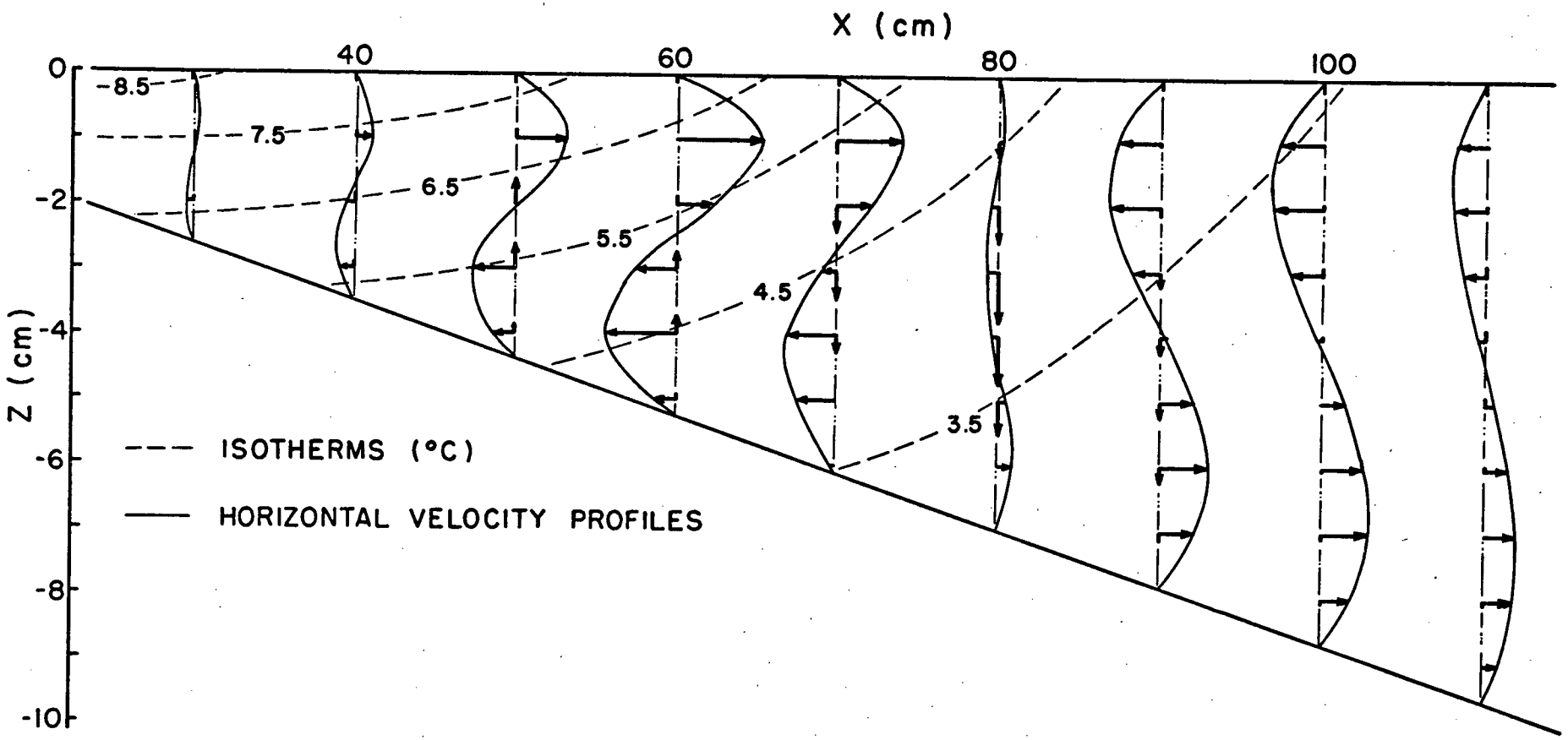

Figure 17a. Calculated velocity field. Velocities are shown by arrows, their length indicating the motion in a minute (i.e. cm min^{-1}) in the same scales as used for the axes. The analytical temperature field used is shown by dashed lines (°C). The solid curves are the horizontal velocity profiles. Compare with Figure 6 (p.15).

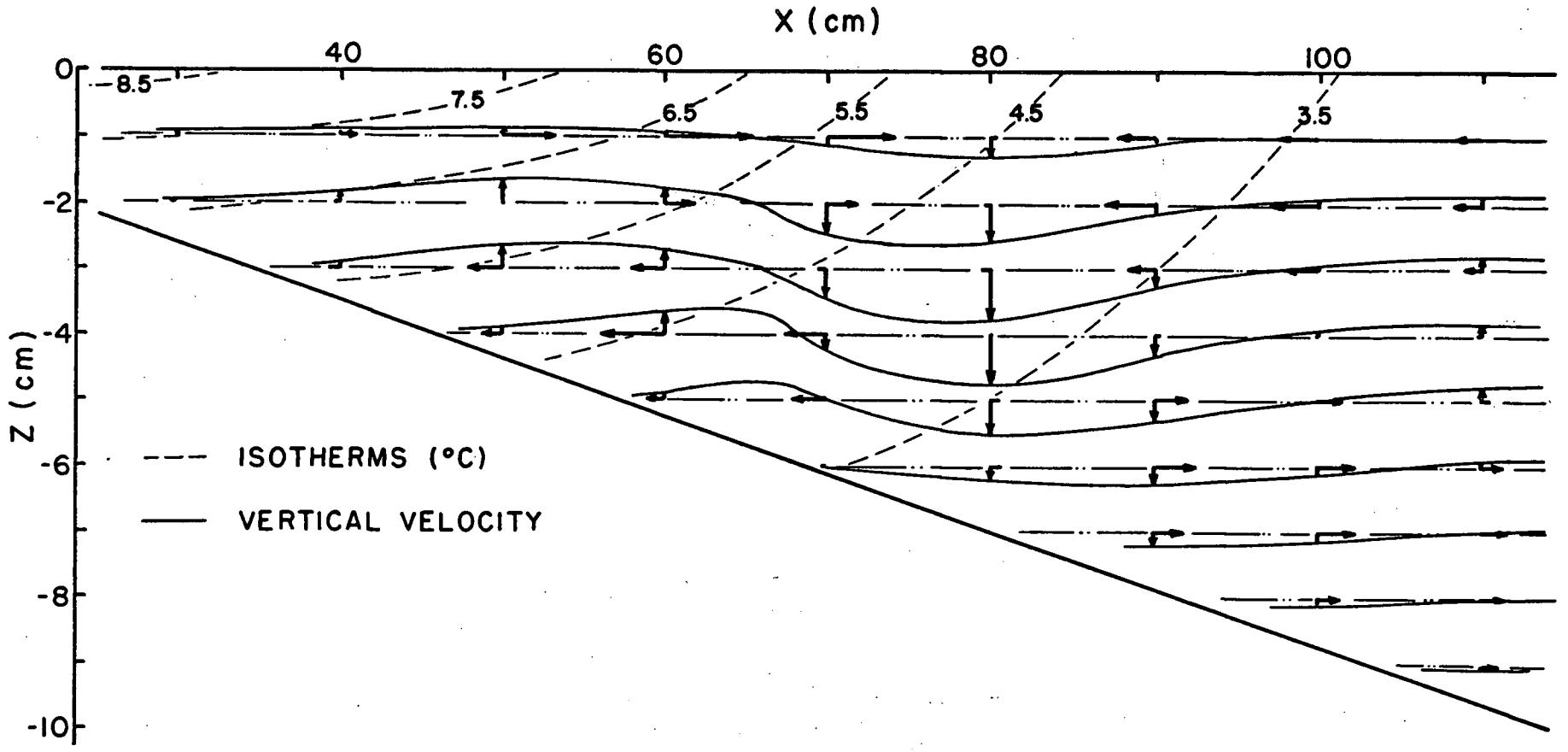

Figure 17b. Calculated velocity field. Velocities are shown by arrows, their length indicating the motion in a minute (i.e. cm min^{-1}) in the same scales as used for the axes. The analytical temperature field used is shown by dashed lines (°C). The solid curves are for the vertical velocity.

velocities drops off at the extrema of the plot since the hyperbolic tangent approximation attains maximum and minimum values before the ends of the tank are reached, whereas the observed temperatures did not. The velocities between 50 and 70 centimeters along the tank are up to twice as large as those shown in the generalized velocity field (Figure 6, p.15). This can be attributed to the fact that $\partial\theta/\partial x$ is larger than that for the hyperbolic tangent temperature model in this region. An even closer match to the observed generalized velocity field could probably be made by using a more involved temperature field, however there is little point in such a tedious endeavour in that the temperature fields observed in the tank do vary between runs (see Figure 18) and the associated velocity fields would hence also vary somewhat from the average values shown in Figure 6 (p.15). Also the observed temperature sections are not an instantaneous measurement but rather the temperatures were taken in sequence from the deep end to the shallow end during which time the bar progressed about 10 cm. Variations in the temperature field similar to those found in the tank have been observed for the bar in Lake Ontario (Rodgers, 1968).

It ought to be noted that a different hyperbolic tangent approximation will need to be made for any other position of the bar that is not within about 10 cm of the position chosen for the calculation. This is due to the fact that the temperature field changes with time, particularly in magnitude. Such approximations could be based on the temperature field predicted by the mathematical model (equations 3.1.13).

The stream function ϕ is plotted in Figure 19. There is no net transport across any vertical section of the tank, so that ϕ can be set

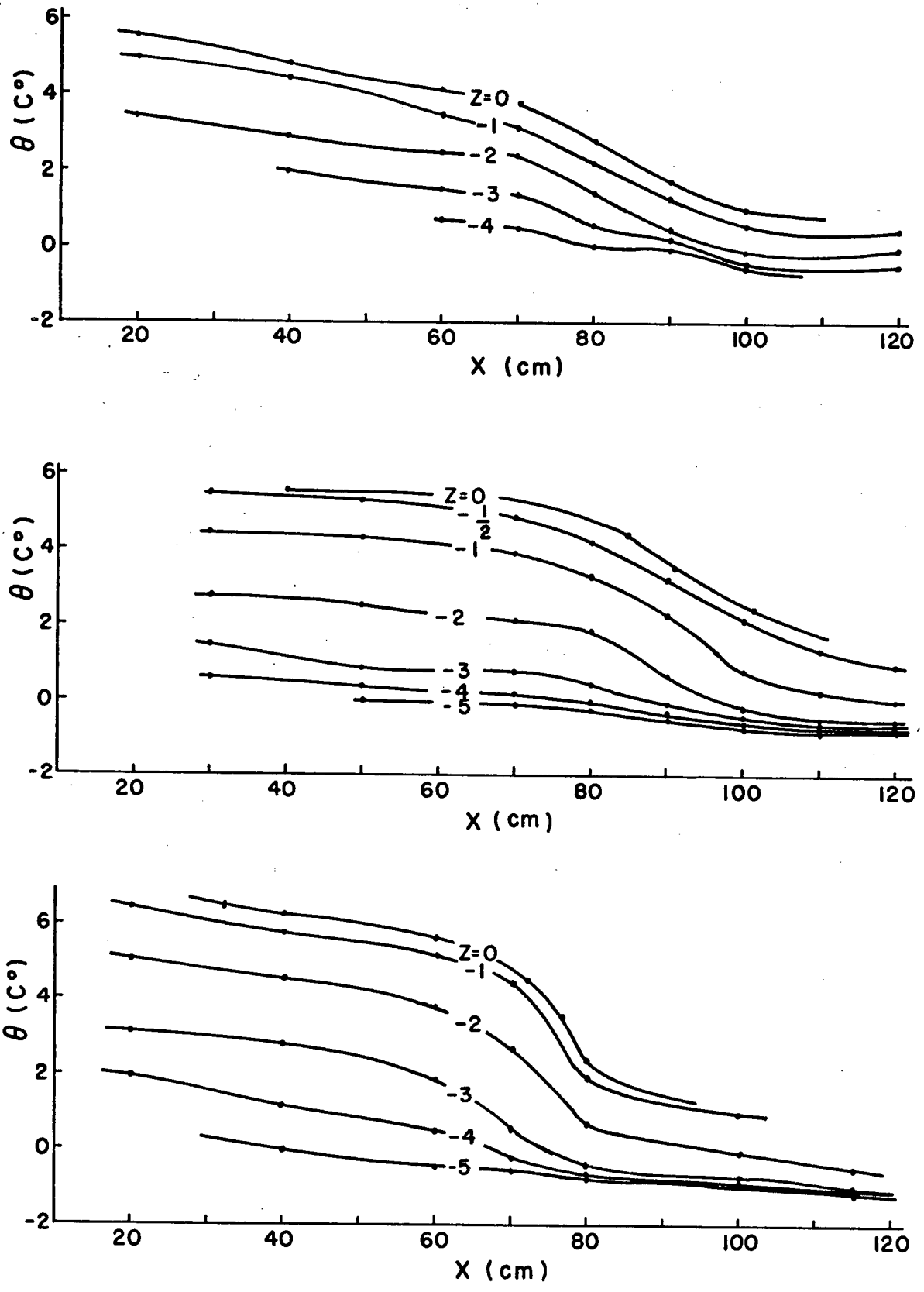

Figure 18. Actual θ (in C°) against distance along tank (x, in cm) plotted from laboratory observations.

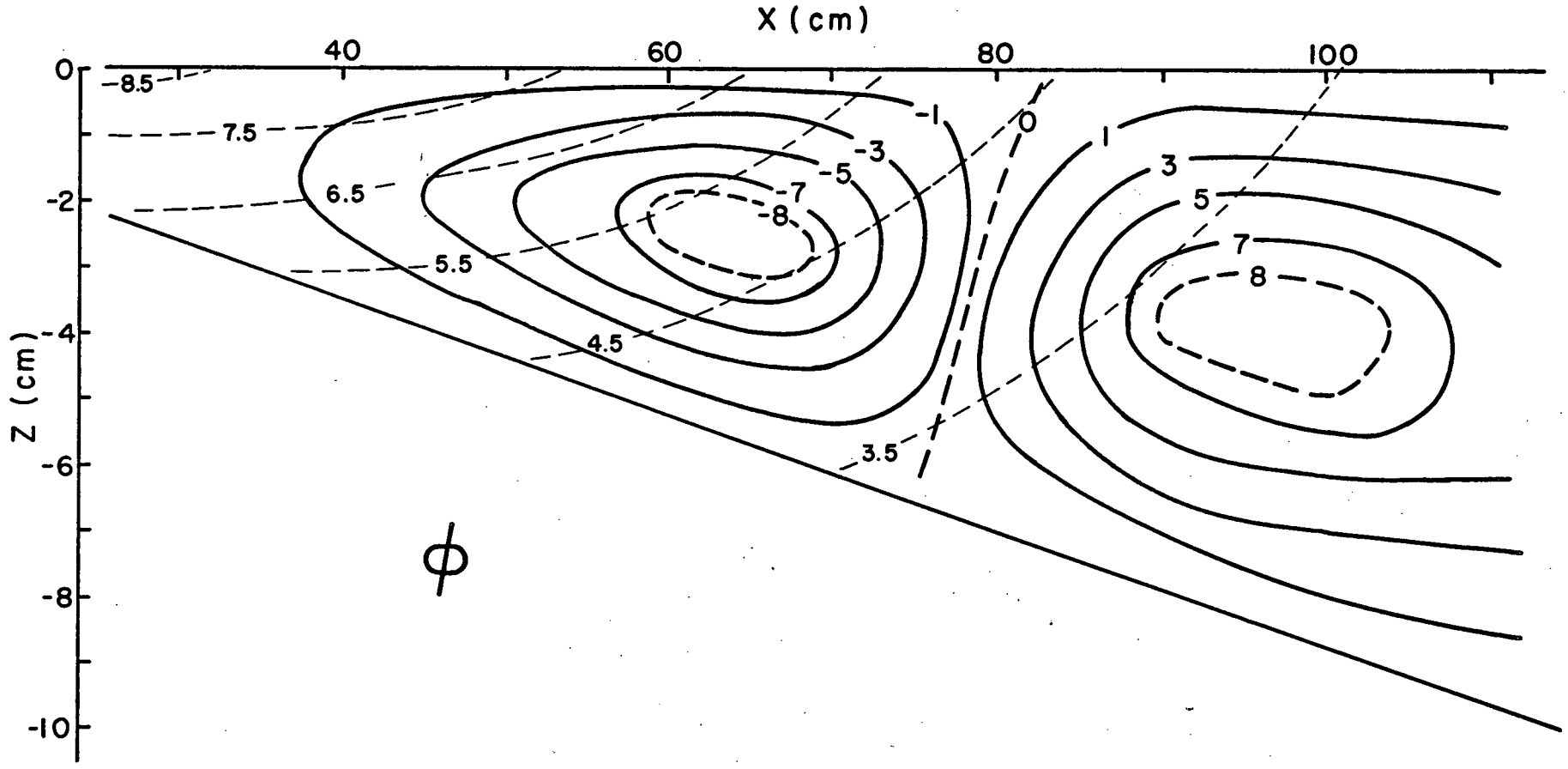

Figure 19. Calculated stream function ϕ in $cm^2\ min^{-1}$. The analytical temperature field used is shown by dashed lines (°C).

equal to zero at the top and bottom.

Figure 19 must be interpreted with care. One must keep in mind that this is the picture of ϕ at $t = 90/S$ in the tank. As time increases heating continues, the temperature field changes and the 'bar' defined as the 4°C surface isotherm progresses down the tank. Thus the density driven velocity field is also moving down the tank, changing slowly. In terms of the stream function ϕ (Figure 19) this means that the two sets of closed streamlines are moving along the tank at the speed of the 'bar' and hence must be slowly expanding vertically. The assumption, used to derive the circulation, that the $\partial/\partial t$ term in equation 3.2.4 can be neglected is thus only valid when changes are slow enough. The negative set of streamlines on the shallow side must also slowly expand horizontally while the positive set on the deep side must be slowly shrinking.

With this in mind one can see that this picture does not contradict the laboratory observations which clearly showed that water from the warmer, stable thermocline was not involved in any mixing or downward flow at the bar. This stable thermocline involves the water at temperature above 4.5°C. Looking at ϕ (Figure 19, p.49) and the velocity field (Figure 17b, p.47) from the mathematical model, and recalling that the average bar speed used in this model is about 2.5 cm min^{-1}, it can be seen that the downward velocities in the region warmer than 4.5°C serve only to thicken the thermocline region. In fact, by the time the bar has travelled roughly a further 10 cm down the tank, the w velocities observed at, say, 70 cm, will probably all be positive. The flow underneath the warmer water on the shallow side is fed by the flow towards the bar from the deeper side. This model is not steady state, thus

streamlines are not pathlines.

The streamlines shown in Figure 19 (p.49) close more rapidly at the two ends of the tank in the mathematical model than they probably do in the laboratory experiments since the hyperbolic tangent temperature approximation has reached its maximum and minimum values before the ends of the tank, whereas the observed temperatures has not. Such more gradual closings of the streamlines would tend to decrease the magnitudes of w away from the region of the bar.

3.3 Validity of the Velocity Model

Before extending the mathematical model to compare it with the lake it is necessary to consider the size of the neglected terms in the vorticity equation. Now including advection terms, 3.2.2 becomes

$$\frac{\partial \omega_2}{\partial t} + \underset{\sim}{v} \cdot \nabla \omega_2 = \frac{g}{\rho} \frac{\partial \rho}{\partial x} + \nu \left(\frac{\partial^2}{\partial x^2} + \frac{\partial^2}{\partial z^2} \right) \omega_2 \qquad (3.3.1)$$

where $\omega_2 = \frac{\partial u}{\partial z} - \frac{\partial w}{\partial x}$. The size of these terms was evaluated at several positions along the tank from the velocity field calculated from equation 3.2.7. This thus provides an internal consistency check on the solution of equation 3.2.7 and therefore on the assumptions used to derive it.

1) $\frac{\partial w}{\partial x}$ with respect to $\frac{\partial u}{\partial z}$ is always less than 1:10 and usually less than 1:100. Thus the assumption that $\frac{\partial w}{\partial x}$ is small with respect to $\frac{\partial u}{\partial z}$ is reasonable everywhere.

2) In the viscous term $\frac{\partial^2 u}{\partial x^2}$ was neglected with respect to $\frac{\partial^2 u}{\partial z^2}$. The ratio of these two terms is also 1:10 or less everywhere.

3) The $\partial/\partial t$ term can be compared to the buoyancy term and is found to be generally less than 1:10 except, of course, where the buoyancy term is zero; that is, right at the bar ($\theta = 0$) and at the extrema of the hyperbolic tangent temperature approximation where $\frac{\partial \theta}{\partial x} = 0$. The latter lies well to the extrema of the plots. It is possible to calculate the size of the $\partial/\partial t$ term since the buoyancy term depends on time.

4) Non-linear terms are generally less than one tenth of the buoyancy term except, of course, where the buoyancy term is zero, as mentioned above. In the immediate vicinity of the 4°C isotherm ($\theta = 0$) the vorticity balance would shift to include $\partial/\partial t$, advective and viscous terms.

Thus the assumptions made in deriving the mathematical model appear to be reasonable, as the comparison between the calculated and observed velocity fields would suggest and the model provides a useful approximation to the circulation.

3.4 Extension to a Lake

The laboratory studies suggested that the tank could be viewed as a section of a lake from shore to deeper regions using a vertical scaling of about 1/1000 (see p.12). The 5° bottom slope, compared to the north shore bottom slopes of Lake Ontario, then suggests a horizontal scaling of about 1/20,000. The average speed of the bar in Lake Ontario is about 20 times that in the tank with the 5° bottom slope. Using these scales for z, x, and t and assuming that the equations (3.1.13 and 3.2.7) used

can be applied to the lakes simply by making the appropriate scale changes, the value of vertical eddy diffusivity must be about 6 $cm^2\ sec^{-1}$ and vertical eddy viscosity about 38 $cm^2\ sec^{-1}$. Now it is not unreasonable that these values be different, especially in a stable situation as on the shallow side of the 'bar'. In fact, experimental values given for Lake Michigan (Huang, 1969) are 1-10 $cm^2\ sec^{-1}$ for vertical eddy diffusivity and 1-100 $cm^2\ sec^{-1}$ for vertical eddy viscosity. A ratio of 1:2 (vertical eddy diffusivity to vertical eddy viscosity) might be more realistic. If the vertical eddy diffusivity is arbitrarily set at 11 $cm^2\ sec^{-1}$, which, when applied to equation 3.1.13 does not give an unrealistic temperature field, the corresponding vertical eddy viscosity, from equation 3.2.7, is 21 $cm^2\ sec^{-1}$.

Such an extension as this should, of course, only be applied to large dimictic freshwater lakes, such as the Great Lakes, in which the bar could be expected to exist.

However, when equation 3.2.7 is applied to a lake there are additional terms that have been neglected, those associated with the Coriolis force. In the vorticity equation 3.2.1 these are included by replacing $\underset{\sim}{\omega}$, the relative vorticity, by $(\underset{\sim}{\omega} + 2\underset{\sim}{\Omega})$ where $2\underset{\sim}{\Omega}$ is the 'planetary vorticity'. From Veronis' (1963) estimates, based on Ertel's circulation theorem as applied to a stratified fluid, the ratio of horizontal to vertical scales in the thermal bar phenomenon is such that the component of planetary vorticity parallel to the earth's surface may be safely neglected. Because of the presence of the vertical component of planetary vorticity (f), the density induced pressure gradients in a lake will tend to be

balanced by a geostrophic current. However a time of O(1/f) is necessary to achieve such an equilibrium, during which the position of the bar changes appreciably. This leads me to believe that geostrophic equilibrium may not be attained while the bar is moving and that on a short time scale the circulation is roughly due to the same dynamic balance as in the model. A fossil geostrophic circulation due to the density gradients associated with the bar may continue to exist after the bar has disappeared.

The validity of equation 3.2.7 was checked for Lake Ontario by evaluating, from the scaled results of 3.2.7, the size of the neglected terms in the shallow and deeper regions and in the vicinity of the 'bar'. It is possible that the relative size of these terms may be different from those in the tank since there are different scales used for horizontal and vertical distances as well as time. It was found that the basic balance between the buoyancy and the approximated viscous effects as used in equation 3.2.7 is valid for the lake, except again right in the vicinity of the bar. The non-linear terms are more important near the bar in Lake Ontario than they were in the tank. Nevertheless the mathematical model probably gives a reasonable, if rough, approximation of what occurs in the lakes since the assumptions are nearly satisfied, except for the zero surface velocities (p.16).

Considering the plot of the calculated streamlines, Figure 19(p.49) in the light of a possible extension to lakes it is worth remarking on the situation of the 'stationary thermal bar'; for example, the case of Lake Geneva (Forel, 1880) (mentioned earlier) or the case of effluents warmer than 4°C being dumped into a lake that is cooler than 4°C (see section 2, p.29 and Appendix D). As observed in the laboratory, Figure 19(p.49) suggests two cells, in this case fixed in position, with clockwise motion

on the shallow side and counter-clockwise motion on the deep side and mixing and sinking between the two cells. It must be emphasized that this is NOT what has been observed for the 'migrating thermal bar' in the laboratory model. Streamlines are pathlines only when flow is stationary!

It would appear from the way in which the mathematical model as well as the tank can approximate the temperature fields observed in Lake Ontario, that the velocity field observed in the laboratory and calculated from a simple vorticity balance which also holds for the lake might also be that associated with the 'bar' in lakes. However it will probably be very difficult to determine this by direct measurements as the velocities expected, for example in Lake Ontario, are only of the order of 1 cm sec^{-1} and there are many other flows present in lakes that are not directly associated with the thermal bar.

4. SUMMARY

The 'migrating thermal bar' phenomenon which is known to occur in certain large dimictic freshwater lakes has been studied in a two-dimensional laboratory model. The temperature fields agree with those observed in the Great Lakes.

A linear model is used to describe the speed of the 'thermal bar'. The effects of variation of the parameters of heat input, bottom slope, and initial temperature on the speed of the bar were measured and found to agree with this simple model. The linear model gives a reasonable first approximation to the speed of the 'thermal bar' in both the experimental model and the Great Lakes.

Since the observed temperature field and speed of the bar appear to model conditions in the lakes it seems possible that the associated observed velocity fields may do this as well. On the shallow side of the 'migrating thermal bar' temperature observations showed that a stable thermocline developed which progressed towards the deep end, its front end marking the boundary between the stable shallower region and the convecting deeper region. In the laboratory model a mean flow towards the deep end was observed in the thermocline with a counter-flow underneath. In the deep end of the model a flow near the surface travelled toward the stable thermocline. This current sank at the front edge of the thermocline and divided, a part feeding the upslope current in the shallow end, the other part providing the downslope current in the deep end. The water in this sinking zone or 'bar zone' was from the deep end of the model and did not include water from the thermocline

on the shallow side.

On the basis of this laboratory model which indicated that horizontal advection and diffusion were not of primary importance a mathematical model was developed. First the temperature field was calculated from the one-dimensional heat diffusion equation. Then the velocity field was calculated assuming that the flow was driven by buoyancy forces and balanced by viscous forces. Since there is a great similarity between the calculated and observed temperature and velocity fields, the assumptions on which the vorticity balance is based are obviously nearly satisfied in the laboratory model.

Because of the similitude between the experimental and calculated temperature fields and those observed in lakes, the observed and calculated velocity field may model the flows associated with the thermal bar in the lakes. In this case the balance would be between buoyancy forces and eddy viscosity effects except possibly in the immediate vicinity of the 'bar' where non-linear terms would be important. The velocities expected in Lake Ontario would be of the order of 1 cm sec^{-1}.

From the laboratory and mathematical studies it is also possible to describe the behaviour associated with the 'stationary thermal bar' which would be expected in the case of waters warmer than 4°C being dumped into waters cooler than 4°C. In this case the 'bar' would be expected not to move and the circulation would consist of two cells with mixing and sinking at the 'bar'. This is quite different from the behaviour observed for the 'migrating thermal bar' in the laboratory.

BIBLIOGRAPHY

Arlinger, B., 1965. Calculation of temperature in an infinite wedge with given heat flux through its bounding surfaces. Saab TN 59, Saab Co., Linköping, Sweden, 30pp.

Chermack, E.E., 1970. Study of thermal effluents in southeastern Lake Ontario as monitored by an airborne radiation thermometer. Paper presented at the 13th Conf. Great Lakes Res. (International Assoc. Great Lakes Res.), Buffalo, N.Y., April, 1970.

Church, P.E., 1942. The annual temperature cycle of Lake Michigan. University of Chicago, Department of Meteorology, Misc. Reports Nos. 4 and 18, 148pp.

Davies, J.T. and E.K. Rideal, 1961. Interfacial Phenomena. Academic Press, N.Y., 474pp.

Dorsey, N.E., 1940. Properties of Ordinary Water-Substance. Reinhold Publishing Corp., N.Y., 327.

Elder, F.C. and R.K. Lane, 1970. Some evidence of meteorological related characteristics of lake surface temperature structure. Paper presented at the 13th Conf. Great Lakes Res. (International Assoc. Great Lakes Res.), Buffalo, N.Y., April, 1970.

Elliott, G.H. and J.A. Elliott, 1969. Small-scale model of the 'thermal bar'. Proc. 12th Conf. Great Lakes Res.; International Assoc. Great Lakes Res., 553-557.

_____ and _____, 1970. Laboratory studies on the 'thermal bar'. Proc. 13th Conf. Great Lakes Res.; International Assoc. Great Lakes Res., (in the press).

Forel, F.A., 1880. La congélation des lacs suisses et savoyards pendant l'hiver 1879-1880, Lac Léman. L'Echo des Alpes, Genève, 3, 149-161.

Handbook of Chemistry and Physics, 1969-70. The Chemical Rubber Co., Cleveland, Ohio, page F-4.

Huang, C.K., 1969. The thermal current structure in Lake Michigan, A theoretical and observational model study. University of Michigan, Great Lakes Res. Div., Special Report No. 43, 169pp.

Richards, T.L., J.G. Irbe and D.G. Massey, 1969. Aerial surveys of Great Lakes water temperatures April, 1966 to March, 1968. Department of Transport, Meteorological Branch, Climatological Studies No. 14, 55p.

_____, _____ and _____, 1969-1970. Unpublished data.

Rodgers, G.K., 1965a. The thermal bar in the Laurentian Great Lakes. Proc. 8th Conf. Great Lakes Res.; Univ. Michigan, Great Lakes Res. Div. Pub. 13, 358-363.

_____, 1965b. Unpublished data.

_____, 1966a. The thermal bar in Lake Ontario, Spring 1965 and Winter 1965-66. Proc. 9th Conf. Great Lakes Res.; Univ. Michigan, Great Lakes Res. Div. Pub. 15, 369-374.

_____, 1966b. A note on thermocline development and the thermal bar in Lake Ontario, Symposium of Garda, I.A.S.H. Pub. No. 70, 401-405.

_____, 1967. Thermal régime and circulation in the Great Lakes. Royal Society of Canada, Water Resources of Canada Symposia, 87-95.

_____, 1968. Heat advection within Lake Ontario in spring and surface water transparency associated with the thermal bar. Proc. 11th Conf. Great Lakes Res.; International Assoc. Great Lakes Res., 480-486.

_____ and D.V. Anderson, 1961. A preliminary study of the energy budget of Lake Ontario. J. Fish. Res. Bd. Canada, 18, 617-636.

_____ and _____, 1963. The thermal structure of Lake Ontario. Proc. 6th Conf. Great Lakes Res.; Univ. Michigan, Great Lakes Res. Div. Pub. 10, 59-69.

Sato, G.K., 1969. Prediction of the time of disappearance of the thermal bar in Lake Ontario, Univ. Toronto, M.A.Sc. dissertation, 114pp.

Sverdrup, H.U., M.W. Johnson and R.H. Fleming, 1942. The Oceans. Prentice-Hall, Inc., N.Y., 80, 81, 105.

Tikhomirov, A.I., 1963. The thermal bar of Lake Ladoga. Bull. (Izvestiya) All-Union Geogr. Soc., 95, 134-142. Am. Geophys. Union translation, Soviet Hydrology: Selected Papers, No. 2.

Veronis, G., 1963. On the approximations involved in tranforming the equations of motion from a spherical surface to the β-plane. II. Baroclinic systems. J. Marine Res., 21, 199-204.

APPENDIX A: Cooling Experiment

Figure 20 shows a temperature section and temperature anomaly section for surface cooling of water initially above 4°C. For the temperature anomaly (see p.24) section it was necessary to estimate the heat loss from the temperature section. The section is similar to measurements made in Lake Ontario (Figure 20). The flow pattern observed in the laboratory experiment was the same as that encountered in the heating experiments (see Figure 6, p.15).

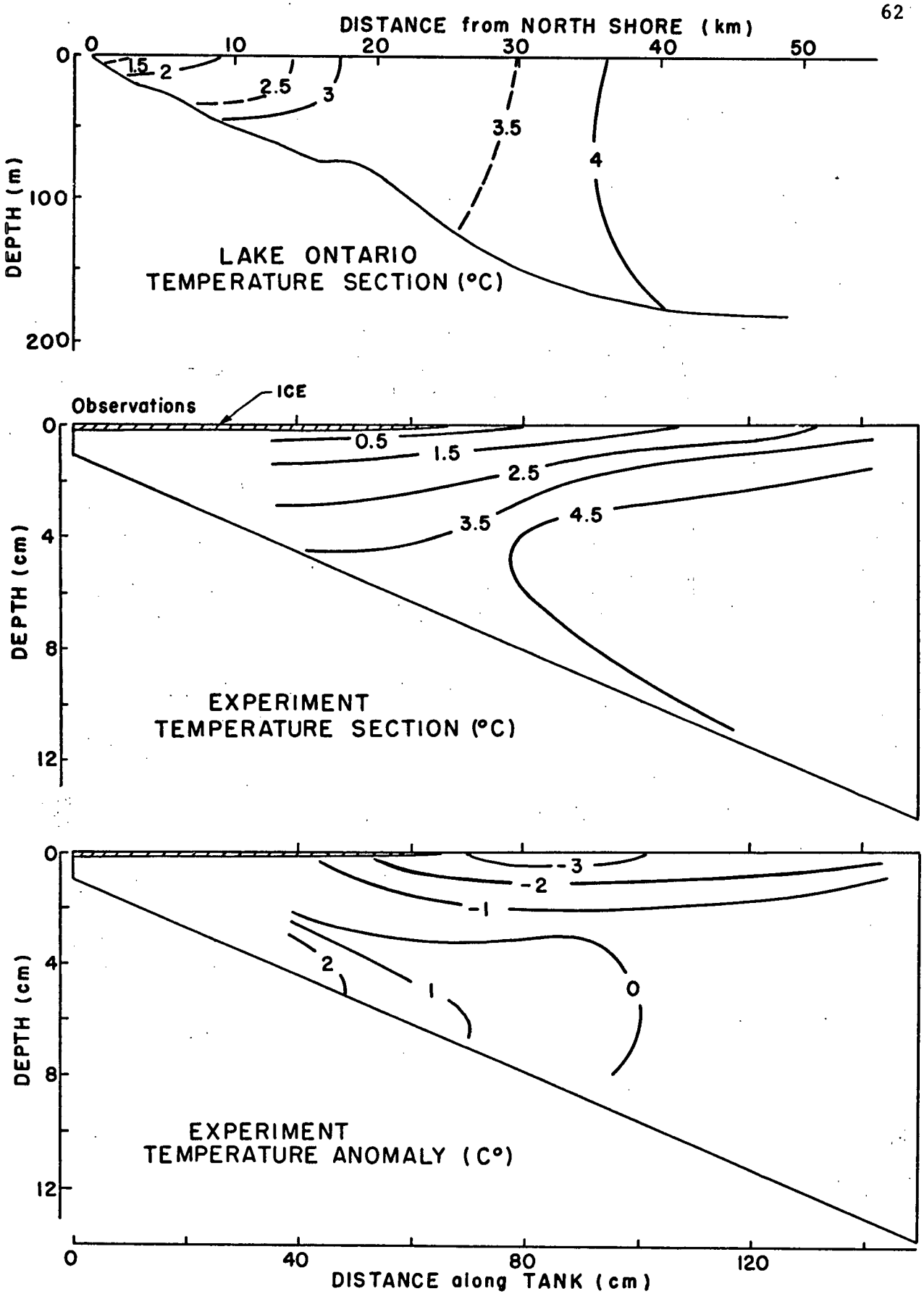

Figure 20. Temperature section from Lake Ontario (Rodgers, 1966a); mid-lake N-S section taken mid-January 1966.
Temperature and temperature anomaly sections for the case of cooling (fall simulation) with 5° bottom slope.

APPENDIX B: Temperature Data: constant slopes

Figures 21 to 27 are temperature data for runs simulating spring warming. They include a temperature section, mean temperatures, changes in heat content, and a temperature anomaly section (p.24) for different slopes, different heating rates, and different positions of the 'thermal bar'. Also shown are the curves for mean temperature and change in heat content predicted by the assumptions used in the linear model for the speed of the bar. There is a possible further parallel between the tank and the observations in Lake Ontario (Rodgers 1968); the advection of heat towards the deep end of the tank or centre of the lake appears to occur mainly during the early stages when the thermal bar is near the shore (Figure 28 p.77, and Figure 12, p.25). However this is purely speculation as some of this could be due to the nonuniform distribution of heat flux over the surface of the Lake.

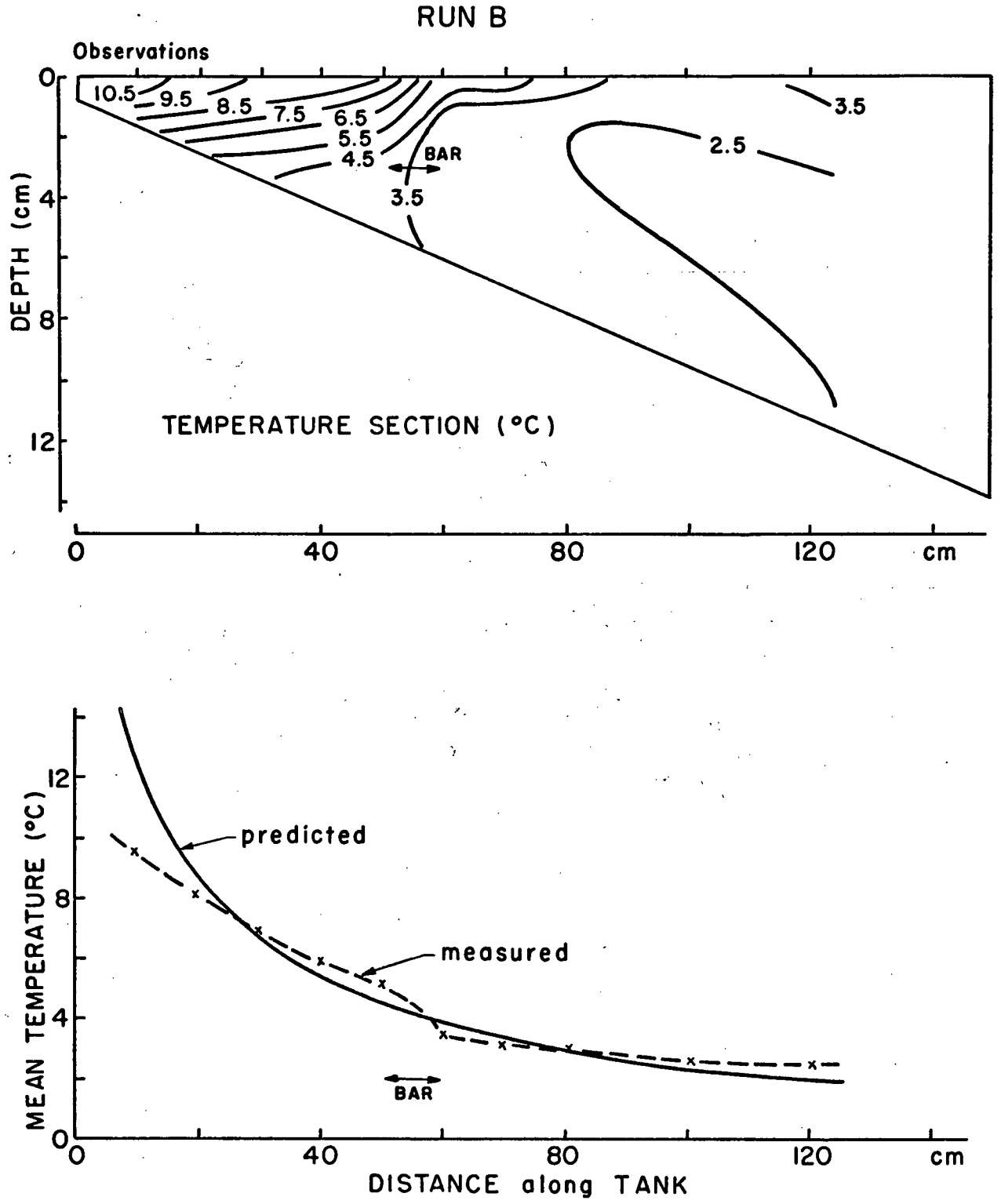

Figure 21a. Temperature section and mean temperatures (vertically averaged) for Run B: 5° bottom slope, standard heating, and Ti, 0°C.

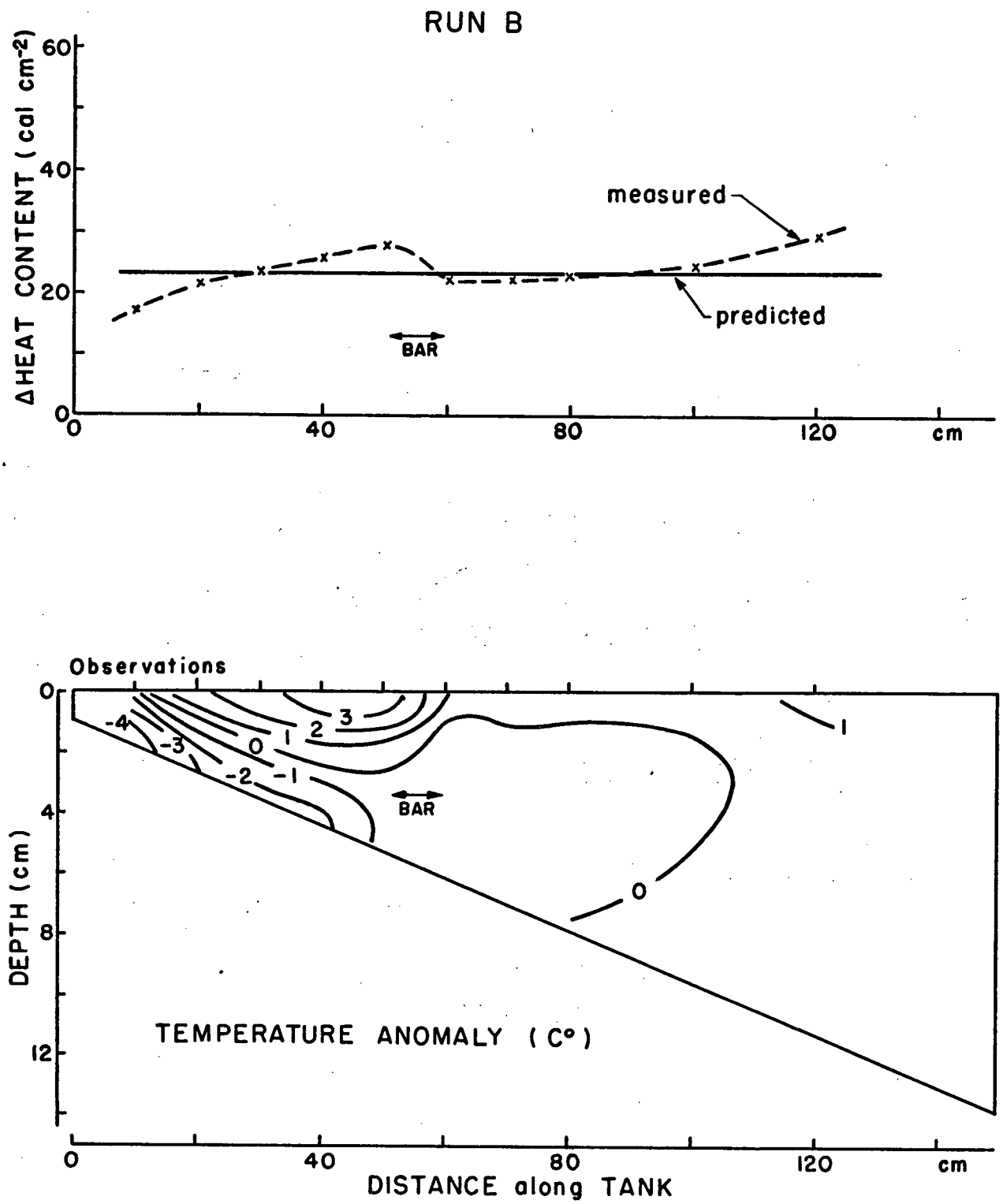

Figure 21b. Changes in heat content and temperature anomaly section for Run B

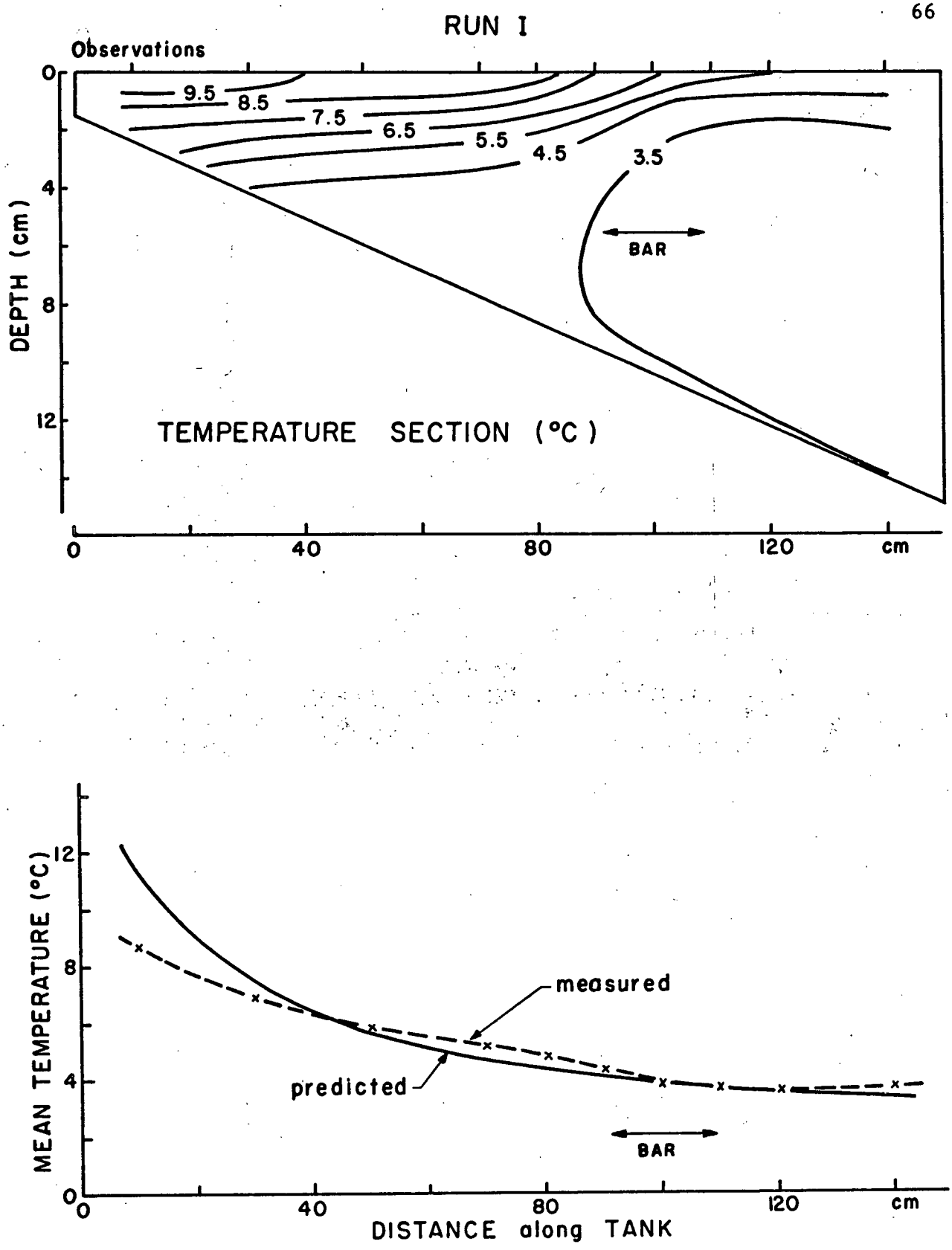

Figure 22a. Temperature section and mean temperatures for Run I: 5° bottom slope, standard heating, and Ti, 1.4°C.

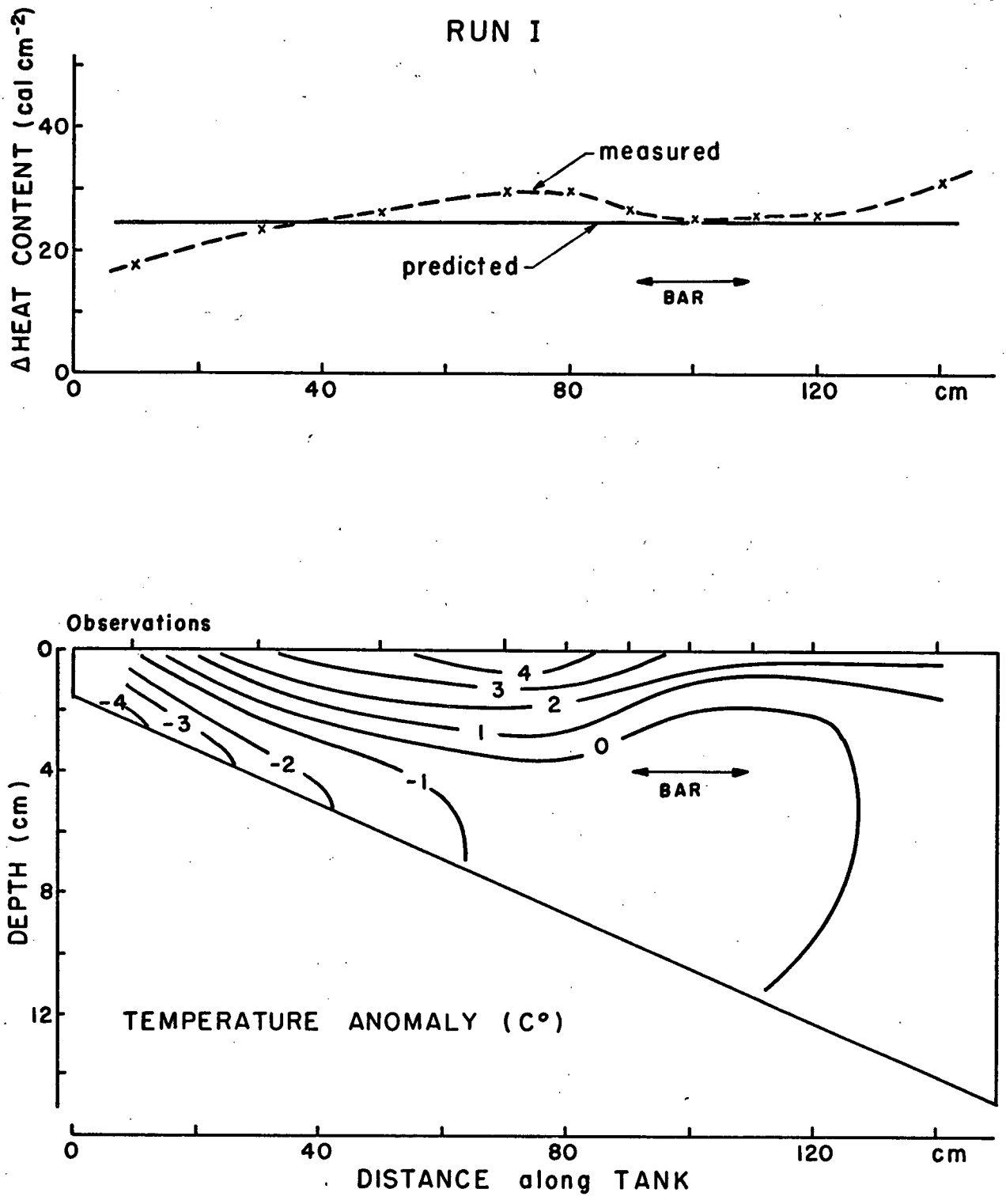

Figure 22b. Changes in heat content and temperature anomaly for Run I.

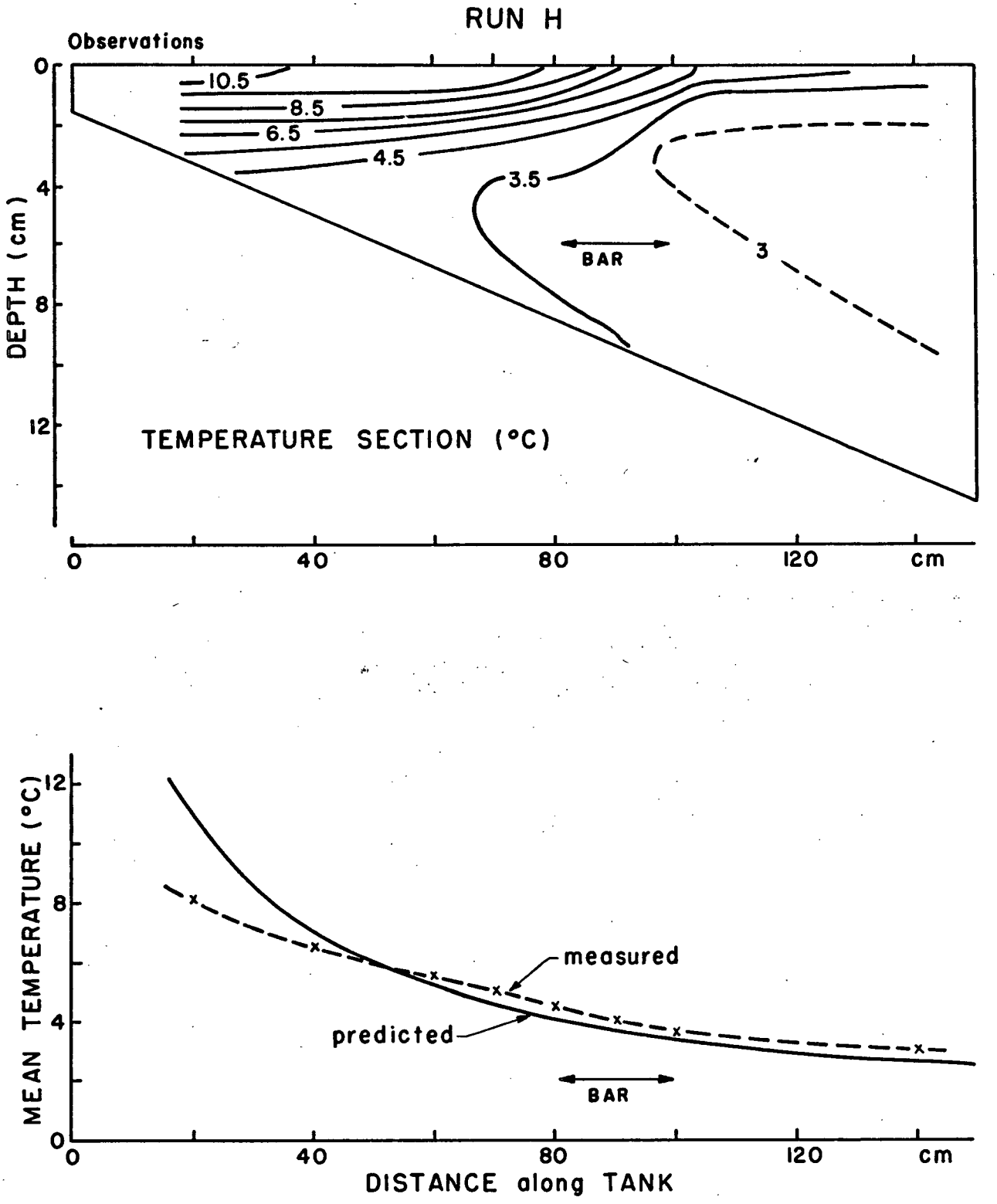

Figure 23a. Temperature section and mean temperatures for Run H: 5° bottom slope, increased heating and Ti, 0°C.

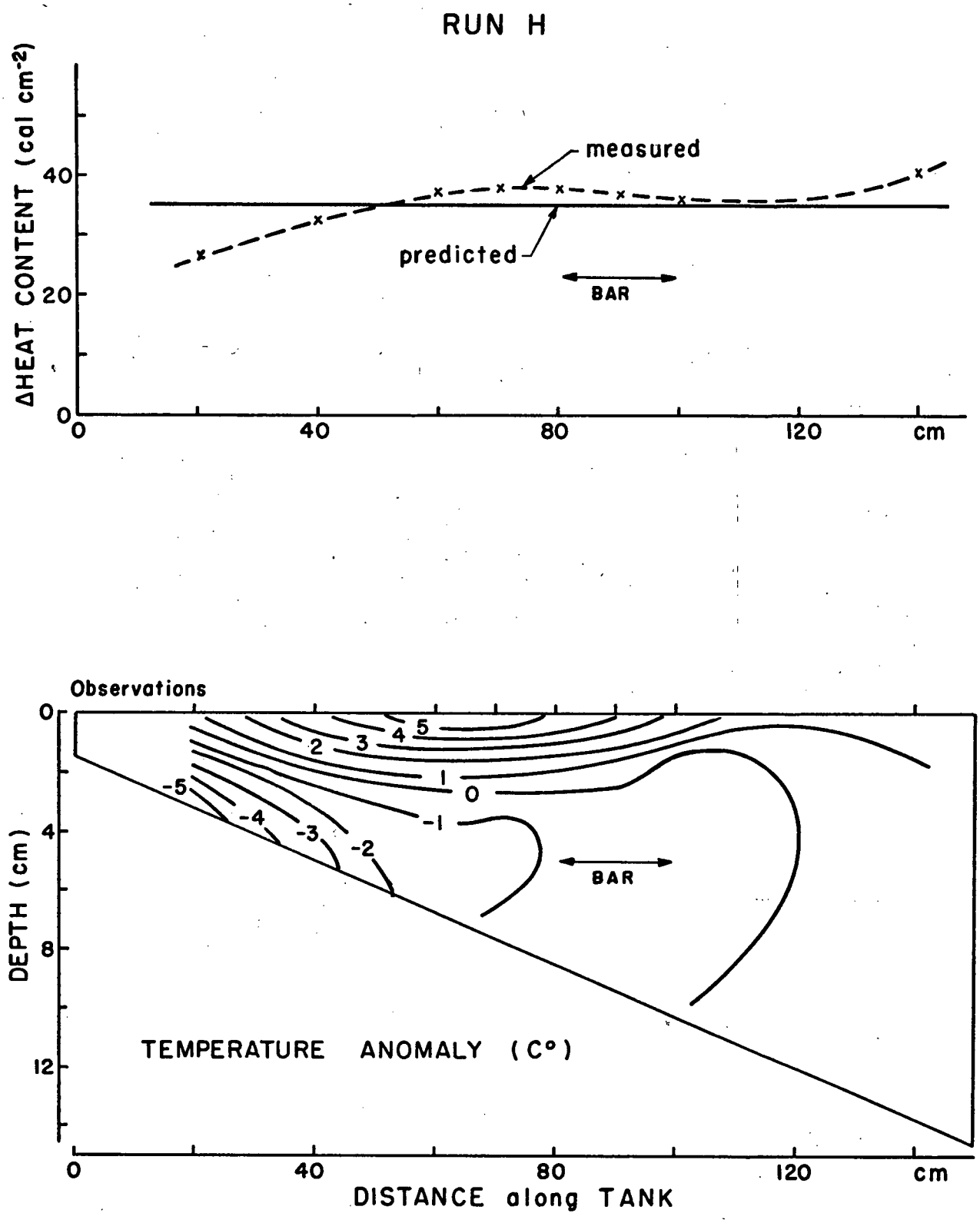

Figure 23b. Changes in heat content and temperature anomaly for Run H.

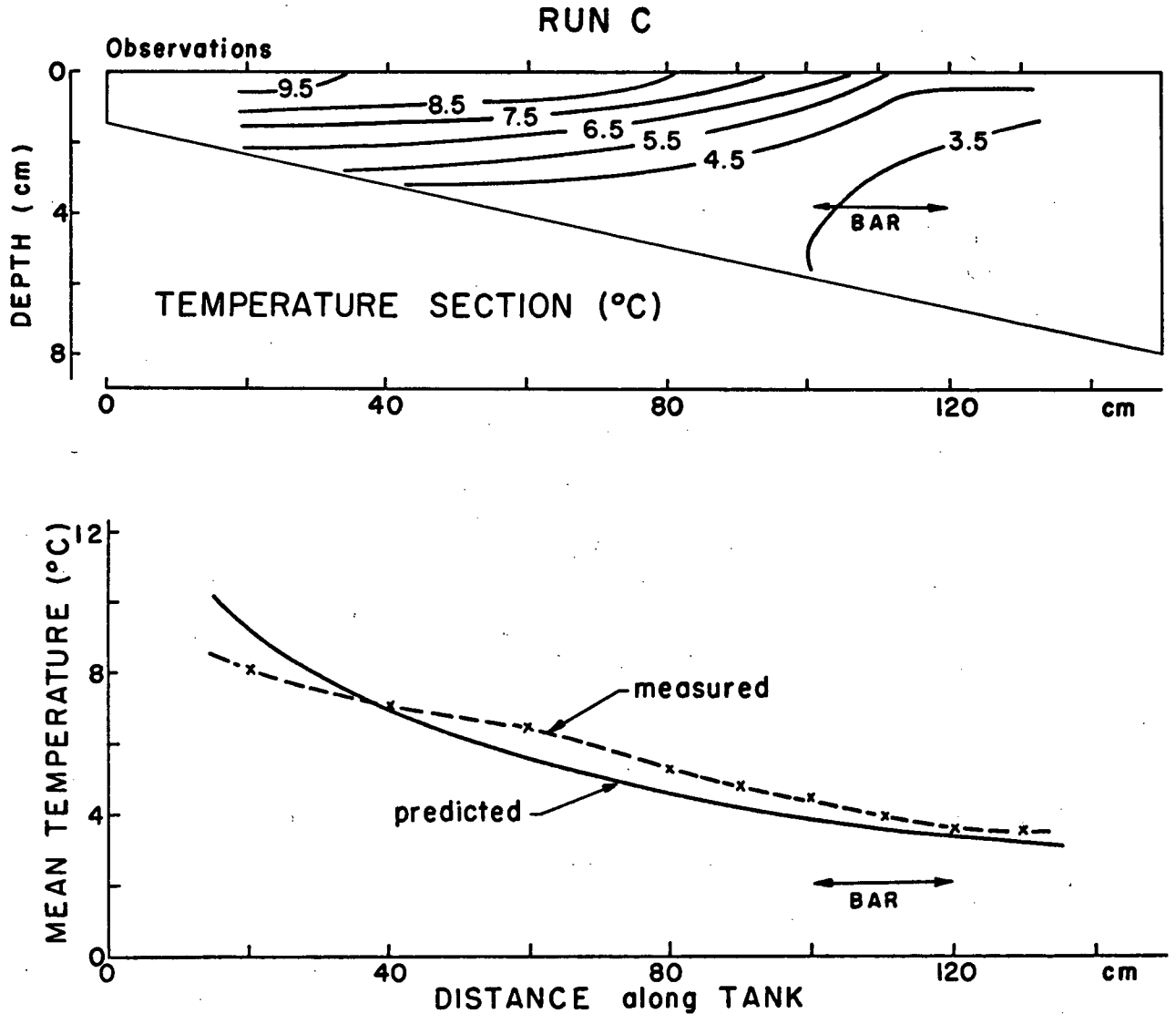

Figure 24a. Temperature section and mean temperatures for Run C: 2.5° bottom slope, standard heating and Ti, 0°C.

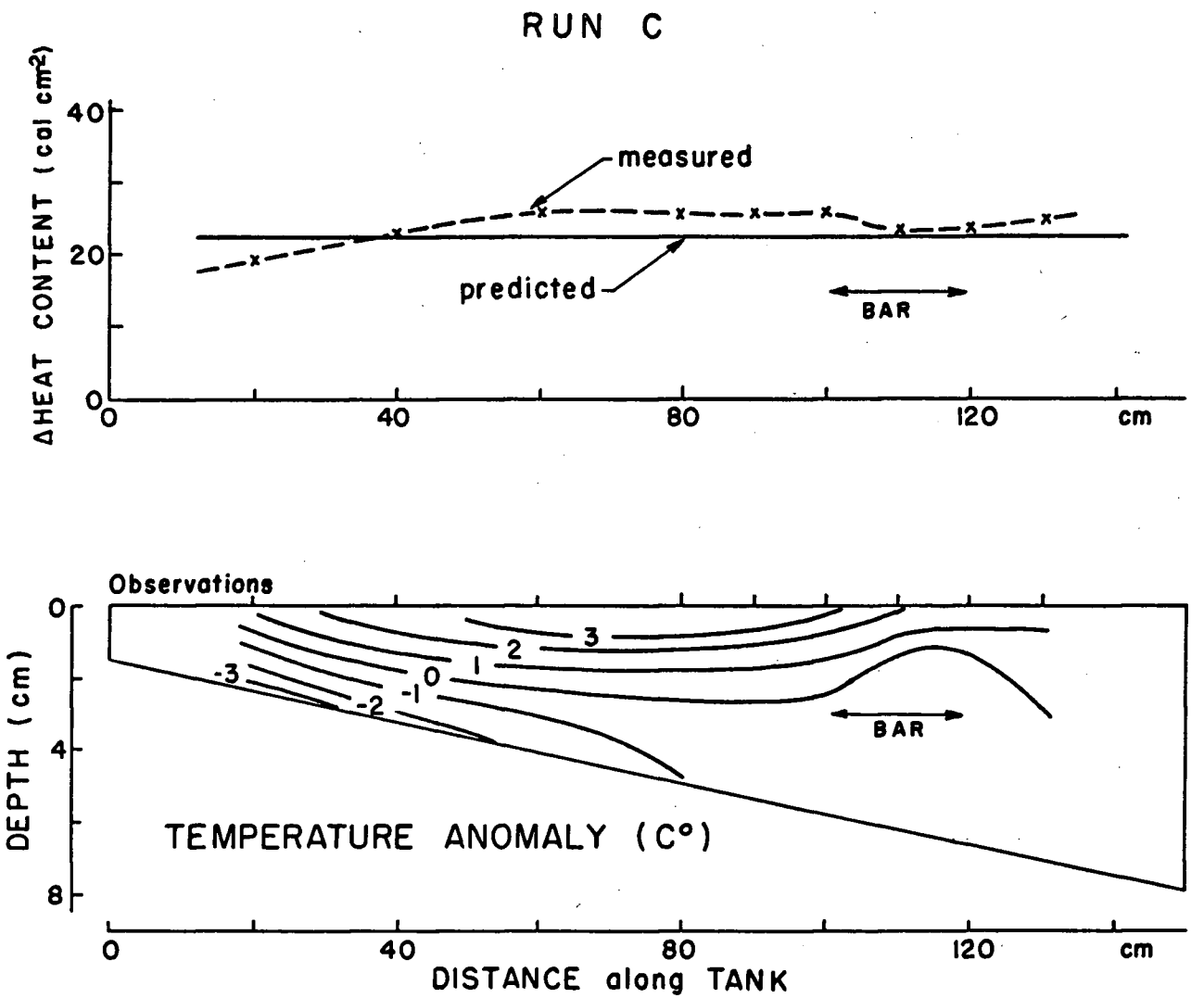

Figure 24b. Changes in heat content and temperature anomaly for Run C

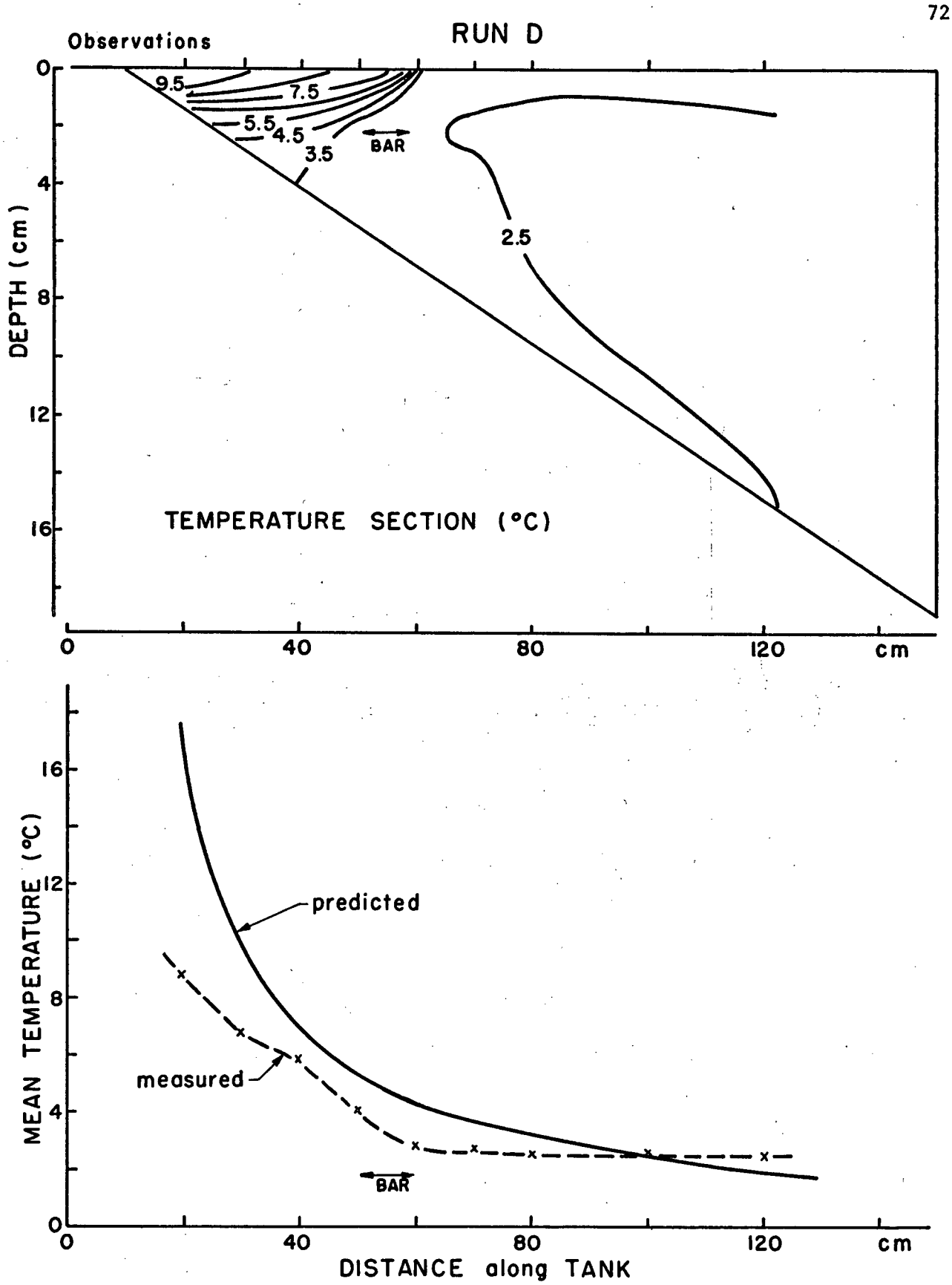

Figure 25a. Temperature section and mean temperatures for Run D: 7.5° bottom slope, standard heating and Ti, 0°C.

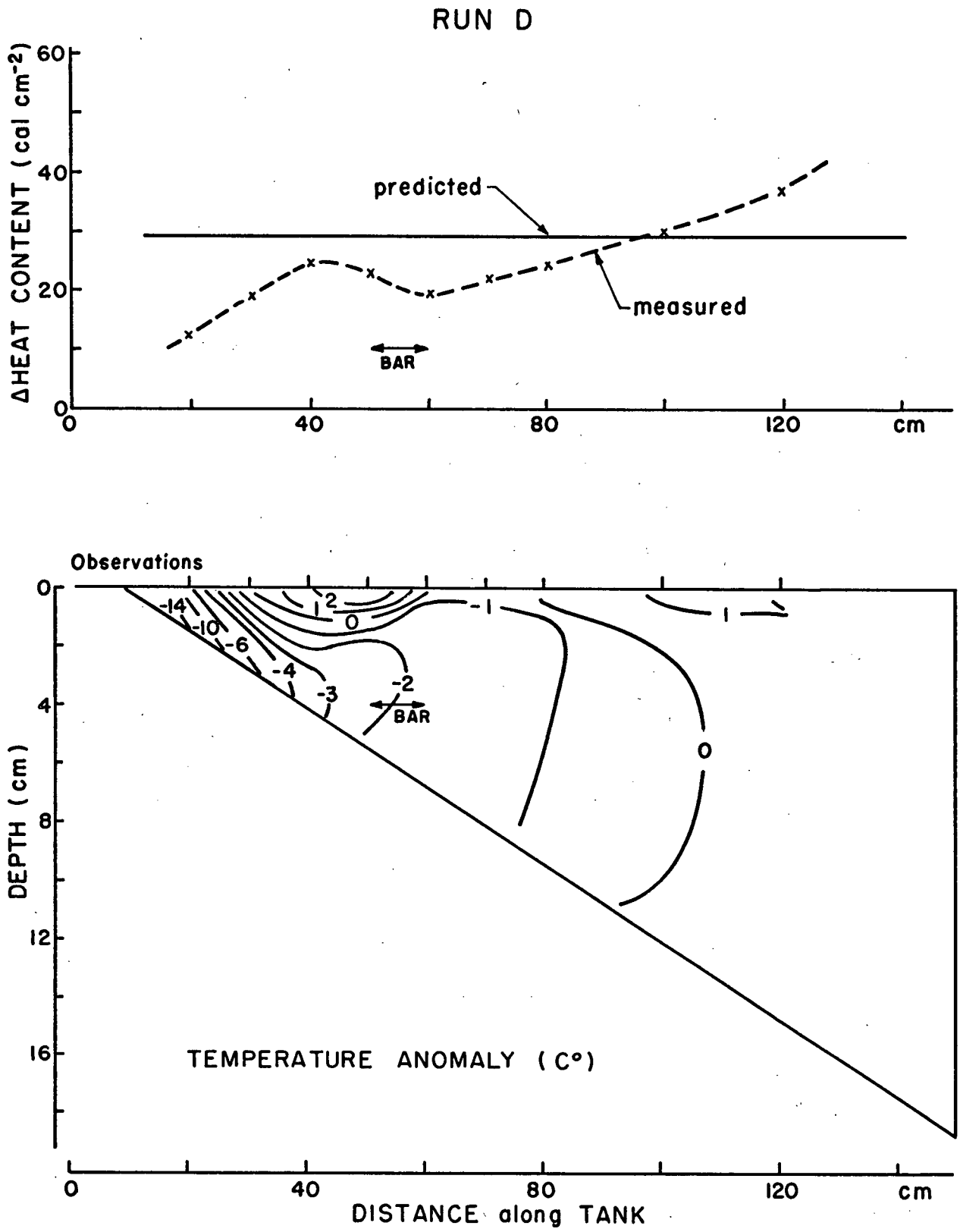

Figure 25b. Changes in heat content and temperature anomaly for Run D

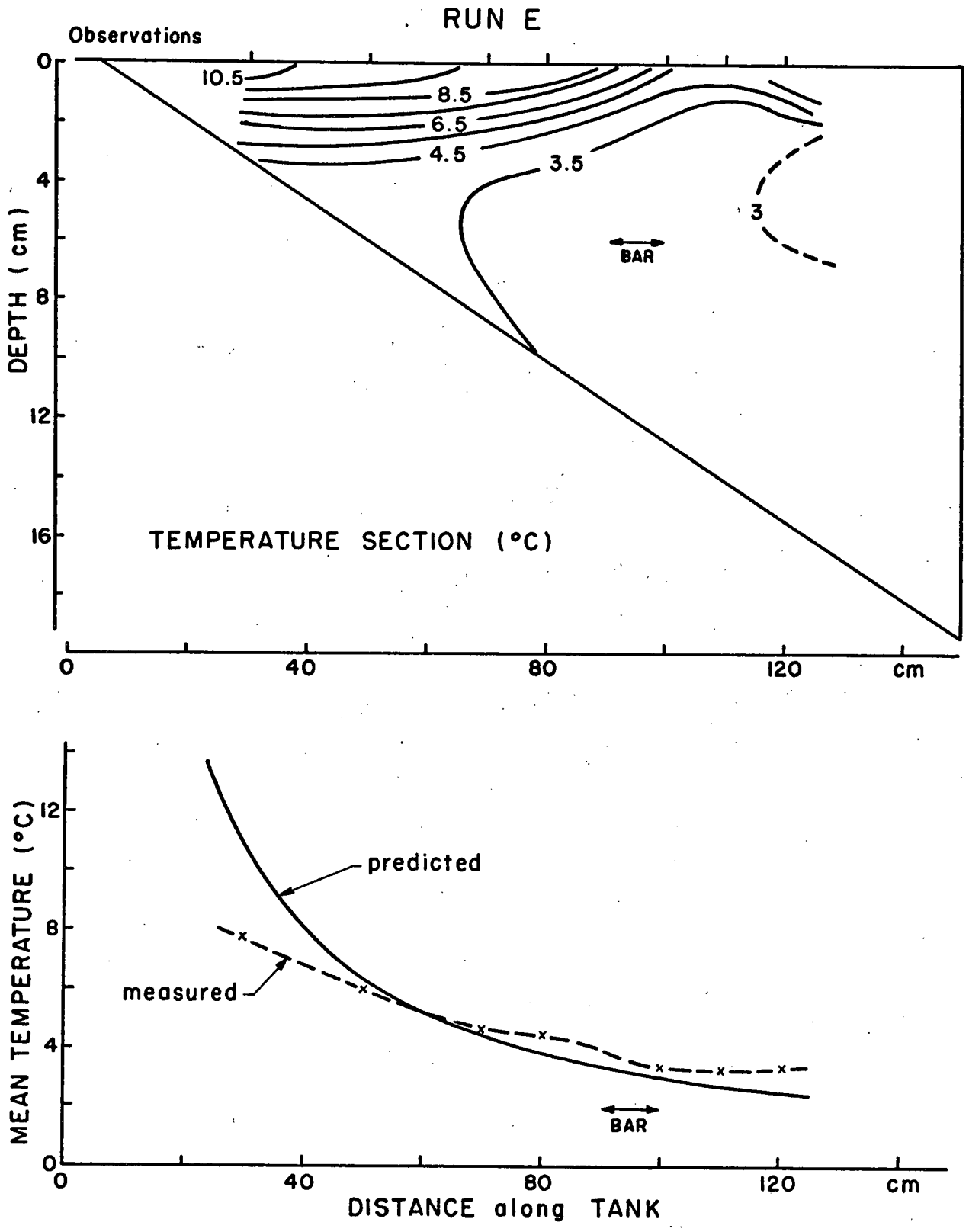

Figure 26a. Temperature section and mean temperatures for Run E: 7.5° bottom slope, standard heating and Ti, 0°C.

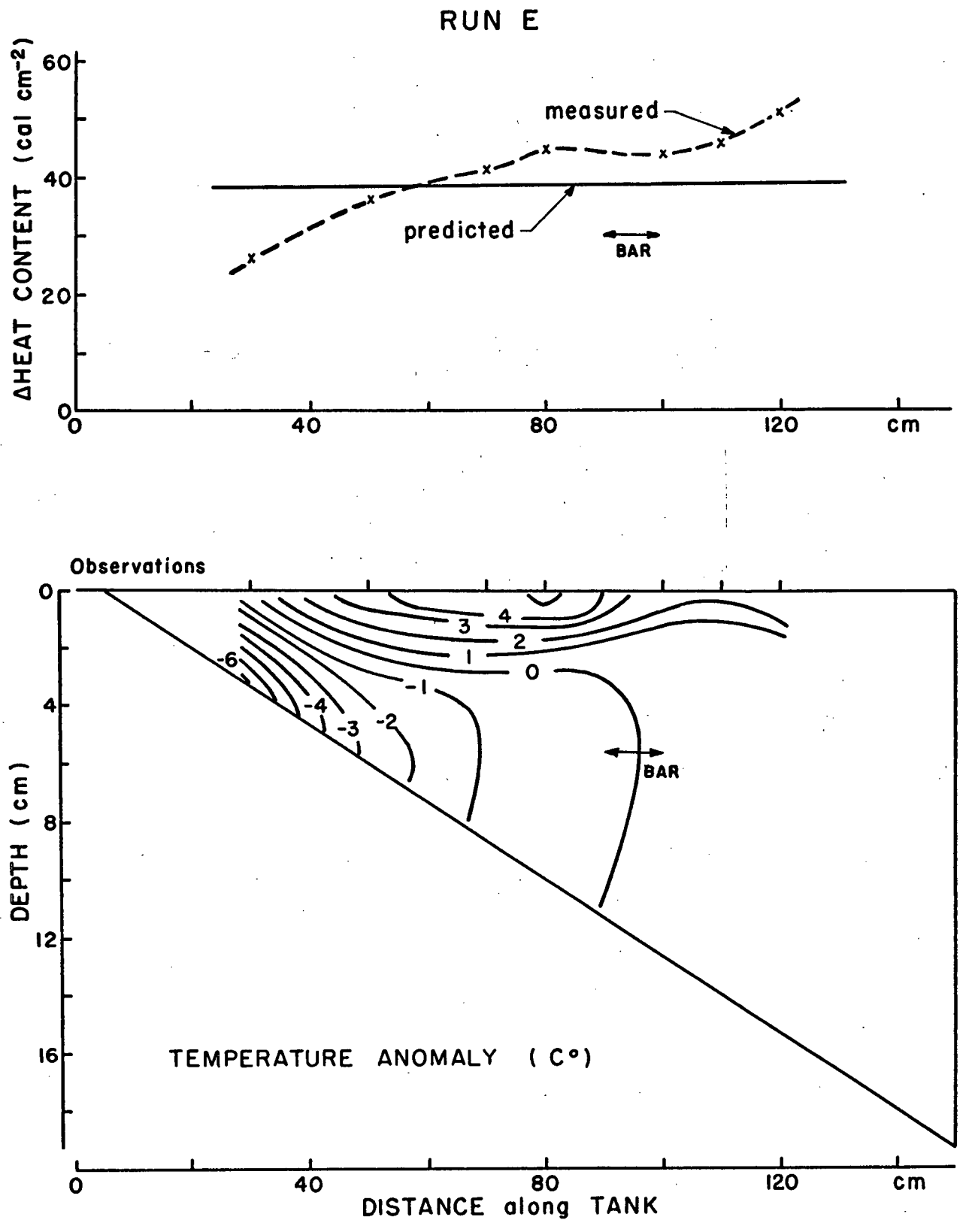

Figure 26b. Changes in heat content and temperature anomaly for Run E

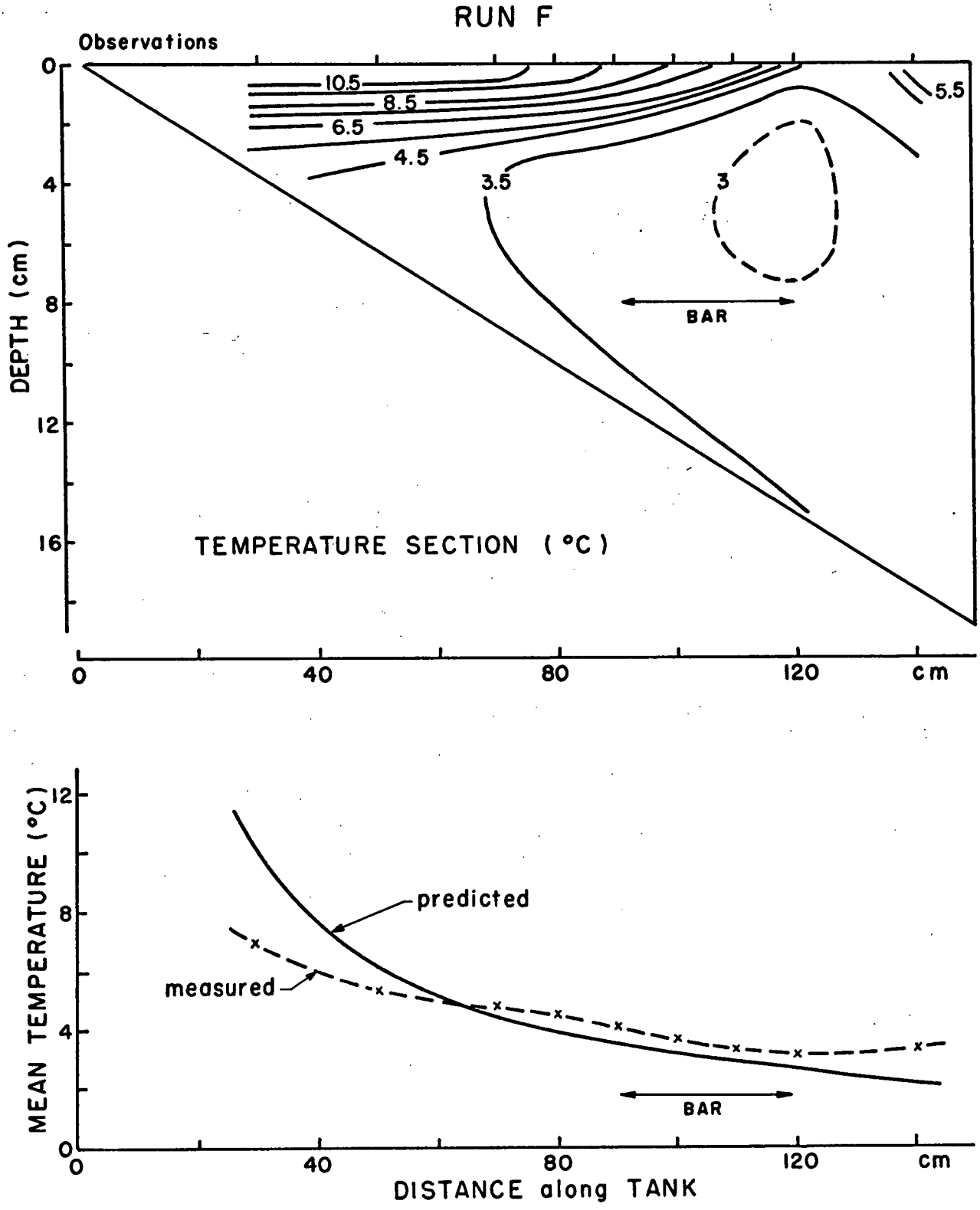

Figure 27a. Temperature section and mean temperatures for Run F: 7.5° bottom slope, increased heating and Ti, 0°C.

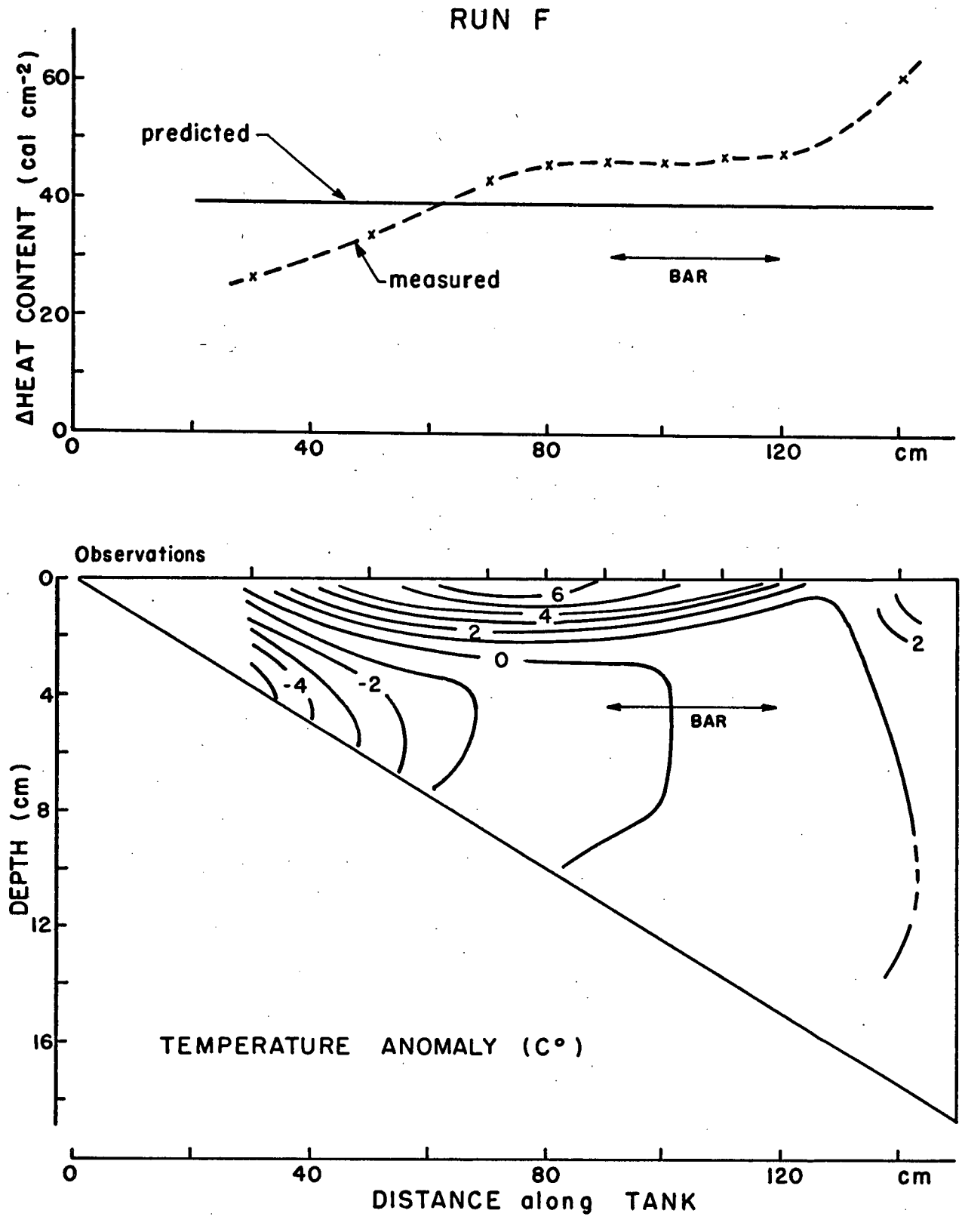

Figure 27b. Changes in heat content and temperature anomaly for Run F

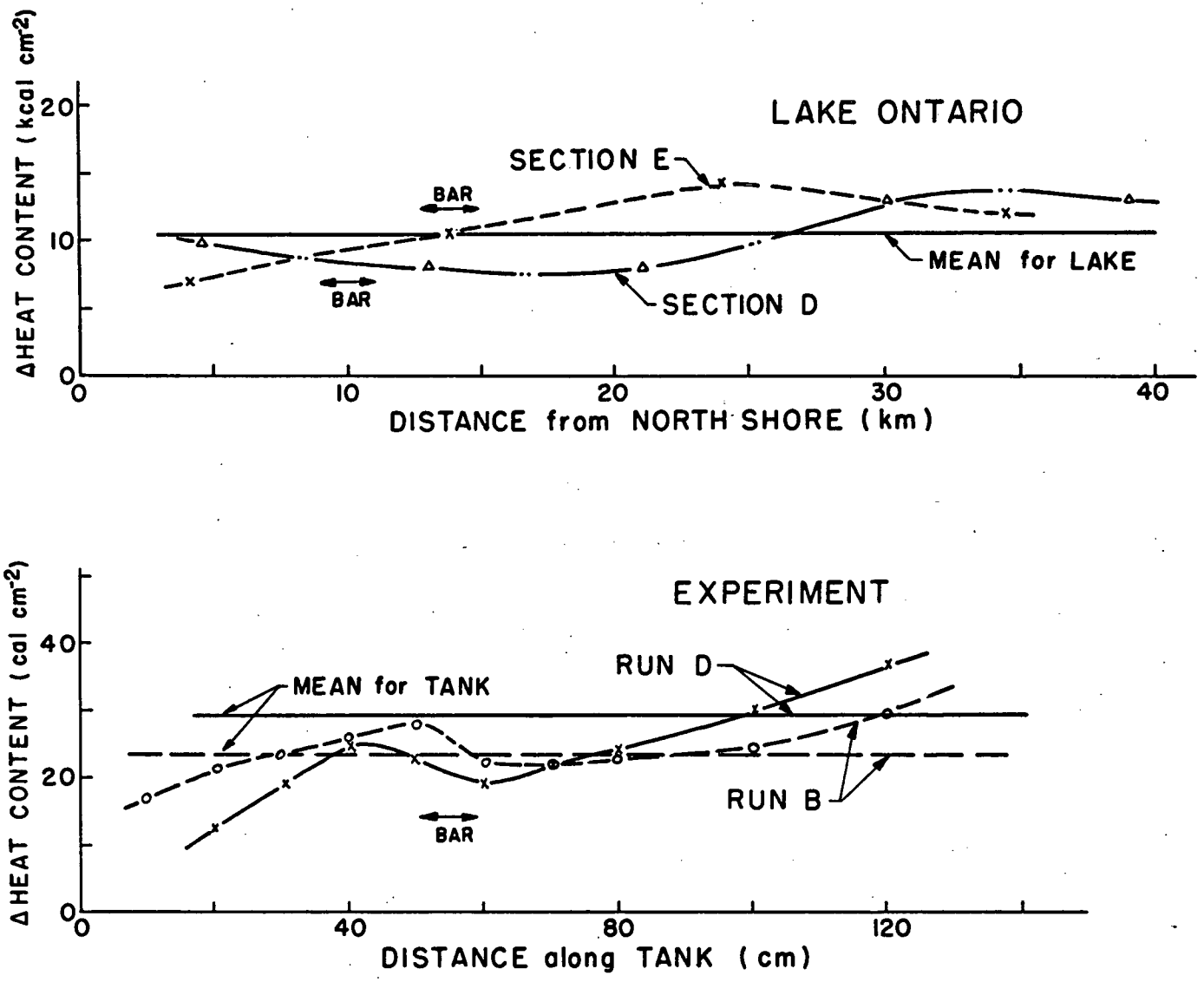

Figure 28. Changes in heat content during the early stages of the thermal bar for Lake Ontario (for sections in Figure 2, p.4) and for the tank experiment.

APPENDIX C: Investigation of the Effects of Bottom Irregularities

Figures 29 and 30 contain temperature data similar to that in Appendix B for the cases of a 5° slope followed by a 0° slope and a 5° slope followed by a vertical dropoff to a 0° slope. Figure 31 shows the bar speeds from these experiments. The results are all similar to the previous cases. However, the linear model for the speed of the bar is not as good an approximation for these extreme changes in bottom topography. The speed of the bar was roughly that which would have been expected from equation 2.5.1 for a bottom slope that was the weighted average of the bottom slopes in each section. There are no abrupt changes in bar speed, temperature field or current structure associated with these bottom irregularities.

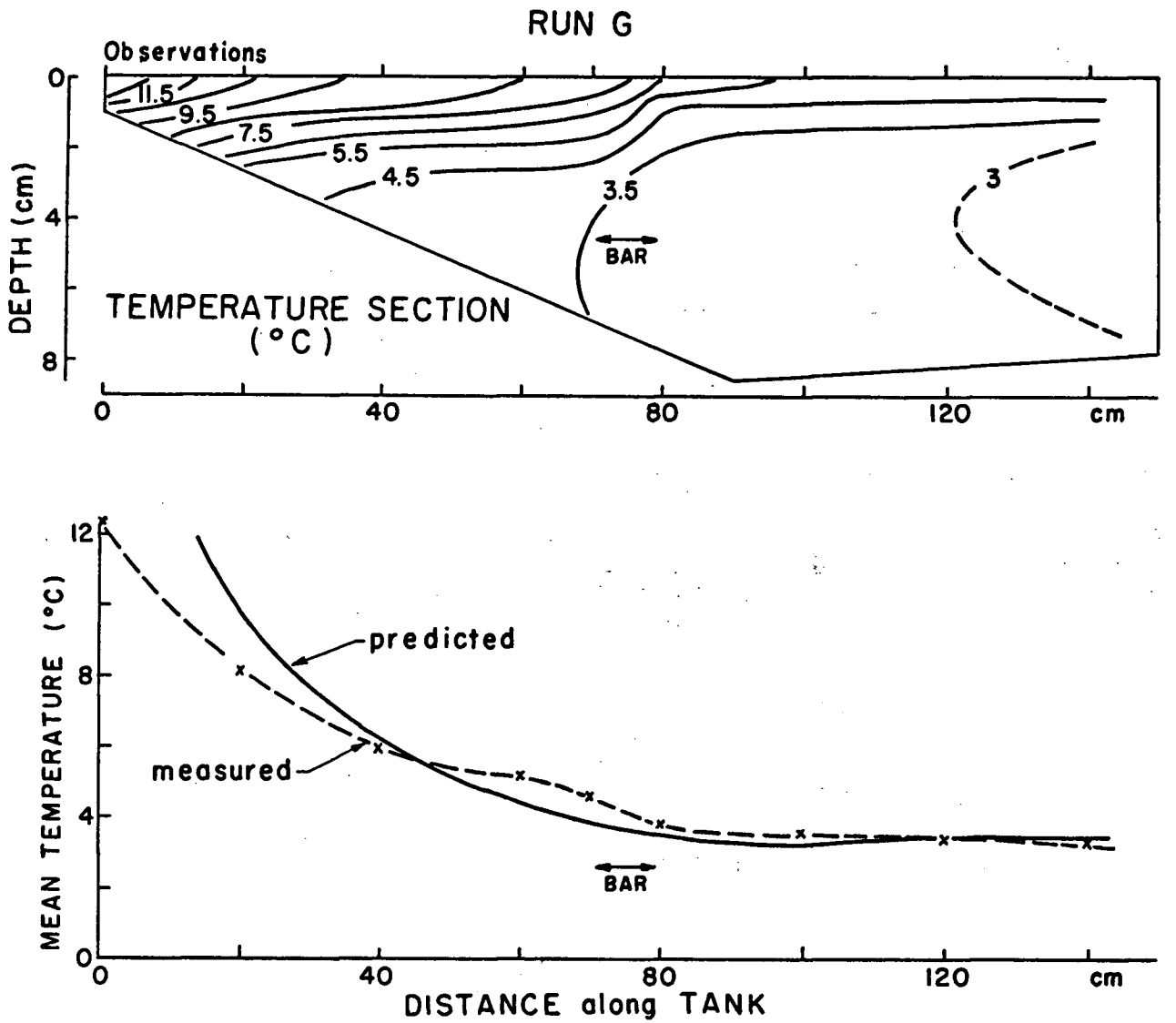

Figure 29a. Temperature section and mean temperatures for Run G: 5°-0° bottom slope, standard heating and Ti, 0°C

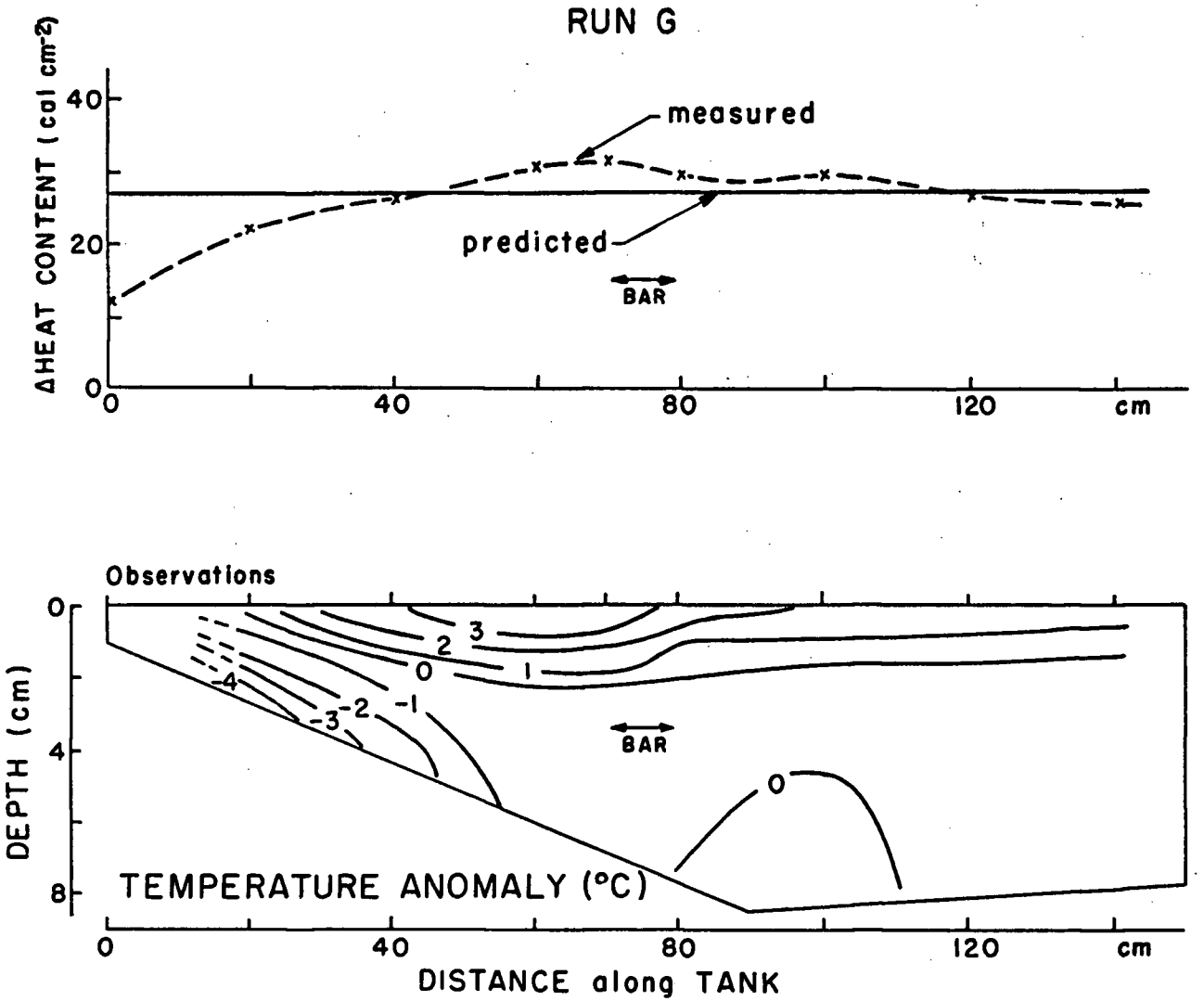

Figure 29b. Changes in heat content and temperature anomaly for Run G

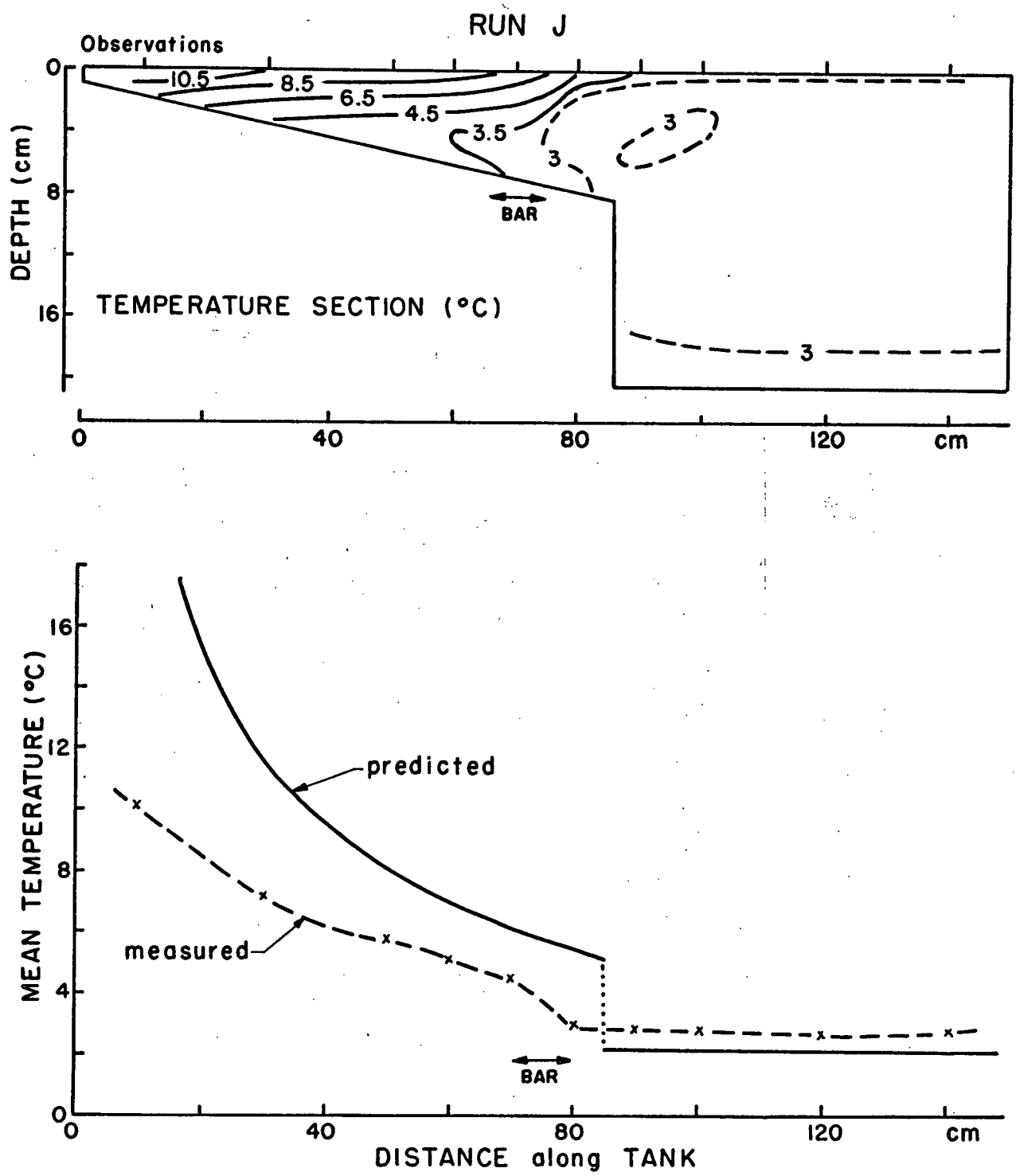

Figure 30a. Temperature section and mean temperatures for Run J: 5°-0° bottom slope with dropoff, standard heating, and Ti, 0°C.

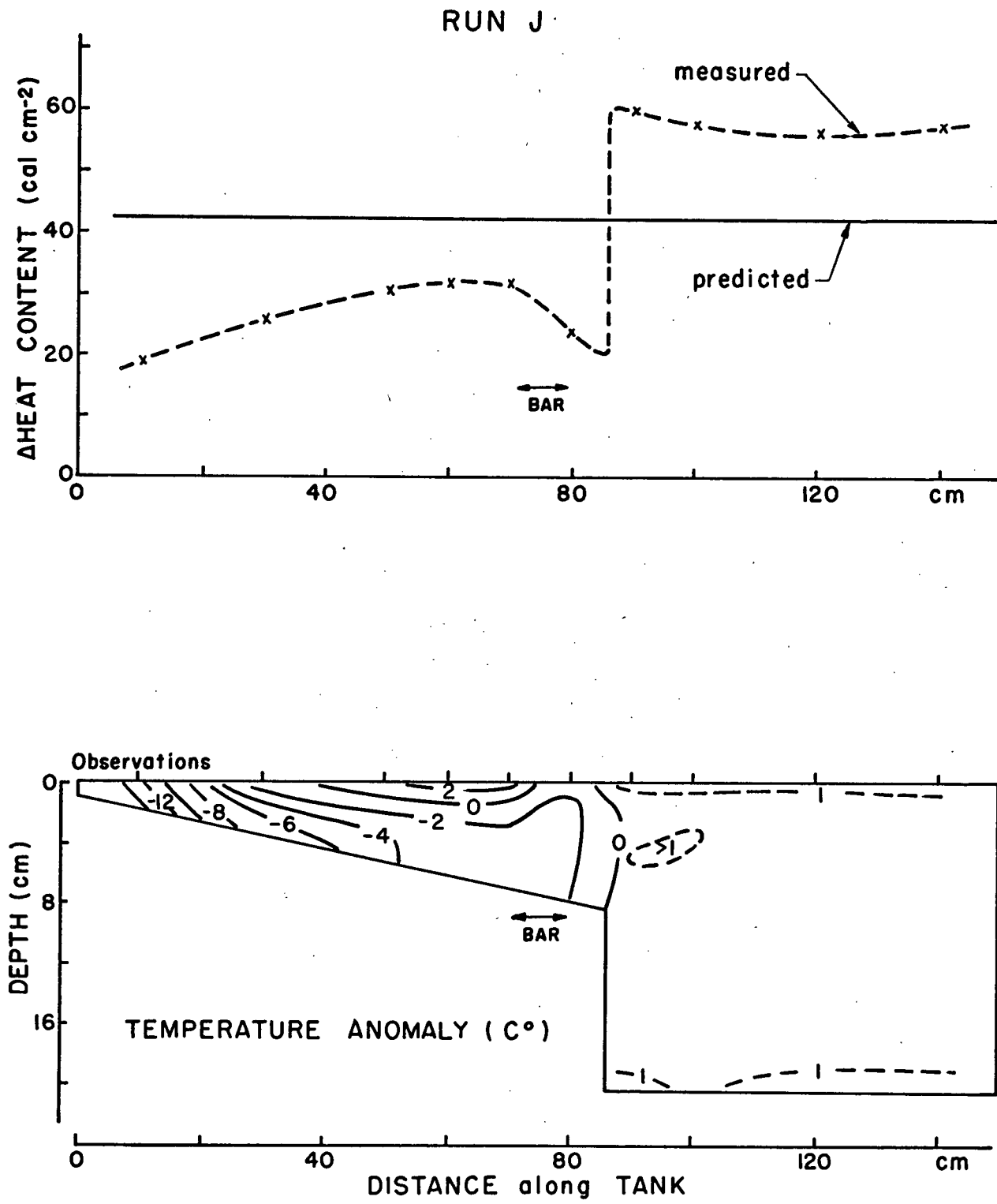

Figure 30b. Changes in heat content and temperature anomaly section for Run J

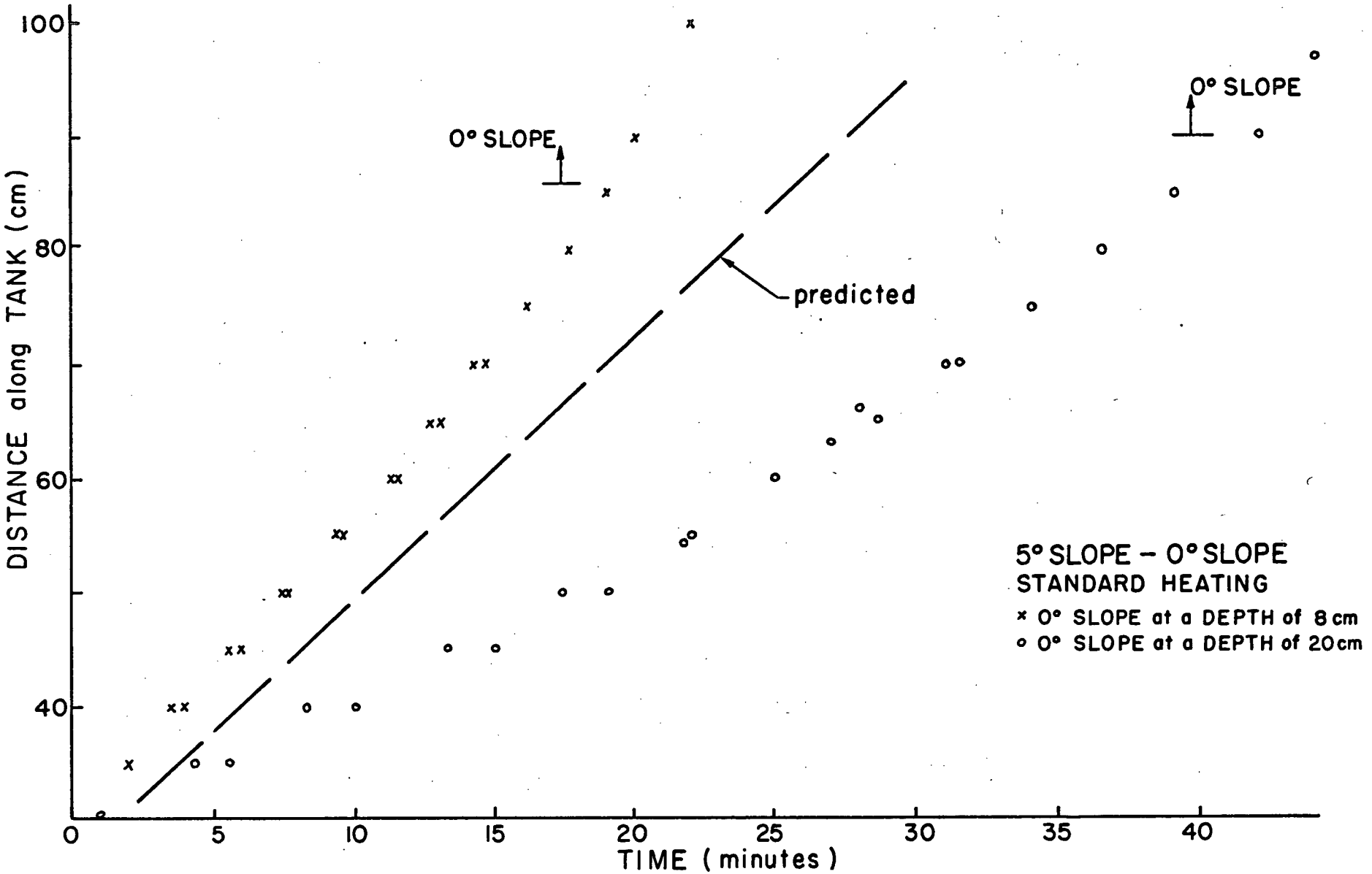

Figure 31. Position of the bar, measured and predicted, for 5°-0° bottom slopes and standard heating. The SLOPE of these curves is BAR SPEED.

APPENDIX D

To show that the thermal bar phenomenon is driven, basically, by the heating of water through its maximum density, as has been proposed in the linear model for the speed of the bar, the following two experiments were performed.

1. Sliding Door Experiment

Figure 32 shows the temperature section and mean temperatures 20 minutes after 2°C and 8°C water were brought together. There was no heating (heat lamps were turned off). This represents the behaviour of flow which could be expected when 'fresh' water colder than 4°C flows into water warmer than 4°C (for example, at the foot of a glacier) or when water warmer than 4°C flows into water colder than 4°C (for example, effluents). The behaviour is not similar to the migrating thermal bar in that the resulting current pattern does not move and the active sinking zone between the two water masses involves water from both sides. This circulation results from the production of dense, 4°C water at the contact between the two water masses. The horizontal velocity profiles are S-shaped, similar to those shown in Figure 6 (p.15) for the migrating thermal bar experiments. This current structure, superimposed on the temperature section, is a clockwise circulation in the shallower water and a counter-clockwise circulation in the deeper water, with most of the sinking between the 3.5 and 4.5°C isotherms (as indicated by arrows). In a manner similar to the migrating thermal bar phenomenon, the sinking prevents flow due

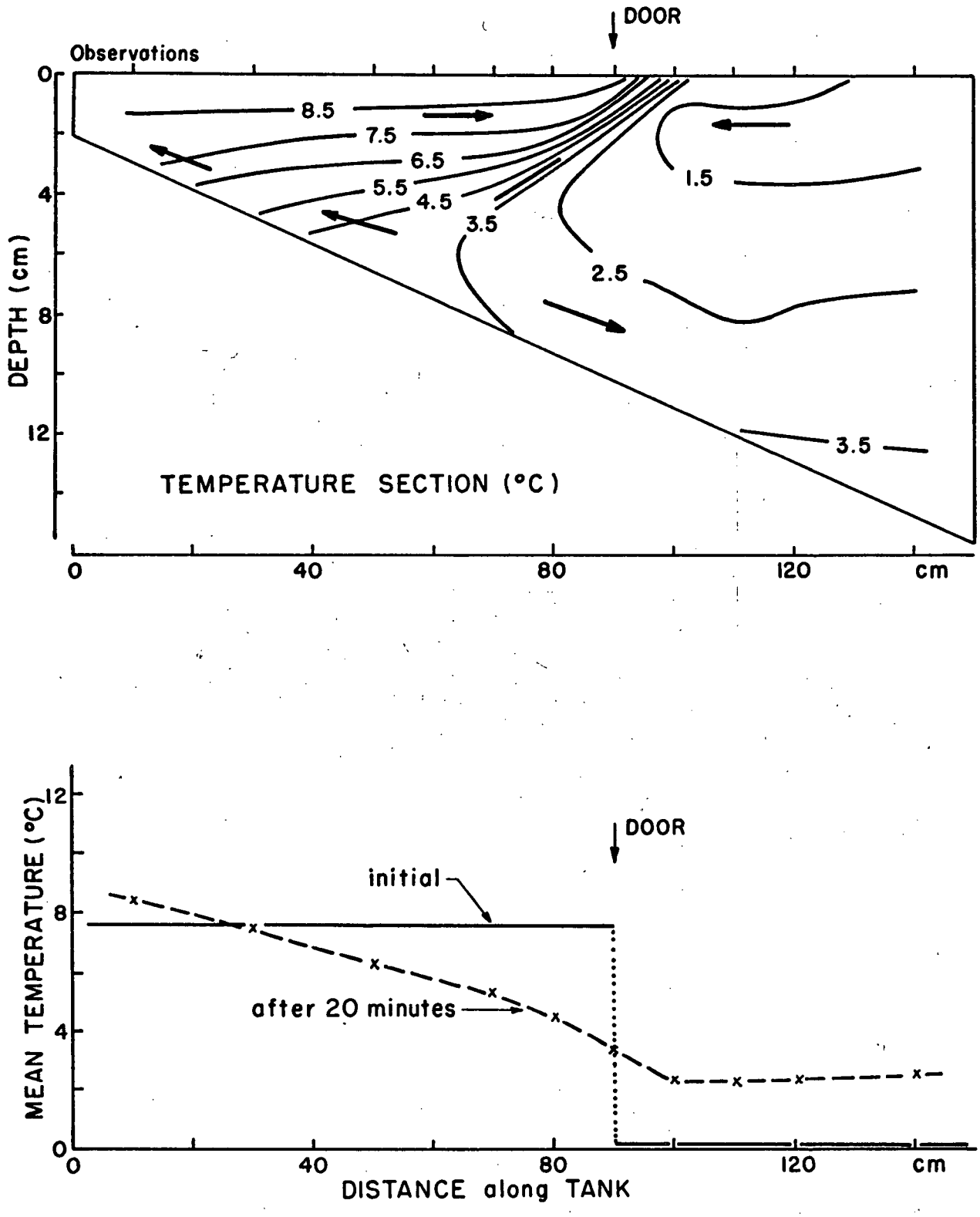

Figure 32. Temperature section and mean temperatures for sliding door experiment (5° bottom slope).

to the horizontal density gradients.

Actual examples of water warmer than 4°C being dumped into water colder than 4°C were presented by Chermack (1970) at the 13th Conference on Great Lakes Research, April, 1970. His work involved airborne radiation thermometer studies of effluents from nuclear power plants on southeastern Lake Ontario. In each case these effluents were confined to an arc of radius of the order of a kilometer from the point of discharge. This confinement agrees with the results of this 'sliding door' experiment.

2. Heating Water Warmer than 4°C

Figure 33 shows the temperature section associated with heating water that is all at a temperature greater than 4°C. The flow is towards the deep end in the upper layers and towards the shallow end in the deeper layers. The temperature structure bears no resemblance to the thermal bar case. The velocities involved are considerably less than the speed of the migrating thermal bar (about 1/10). This flow is driven by the horizontal density gradients set up by uniform surface heating and a sloping bottom since the temperature rises faster in the shallow end of the tank.

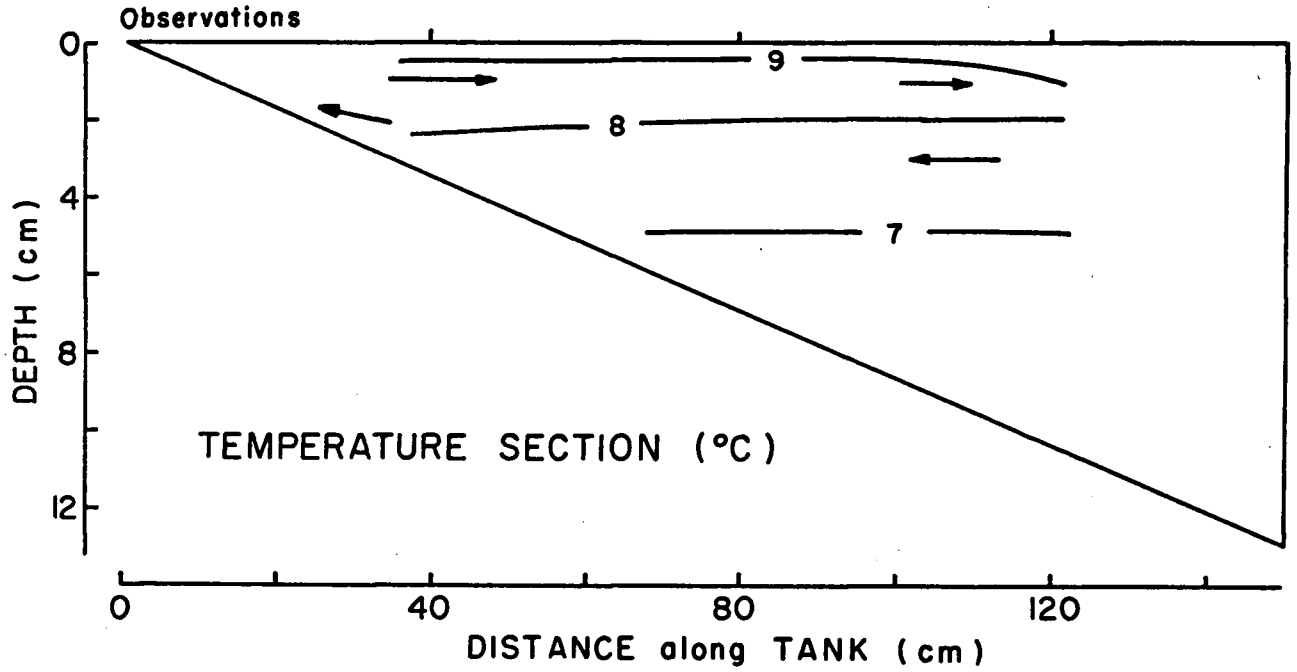

Figure 33. Temperature section for heating water warmer than 4°C, with a 5° bottom slope, standard heating and Ti, about 7°C.

APPENDIX E: Calculation of the Stream Function

The stream function ϕ is calculated from equation 3.2.7, using the analytical temperature function given in equation 3.2.9 and satisfying the boundary conditions given in equations 3.2.8. The streamline along $z = 0$ and $z = -D$ is set equal to zero.

$$\phi = \frac{2Ag}{\nu} (2.9)\ (0.0392)\ \mathrm{sech}^2(0.392[\ \frac{St-x}{10} - 2\ ])$$

$$\cdot\{\ \frac{0.001}{36} z^6 + \frac{0.01}{6} z^5 + \frac{1}{24} z^4$$

$$+ z^3\ (\ \frac{0.001}{9} D^3 - \frac{0.01}{2} D^2 + \frac{1}{12} D\ )$$

$$+ z^2\ (\ \frac{0.001}{12} D^4 - \frac{0.01}{3} D^3 + \frac{1}{24} D^2\ )$$

$$- 2.9\ [\ 1 + \tanh(0.392[\ \frac{St-x}{10} - 2\ ])]$$

$$\cdot[\ \frac{0.00001}{168} z^8 + \frac{0.0001}{21} z^7 + \frac{0.001}{6} z^6 + \frac{0.01}{3} z^5$$

$$+ \frac{1}{24} z^4 + z^3\ (\ \frac{0.00001}{28} D^5 - \frac{0.001}{42} D^4 + \frac{0.01}{15} D^3$$

$$- 0.01\ D^2 + \frac{1}{12} D\ ) + z^2\ (\ \frac{0.0001}{336} D^6 - \frac{0.002}{105} D^5$$

$$+ \frac{0.001}{2} D^4 - \frac{0.1}{15} D^3 + \frac{1}{24} D^2\ )\ ]\ \}$$

where $A = 8 \times 10^{-6}\ C^{\circ\ -2}$,

g is the acceleration due to gravity ($\simeq 10^3$ cm sec^{-2}),

ν is viscosity (= 1.5 x 10^{-2} cm^2 sec^{-1} for the laboratory model),

S is the speed of the bar,

$D = \alpha x$ is the depth of the bottom and α is bottom slope.

From this ϕ, u and w can be found since

$$u = \frac{\partial \phi}{\partial z} \quad \text{and} \quad w = -\frac{\partial \phi}{\partial x} \quad .$$